

**DEVELOPMENT OF TARGETED DRUG DELIVERY
SYSTEM FOR BREAST CANCER**

Thesis submitted in fulfillment of the requirements for the Degree of

**DOCTOR OF PHILOSOPHY
IN
PHARMACEUTICAL SCIENCES**

**BY
ARUN SHARMA**



**DEPARTMENT OF PHARMACY
JAYPEE UNIVERSITY OF INFORMATION TECHNOLOGY
WAKNAGHAT, DISTRICT SOLAN, H.P., INDIA**

JULY 2018

**DEVELOPMENT OF TARGETED DRUG DELIVERY
SYSTEM FOR BREAST CANCER**

Thesis submitted in fulfillment of the requirements for the Degree of

**DOCTOR OF PHILOSOPHY
IN
PHARMACEUTICAL SCIENCES**

**BY
ARUN SHARMA**



**DEPARTMENT OF PHARMACY
JAYPEE UNIVERSITY OF INFORMATION TECHNOLOGY
WAKNAGHAT, DISTRICT SOLAN, H.P., INDIA**

JULY 2018

@ Copyright

JAYPEE UNIVERSITY OF INFORMATION TECHNOLOGY, WAKNAGHAT

July 2018

All Rights Reserved

ii

Arun Sharma, Ph.D. Thesis, Jaypee University of Information Technology, July 2018

“Every challenging work needs self-efforts as well as support from your love one”

DEDICATED TO MY LOVING PARENTS AND
BROTHERS

Mr. and Mrs. *J.P. Sharma*

Nikhil Sharma & Sanjay Sharma

TABLE OF CONTENT

CONTENTS	Page No.
Table of Contents	iv-ix
Declaration	x
Certificates	xi-xii
Acknowledgement	xii-xiv
Abstract	xv-xvi
Abbreviations	xvii-xxi
Table of figures	xxii-xxvi
List of Tables	xxvii
INTRODUCTION.....	1-5
Scope and outline of the thesis	
CHAPTER-1.....	6-39
1.1 Breast cancer	
1.2 Epidemiology of Breast cancer	
1.2.1 Worldwide Scenario	
1.2.2 India	
1.3 Types of Breast Cancer	
1.3.1 Ductal Carcinoma In-Situ (DCIS)	
1.3.2 Lobular Carcinoma In-Situ (LCIS)	
1.3.3 Invasive Ductal carcinoma (IDC)	
1.3.4 Invasive Lobular carcinoma (ILC)	
1.4 Breast cancer classification: based Molecular subtype	
1.4.1 Luminal-A subtype	
1.4.2 Luminal-B subtype	
1.4.3 Triple negative subtype	
1.4.4 HER2-enriched subtype	
1.5 Other rare breast cancers	
1.5.1 Tubular carcinoma in Breast	
1.5.2 Medullary carcinoma in Breast	
1.5.3 Mucinous carcinoma in Breast	

- 1.5.4 Papillary carcinoma in Breast
- 1.5.5 Cribriform carcinoma in Breast
- 1.5.6 Paget's Disease of the Nipple
- 1.5.7 Phyllodes tumors in Breast
- 1.5.8 Male breast cancer

1.6 Metastatic breast cancer

1.7 Breast cancer treatment

1.7.1 Local treatment

1.7.1.1 Surgery

1.7.1.2 Radiation therapy

1.7.2 Systemic treatment

1.7.2.1 Chemotherapy

1.7.2.2 Hormone therapy

1.7.2.3 Targeted therapy

1.8 Chemotherapy: mainstay for breast cancer treatment

1.9 Chemotherapy for more aggressive and advanced breast cancer

1.10 Taxanes

1.11 Paclitaxel and its mechanism of action

1.11.1 Associated side of Paclitaxel

1.12 Chemotherapy combination

1.12.1 Advantages of combinational strategies in cancer therapy

1.13 Commonly employed combination therapy for cancer treatment

1.13.1 Radiotherapy along with chemotherapy

1.13.2 Chemotherapy along with hormone therapy

1.13.3 Immunotherapy with chemotherapy

1.14 Clotrimazole

1.14.1 Mechanism of Action Against Tumor

1.15 Nanotechnology- chemotherapeutics

1.16 Nanoparticles Targeting Approaches

1.16.1 Passive targeting

1.16.1.1 Targeting via Enhanced Permeability and Retention (EPR) effect

1.16.1.2 Targeting via Enhanced Permeability and Retention (EPR) effect

1.16.2 Active targeting

1.17 Sialic acid

1.18 Different types of nanocarrier systems

1.19 Polymeric nanoparticles

1.19.1 Advantages of polymeric nanoparticles

1.19.2 Selecting a Polymeric Drug Delivery

1.19.3 Types of polymer available for drug delivery

1.19.3.1 Natural polymers

1.19.3.2 Synthetic polymers

1.20 Polycaprolactone

1.20.1 Methods for preparation of nanoparticles

1.20.1.1 Solvent Evaporation method

1.20.1.2 Nanoprecipitation method

1.20.1.3 Dialysis method

1.20.1.4 Emulsification/solvent diffusion (ESD) technique

CHAPTER-2..... 40-56

2.1 Introduction

2.2 Material and Method

2.2.1. Materials

2.2.2. Fourier transform infrared spectroscopy (FTIR) analysis

2.2.4 Cell lines maintenance and culturing

2.2.4. Cell cytotoxicity analysis and drug combination

2.2.5 Microscopical evaluation cell death

2.2.5.1 Acridine orange (AO) and ethidium bromide (EtBr) staining to identify apoptosis.

2.2.5.2 4'-6- diamidino-2-phenylindole (DAPI) and propidium iodide (PI) staining

2.2.6 Estimation of Reactive oxygen species (ROS)

2.2.7 Estimation of Reactive nitrogen species (RNS)

2.2.8 Comet assay

2.2.9 Glucose consumption

2.2.10 Statistics

2.3 Results and Discussion

2.3.1 Physicochemical characterization of PAX/CLZ mixture

2.3.2 Cell cytotoxicity analysis and selection of drug combination

2.3.3 Microscopical evaluation of cell death

2.3.3.1 Acridine orange (AO) and ethidium bromide (EtBr) staining to identify apoptosis

2.3.3.2 4'-6- diamidino-2-phenyl-indole (DAPI) and propidium iodide (PI) staining

2.3.4 Estimation of Reactive oxygen species (ROS)

2.3.5 Estimation of Reactive nitrogen species (RNS)

2.3.6 Comet assay

2.3.7 Glucose consumption

2.4 Summary Points

CHAPTER-3 57-71

3.1 Introduction

3.2. Materials and Methods

3.2.1 Materials

3.2.2 Preparation of PSA - PCL polymeric NPs

3.2.2.1 Fabrication of PCL-polymeric NPs

3.2.2.2 Synthesis of PSA-PCL NPs

3.2.3 Particle size distribution and zeta potential analysis

3.2.4 Morphological analysis

3.3.5 Fourier Transform Infrared (FTIR), Ultra violet (UV)-Visible Spectrophotometer analysis and X-Ray diffraction (XRD) analysis.

3.3.6 Quantification of drug encapsulation and drug loading

3.3.7 In-vitro drug release study

3.3.8 Cell line and culture

3.2.8.1 In-vitro cytotoxicity studies

3.3.9 Photoluminescence spectrophotometric analysis for cellular uptake

3.3.10 Fluorescent microscopic analysis of cellular uptake

3.2.11 Statistical analysis

3.3 Results and Discussion

3.3.1 Characterization of synthesized nanoparticles

3.3.2 Drug encapsulation efficiency, loading and release

3.3.3 Cell cytotoxicity

3.3.4 Photoluminescence analysis

3.3.5 Microscopic analysis of cellular uptake

3.4 Summary Points

CHAPTER-4 72-85

4.1 Introduction

4.2 Material and Methods

4.2.1 Materials

4.2.2 Fabrication of PCL-polymeric NPs

4.2.3 Particle size distribution analysis

4.2.4 Quantification of drug encapsulation and drug loading

4.2.5 Identification of critical variables and preliminary investigation

4.2.6 Optimization of Nanoparticles using Box-Behnken response surface methodology.

4.2.7 Statistical analysis

4.3 Result and Discussion

4.3.1 Preliminary investigation

4.3.2 Response surface methodology and Box-Behnken design

4.3.3 Effect of variables on particle size (PS) studied through-BBD

4.3.4 Effect of variables on entrapment efficiency (%EE) studied through (BBD)

4.3.5 Optimization of variable through desirability plot

4.4 Summary Points

CHAPTER-5 86-100

5.1 Introduction

5.2 Material and Methods

5.2.1. Materials

5.2.2. Ingredient volume selection from previously optimized concentrations

5.2.3. Fabrication of drug loaded PCL-nanoparticles

5.2.4. Functionalization of Sialic Acid (SA) on PCL NPs

5.2.5. Surface morphological investigation

5.2.6. Fourier Transform Infrared (FTIR) analysis

5.2.7. Particle size distribution and zeta potential analysis

5.2.8. Quantification of drug encapsulation and drug loading

5.2.9. In-vitro drug release study

5.2.10. Cell line and culture

5.2.10.1. *In-vitro cytotoxicity studies*

5.2.11. Acridine orange (AO) and ethidium bromide (EtBr) staining to identify apoptosis

5.2.12. Statistical analysis

5.35.3 Results and Discussion

5.3.1. Scanning electron microscopy, particle size distribution and % entrapment efficiency.

5.3.2. Fourier-transform infrared spectroscopic analysis

5.3.3. In-vitro Drug release studies

5.3.4. In-vitro cell cytotoxicity studies

5.3.5. Acridine orange (AO) and ethidium bromide (EtBr) staining to identify cell death

5.4 Summary Points

APPENDIX101-114

REFERENCES115-129

PUBLICATION AND CONFERENCES130-133

DECLARATION BY THE SCHOLAR

I, Arun Sharma, hereby claim that the work described in the Ph.D. thesis entitled “**Development of targeted drug delivery system for breast cancer**” submitted at the **Jaypee University of Information Technology, Wagnaghat, India**, is an authentic record of my work carried out under the guidance of **Dr. Udayabanu Malairaman**. This work has not been submitted elsewhere for any other degree or diploma. I am totally accountable for the contents of my Ph.D. thesis.

Arun Sharma

Date:

Enrolment Number: 136752

Department of Pharmacy

Jaypee University of Information Technology,

Wagnaghat, Solan, H.P., Indian

SUPERVISOR'S CERTIFICATE

This is to certify that the work described in the Ph.D. thesis entitled “**Development of targeted drug delivery system for breast cancer**” submitted by **Arun Sharma** at the **Jaypee University of Information Technology, Wagnaghat, India**, is a bonafide record of his original work carried out under my guidance.

Certified further, that to the best of my knowledge the work reported herein does not resemble any other thesis or dissertation and this work has not been submitted elsewhere for any other degree or diploma.

Dr. Udayabanu Malairaman

Date:

Assistant Professor

Department of Pharmacy

Jaypee University of Information Technology,

Wagnaghat, Solan, H.P., Indian

CO-SUPERVISOR'S CERTIFICATE

This is to certify that the work described in the Ph.D. thesis entitled “**Development of targeted drug delivery system for breast cancer**” submitted by **Arun Sharma** at the **Jaypee University of Information Technology, Wagnaghat, India**, is a bonafide record of his original work carried out under my co-guidance.

Certified further, that to the best of my knowledge the work reported herein does not resemble any other thesis or dissertation and this work has not been submitted elsewhere for any other degree or diploma.

Dr. Abhishek Chaudhary

Date:

Assistant Professor
Department of Biotechnology and Bioinformatics
Jaypee University of Information Technology,
Wagnaghat, Solan, H.P., Indian

ACKNOWLEDGEMENT

One of the joyful moments is to look over the past journey and remember all those special people without whom this achievement would never have been possible. At this juncture my head bows before the *Almighty* for blessing me with the right kind of individuals who have loved, encouraged and supported me throughout.

This piece of work is not an acknowledgement; it's a gratitude for all those who helped me to achieve this work.

*First and foremost, I offer my sincerest gratitude to my mentor, **Dr. M. Udayabanu**, for his immaculate guidance with wisdom and knowledge whilst allowing me the room to work in my own way. All the more, his efforts and skills reflect in the pages of this thesis which my labors will never stand upto. I could not have asked for a better role model, all inspirational, supportive, and patient as his and hope that I can in turn pass on the research values and the dreams that he has imparted to me.*

*I express my heartfelt thanks to my co-guide **Dr. Abhishek Chaudhary**, for contributing his valuable time to discuss and make appropriate suggestions all through the period of my study.*

*I gratefully acknowledge the help rendered by **Prof. R.S. Chauhan** (Ex-Dean & HOD, Dept of BT, BI & Pharmacy) and **Dr. Sudhir Kumar** (Current-HOD, Dept. of BT, BI & Pharmacy) for their encouragement, timely help and cooperation throughout my research work. I wish to convey my sincere thanks to all the faculty members of Department of Biotechnology, Bioinformatics and Pharmacy especially **Dr. Hemant Sood**, for her sustained support and ever needed cooperation throughout the study.*

*I am grateful to **Jaypee University of information Technology (JUIT) Administration, Professor (Dr.) Vinod Kumar** (Vice-chancellor JUIT), **Professor (Dr.) Samir Dev Gupta** (Director & Academic Head), **Major General (Retd) Rakesh Bassi** (Registrar & Dean of Student Welfare), **Brigadier (Retd.) K.K. Marwah** (Ex- Registrar & Dean of Student Welfare)*

and **Brigadier (Retd.) Balbir Singh** (Ex- Registrar & Dean of Student Welfare) for providing the financial assistance and infrastructure for my research work.

This document would be remained an infant had it not received its necessary 'diet' in the form of comments, suggestions made by DPMC members **Dr. Gopal Singh Bisht, Dr. Poonam Sharma & Dr. Rajesh Kumar**. I am short of words in expressing my thanks to them, for their innovative ideas that shaped this document.

I wish to acknowledge the **Department of Science and Technology**, Government of India, for providing me **INSPIRE Fellowship (IF-140274)**.

I acknowledge my gratitude to students, technical and non-technical staff of the department especially **Mrs. Sonika Gupta, Mrs. Somlata Sharma, Mrs. Mamta Mishra, Mr. Baleshwar, Mr. Ismail Siddiqui and Mr. Kamlesh** for their assistance and valuable contributions.

The constant pursuit to achieve my goals may not have been fuelled, if not for the energy, cheerfulness and unflinching help of friends. I extend my heartfelt thanks to **Dr. Rishi Mahajan, Dr. Rohit Randhawa, Mr. Vineet Mehta, Mr. Arun Parashar, Mrs. Jyoti Kaushik, Ms. Deepika Sharma, Mr. Sampan Attri, Ms. Kavita Sharma, Mr. Sanjay Sange, Mr. Vikrant Sharma & Mr. Deepak Sharma** for their invaluable help

Thanks would be as small word for what I owe my parents, **Dr. J.P. Sharma and Mrs. Neelam Sharma** and my younger brother **Nikhil Sharma**. I would like to express my hearty thanks to **Ms. Ritika Thakur** for understanding, patient waiting and constant praying for completion of my work. It was because of their love & blessing that I was able to strongly steer through the rough winds of time. They have paved the path before me and upon whose shoulder I stand today.

I would once again thank GOD for always listening to me and giving me enough strength to stand by in hard times, for always holding my hand and letting me though.

My very special thanks are due to many others who provided their relentless support and helped me in one way or other during this work.

No one is forgotten, although, not mentioned.

Arun Sharma

The background of the entire page is a monochromatic blue-toned landscape. At the top, a large, pale blue circle representing the moon is positioned in the upper left quadrant. Below it, a series of jagged mountain peaks are visible, receding into the distance through atmospheric haze. The lower half of the image shows rolling, smooth hills or dunes, also receding into the distance. A dark blue horizontal band with a white border runs across the middle of the page, containing the word 'ABSTRACT' in white, bold, serif capital letters.

ABSTRACT

The present investigation was aimed to develop a targeted co-delivery system of paclitaxel (PAX) and clotrimazole (CLZ) through polycaprolactone (PCL) nanoparticles (NPs). Sialic acid (SA) was employed to acquire active targeting towards breast cancer cells. To accomplish this objective, initially, we optimized the concentration of PAX and CLZ by determining cell viability through MTT assay. CompuSyn software was used to depict the synergistic, additive or antagonist effect of PAX and CLZ in combination. MTT assay and CompuSyn simulations suggest the synergistic activity of PAX & CLZ at 12.5-nM & 25- μ M respectively and nominated as PACL. Fluorescent microscopy also supports our finding, where PACL significantly induced nuclear damage in breast cancer cells (MCF-7 & MDA-MB-231). Oxidative stress and nitrogen stress was also aggravated by PACL when compared to individual drug concentration. PACL exhibited significant genotoxicity in cancerous cells whereas glucose uptake was inhibited remarkably through PACL in contrast to individual drug concentration. The second objective was to formulate surface functionalized SA polymeric nanoparticles (SA-PCL-NPs) of PAX. Carbodiimide reaction was exploited to mount SA on the surface of PCL-NPs. Characterisation reveals that SA-PCL-NPs were having spherical morphology with a size range of 151.5 nm to 179.47 nm. SA-PCL-NPs profoundly homed themselves inside the cancer cells and induces apoptosis as suggested by MTT assay and photoluminescence study.

While in the third objective different variables, that play an integral role in the development of nano-formulation were optimized through response surface methodology (RSM). Box Behnken Design (BBD) was employed to generate 3-dimensional surface plots and further analyzed to study the effect of variables on the particle size (PS) and entrapment efficiency % (%EE). Results suggest that when the optimized concentration of variables will be used, there would be 92.4% chances to get PS of 178.7 nm and %EE of 49.13% and witnessed that the obtained results were close to predicted responses. In the final objective, we synthesized the NPs by selecting the drug combination and formulation variables as optimized from 1st and 3rd objective, further the SA was functionalized on the surface of NPs. Resulting SA-co-encapsulated drug-loaded NPs (SA-PACL-NPs) displayed spherical shape, with size ranging from 187 nm to 197 nm. MTT assay revealed increase in cytotoxicity, as an effect of SA-mediated targeting against cancer cells in contrast to normal cells (HEK-293). These results were further confirmed by observing the nuclear morphological alterations in cells, where cancer cells were affected greatly in comparison to normal cells. The obtained results suggest that SA-mediated-NPs were synergistically effective against breast cancer cells whereas possessing minimal effect on normal cells.

LIST OF ABBREVIATION

°C	Celsius
ABC	ATP-binding cassette
AI	Aromatase inhibitor
ADH	Aldehyde dehydrogenase
AO	Acridine Orange
BBD	Box Behnken design
BRCA-1	Breast Cancer Type-1 Susceptibility protein
BRCA-2	Breast Cancer Type-2 Susceptibility protein
BCRP	breast cancer resistance protein
CCD	Central composite design
CDK	Cyclin dependent kinase
CLZ	Clotrimazole
CI	Combination Index
cP	Centi Poise
CO ₂	Carbon di-oxide
CTCF	Corrected total cell fluorescence
DMEM	Dulbecco's Modified Eagle Medium
DAPI	4, 6-diamidino-2-phenylindole
DCIS	Ductal Carcinoma In-Situ
DCM	Dichloromethane
DNA	Deoxyribonucleic acid
DLS	Dynamic Light Scattering
DRI	Dose reduction index

DST	Department of Science and Technology
EDTA	Ethylenediaminetetraacetic acid
EGFR	Epidermal growth factor receptor
EMT	Epithelial mesenchymal transition
EPR	Enhanced permeation and retention
ER	Estrogen receptor
EtBr	Ethidium bromide
ERDs	Estrogen receptor down-regulator
ESA	Epithelial specific antigen
ESD	Emulsification/solvent diffusion
EDC	N-(3-dimethylaminopropyl)-N'-ethylcarbodiimide
eV	Electron volt
FACS	Fluorescence Activated Cell Sorter
FFD	Full factorial design
FBS	Foetal Bovine Serum
FDA	Food and Drug Administration
FTIR	Fourier Transform Infrared Spectroscopy
H	Hour
H ₂ O ₂	Hydrogen peroxide
H ₃ PO ₄	Ortho Phosphoric Acid
HCl	Hydrochloric Acid
HK	Hexokinase
HER	Human epidermal receptor
IL	Interleukin

IL-1 β	Interleukin 1-beta
IDC	Invasive Ductal carcinoma
ILC	Invasive Lobular carcinoma
KBr	Potassium Bromide
kV	Kilovolts
LCIS	Lobular Carcinoma In-Situ
L-15	Leibovitz's
MAPK	Mitogen-activated protein kinase
MDR	Multi drug resistance
MEM	Minimum Essential Medium
MRP-1	Multidrug resistance protein-1
MTT	3-(4,5-dimethylthiazol-2-yl)-2,5-diphenyltetrazolium bromide
ml	Millilitre
N	Normality
NaCl	Sodium Chloride
NPs	Nanoparticles
nm	Nanometer
nM	Nanomole
NHS	N-hydroxy succinimide
NSAID	Non-steroidal anti-inflammatory drugs
NO	Nitic oxide
PAX	Paclitaxel
PACL	Combination of PAX and CLZ
PBS	Phosphate Buffer Saline

PCL	Poly-(caprolactone)
P-gp	P-glycoprotein
PI	Propidium Iodide
PDI	Poly-dispersity index
PS	Particle size
pH	Potenz Hydrogen
PKF	6-phosphofructo-1-kinase
PEG	Poly-ethylene glycol
PR	Progesterone receptor
PVA	poly-vinyl-alcohol
PSA	Poly-sialic acid
ROS	Reactive oxygen species
RNS	Reactive nitrogen species
RSM	Response Surface Methodology
RPM	Rotations per Minute
RES	Reticuloendothelial system
RTK	Receptor tyrosine kinase
Rhd-NPs	Rhodamine loaded nanoparticles
SERMs	Selective estrogen receptor modulator
SEM	Scanning Electron Microscopy
TCN	Targeted combination nanomedicine
UV	Ultra Violet-Visible Spectrophotometer
VEGF	Vascular endothelial growth factor
WHO	World Health Organization

XRD	X-ray Powder Diffraction
Wt%	Percentage Weight
α -TNF	α -Tumor necrosis factor
μ g	Microgram
μ M	Micromole

LIST OF FIGURES

Figure No	Title	Page No.
<i>Chapter-1</i>		
1.1	Breast cancer incidence World wide	7
1.2	Breast cancer incidence in India	8
1.3	Type of Breast cancer based on Invasiveness	9
1.4	Overview of molecular subtype of breast cancer	10
1.5	Schematic representation of the available option for the breast cancer treatment	13
1.6	Schematic representation of various type Mastectomy available for breast cancer treatment	14
1.7	Schematic representation of different types of radiation therapy available for breast cancer	14
1.8	Schematic presentation of systemic treatment given before and after surgery	15
1.9	Different types of targeted therapeutic agents employed to treat breast cancer	17
1.10	Different types chemotherapeutic agents employed to treat breast cancer	18
1.11	Brief description of Paclitaxel	20
1.12	Different types of drug combination used for breast cancer treatment.	24
1.13	Brief Description of clotrimazole	25
1.14	Schematic presentation of different approaches available for targeted nano-delivery system.	27
1.15	Schematic presentation of active targeting approaches.	29
1.16	Chemical structure of Sialic acid and its derivatives. (Image courtesy: Zhang et.al., 2014)	30
1.17	Brief description of different Nano delivery system available	31
1.18	Different type of polymeric nanoparticles. (Image courtesy: Dadwal et.al., 2014)	33
1.19	Facts regarding PCL. (Image courtesy: Wikipedia)	35

1.20	Solvent evaporation technique to formulate polymeric-NPs. (Image courtesy: Nagavarma et.al., 2012)	36
1.21	Nanoprecipitation technique to formulate polymeric-NPs. (Image courtesy: Nagavarma et.al., 2012)	37
1.22	Dialysis technique to formulate polymeric-NPs. (Image courtesy: Nagavarma et.al., 2012)	38
1.23	Emulsification diffusion technique to formulate polymeric-NPs. (Image courtesy: Nagavarma et.al., 2012)	38

Chapter 2

2.1	Chemical structure of (a) Paclitaxel [PAX] and (b) Clotrimazole [CLZ].	46
2.2	FTIR spectroscopic graphs of (a) Paclitaxel, (b) Clotrimazole and (c) physical mixture of PAX and CLZ.	47
2.3	Dose dependent effects of PAX and CLZ on viability of MCF-7 cells (a and b) in the form of percent cell viability relative to untreated control cells. Co-effect of selected PAX and CLZ doses in combination (c) and bars not sharing the same letters are significantly different with $p < 0.05$. Comparative analysis of selected combo on MCF-7, MDA-MB-231 and HEK-293 at 24h (d) and *** indicates $p < 0.001$ when compared with untreated group. All data is presented as mean \pm SEM of three independent experiments.	48
2.4	Combination dose effect curve (a) as an outcome of PAX and CLZ interactions on MCF-& breast cancer cells, (b) mass-action algorithms derived from computerized simulations through Compusyn showing media-effect plot (Chou Plot), (c) FA-CI plot (Chou-Talalay Plot) showing synergism interaction of PAX & CLZ and (d) FA-DRI Plot (Chou-Chou Plot) representing index of dose reduction.	49
2.5	AO/EtBr staining of MCF-7 cells treated with PAX (12.5 nM), CLZ (25 μ M) and PACL (PAX 12.5 nM + CLZ 25 μ M). Cells were observed under fluorescent microscope at 200 X magnification and scale bar corresponds to 50 μ M. Graph characterizes the collective total cell fluorescence ratio for red fluorescence representing PI stained dead cells. * denotes $p < 0.05$, ** denotes $p < 0.01$ and *** denotes $p < 0.001$ when fluorescent intensity was compared with control group. Likewise ### denotes $p < 0.001$ when evaluated against combination treated cells. (CTCF: corrected total cell fluorescence).	50

2.6 AO/EtBr staining of MCF-7 cells treated with PAX (12.5 nM), CLZ (25 μ M) and PACL (PAX 12.5 nM + CLZ 25 μ M). Cells were observed under fluorescent microscope at 200 X magnification and scale bar corresponds to 50 μ M. Graph characterizes the collective total cell fluorescence ratio for red fluorescence representing PI stained dead cells. * denotes p<0.05, ** denotes p<0.01 and *** denotes p<0.001 when fluorescent intensity was compared with control group. Likewise ### denotes p<0.001 when evaluated against combination treated cells. (CTCF: corrected total cell fluorescence). 50

2.7 DAPI/PI staining of MCF-7 cells treated with PAX (12.5 nM), CLZ (25 μ M) and PACL (PAX 12.5 nM + CLZ 25 μ M). Cells were observed under fluorescent microscope at 200 X magnification and scale bar corresponds to 50 μ M. Graph characterizes the collective total cell fluorescence ratio for red fluorescence representing PI stained dead cells. * denotes p<0.05, ** denotes p<0.01 and *** denotes p<0.001 when fluorescent intensity was compared with control group. Likewise, ### denotes p<0.001 when evaluated against combination treated cells. (CTCF: corrected total cell fluorescence).. 52

2.8 DAPI/PI staining of MDA-MB 231 treated with PAX (12.5 nM), CLZ (25 μ M) and PACL (PAX 12.5 nM + CLZ 25 μ M). Cells were observed under fluorescent microscope at 200 X magnification and scale bar corresponds to 50 μ M. Graph characterizes the collective total cell fluorescence ratio for red fluorescence representing PI stained dead cells. * denotes p<0.05, ** denotes p<0.01 and *** denotes p<0.001 when fluorescent intensity was compared with control group. Likewise ### denotes p<0.001 when evaluated against combination treated cells. (CTCF: corrected total cell fluorescence). 52

2.9 Percentage of H₂O₂ and NO level as an effect of PAX (12.5 nM), CLZ (25 μ M) and PACL (PAX 12.5 nM + CLZ 25 μ M) on MCF-7 (a and c) and MDA-MB-231 cells (b and d). Bars represents mean \pm SEM (n = 3). * indicates p<0.05, ** indicates p<0.01 and *** indicates p<0.001 when comparison made with control. Likewise, # indicates p<0.05, ## indicates p<0.01 and ### indicates p<0.001 in comparison to combination group for both cell lines (MCF-7 and MDA-MB-231). 54

2.10 Genotoxic effect of PAX (12.5 nM), CLZ (25 μ M) and PACL (PAX 12.5 nM + CLZ 25 μ M) against MCF-7 and MDA-MB-231 cells. Graph represents the relative percentage of DNA in head and tail of MCF-7 (a) and MDA-MB-231(b) cells. *** specifies p<0.001 when % DNA in head was compared with control and ### indicates p<0.001 55

Likewise $\alpha\alpha\alpha$ denotes $p < 0.001$ when % DNA in tail was correlated with control and $\beta\beta\beta$ denoted $p < 0.001$ when % DNA in tail was compared with combination treated cells for both cells (MCF-7 and MDA-MB-231).

- 2.11** Glucose uptake in MCF-7 (a) and MDA-MB-231 (b) as an effect of PAX (12.5 nM), CLZ (25 μ M) and PACL (PAX 12.5 nM + CLZ 25 μ M). Presented bars denote mean \pm SEM (n = 3). ** express $p < 0.01$ and *** express $p < 0.001$ when comparison made with control cells. Similarly, ## directs $p < 0.01$ and ### directs $p < 0.001$ when compared to combination treated cells. 55

Chapter-3

- 3.1** Surface morphological analysis through visualized through scanning electron microscopy for (a) un-conjugated NPs and (b) sialic acid conjugated NPs. (c) particle size distribution of distinct NPs and (d) zeta potential of the formulated NPs. 65
- 3.2** Presenting (a) Fourier-transform infrared spectroscopic graph of formulated NPs, UV (Ultraviolet-Visible) Spectroscopic Graph, (b) UV (Ultraviolet-Visible) Spectroscopic Graph and (c) XRD (X-Ray Diffraction) analysis of conjugated and un-conjugated nanoparticles. 66
- 3.3** In-vitro drug release profile of PAX from (a) un-conjugated-PCL-NPs and (b) SA-conjugated-PCL-NPs at two different pH (6.8 and 7.4 pH). Data expressed as mean \pm standard deviation, n=3. 66
- 3.4** Time dependent cytotoxic effect of different formulation on breast cancer cells (a) MCF-7, (b) MDA-MB-231 and on normal cells (c). *** designates $p < 0.001$, ** designates $p < 0.001$ and * designates $p < 0.01$ when compared with untreated cells respectively. 67
- 3.5** Representative photoluminescence graph showing effect of rhodamine loaded nanoparticles in different cell lines. 69
- 3.6** Fluorescent images representing the cellular uptake of rhodamine loaded nanoparticles in different cell lines. The scale bar of images corresponds to 50 μ M (200X). Graph represents the corrected total cell fluorescence (CTCF) for red fluorescence indicating dead EtBr stained cells. *** indicates $p < 0.001$ when fluorescent intensity compared with HEK-293. 70

Chapter-4

4.1	Predicated v/s actual pot for particles size of formulated NPs	79
4.2	3D-Response surface plots representing effects of variables on particles size, (a) polymer: drug ratio and surfactant concentration, (b) polymer: drug ratio and organic: aqueous ratio, (c) surfactant concentration and organic: aqueous ratio.	80
4.3	Predicated v/s actual pot for % entrapment efficiency of formulated NPs	81
4.4	3D-Response surface plots representing effects of variables on % entrapment efficiency, (a) polymer: drug ratio and surfactant concentration, (b) polymer: drug ratio and organic: aqueous ratio, (c) surfactant concentration and organic: aqueous ratio.	82
4.5	Obtained desirability plot for optimized nano-formulation	84

Chapter-5

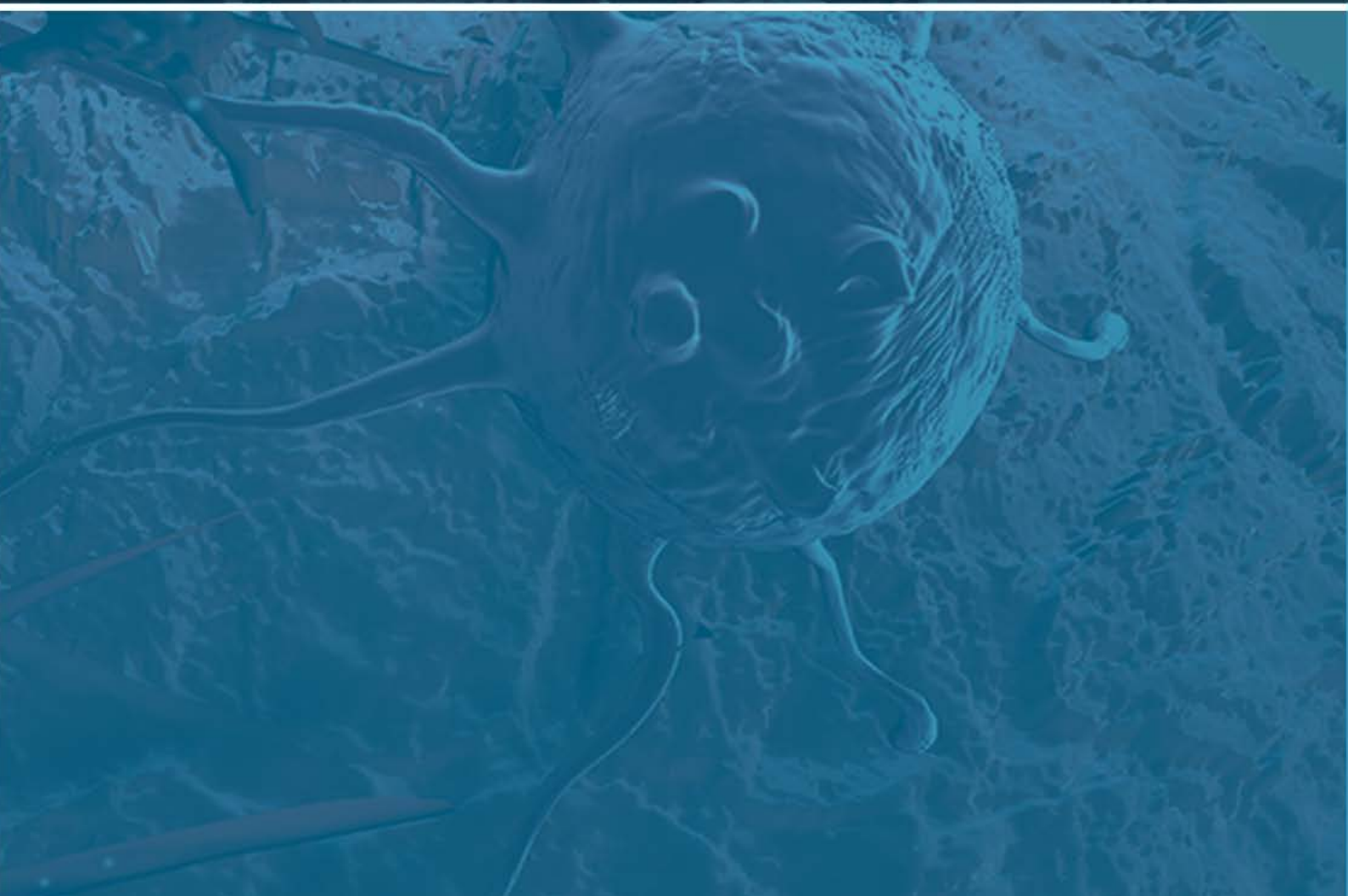
5.1	Optimized concentration of ingredients used for the current synthesis of NPs	90
5.2	Schematic of sialic acid conjugated polymeric nanoparticles by exploiting EDC-NHS conjugation, where inset represents the surface morphology of SA-conjugated-PCL-NPs.	94
5.3	The respective Fourier-transform infrared (FTIR) spectroscopic pattern for a different formulation.	96
5.4	Drug release pattern from the Salic acid formulation (a) PAX and (b) CLZ (See for appendix)	97
5.5	Cytotoxic effect of formulated NPs on (a) MCF-7, (b) MDA-MB-231 and (c) HEK-293 cells. Where * indicates $p < 0.05$, ** indicates $p < 0.01$ and *** indicates $p < 0.001$ when comparison made with PCL-NPs	98
5.6	The scale bar of images corresponds to $50\mu\text{M}$ (200X). The graph represents the corrected total cell fluorescence (CTCF) for red fluorescence indicating dead EtBr stained cells. * indicates $p < 0.05$ and *** indicate $p < 0.001$ when comparison made with HEK-293.	99

LIST OF TABLES

Table No	Title	Page No.
<i>Chapter -1</i>		
1.1	Natural and Synthetic Polymers Used for the Preparation of Nanoparticles	35
<i>Chapter -3</i>		
3.1	Formulation Table	64
<i>Chapter -4</i>		
4.1	Effect of polymer: drug ratio on particle size and % entrapment efficiency	76
4.2	Effect of surfactant concentration on particle size and % entrapment efficiency.	77
4.3	Effect of organic: aqueous Ratio on particle size and % entrapment efficiency	77
4.4	Selected working range of variable of different formulation after conducting preliminary investigation.	78
4.5	Sets of experimental runs suggested by Box-Behnken design and respective particle size analysis and %EE.	78
4.6	Optimized value for the formulation as suggested by desirability plot along with actual obtained values of responses	84
<i>Chapter -5</i>		
5.1	Formulation codes representing amount of ingredients used in different formulations	92



INTRODUCTION



1.1 INTRODUCTION

Cancer is one of the most dreadful disease affecting mankind and is characterized by uncontrolled growth and spreading of cells that may affect almost any tissue of the body [1, 2]. The estimated cancer cases around the world in 2012 had been reported to be 14.1 million as per the world health organization report [3]. Among these, 7.4 million cases accounted for men and 6.7 million for women. This number is projected to rise to a staggering 24 million by the end of 2035 [4]. The rising concern of cancer worldwide draws our immediate attention and has become a prime focus for research in recent decades.

Cancer that progresses from breast tissue is called as breast cancer and it is the most common malignancy among women globally. Breast cancer accounts for 25% of the total number of fresh cases of cancer was diagnosed in 2012 [5, 6]. Like other cancers (skin, lungs, liver, bone, etc), breast cancer is also capable of invading to local regions of the organs, and migrate through lymph nodes, infiltrating into the bloodstream and metastasizing to other distinct organs at advanced stage [7, 8]. Current practice of breast cancer treatment comprises of surgical removal of the cancerous tissue, radiation therapy, hormonal therapy, chemotherapy and poly-chemotherapy [9]. Most commonly and widely employed systemic treatment for breast cancer is chemotherapy, wherein anti-cancerous drugs like, anthracyclines, gemcitabine, alkylating agents, capecitabine, 5-fluorouracil, eribulin, taxane and vinorelbine are administered to the patient [10].

Paclitaxel (PAX) is an anti-cancer chemotherapeutic compound, first isolated from *Pacific yew* in 1971, mostly recommended to treat breast cancer [11]. Major limitation of this compound was its poor aqueous solubility, which further leads to reduced bioavailability. To solve this issue of hydrophobicity, a formulation of paclitaxel was introduced in 1993 with the brand name of Taxol[®], which was approved by World Health Organization's (WHO) and Food and Drug Administration (FDA) in 1994 [12, 13]. This formulation comprises of Cremophore-EL[®], an organic solvent that rectified the hydrophobic associate problem of paclitaxel but was itself a toxic compound [14, 15]. Another new formulation of paclitaxel was introduced with name of Abraxane[®], which was approved by FDA in 2005 [16, 17] and European Medicine Agency in 2008 to treat breast cancer, which is a nano based formulation of albumin conjugated paclitaxel [17]. Nano-delivery systems are advantageous over the conventional drug delivery systems as they enable us with increased solubility, enhanced controlled drug release and by overcoming the side effects of toxic excipients. Here, the Cremophore-EL[®] associated toxic

problems were solved and more over Abraxane[®] was able to target breast cancer through passive targeting, i.e. enhanced permeation and retention (EPR) effect [18].

Because of EPR effect, nano-formulation escapes from the vasculature through leaky endothelium and invades and accumulates into the vicinity of tumor. However, Abraxane[®] suffers from a major drawback of rapid elimination, leading to poor bioavailability of paclitaxel. Further being a costly product, Abraxane[®] limits its use in under developed and developing countries [18, 19].

In this context, surface modified-targeted-nano-delivery systems would be the best alternative resolution, that will not only prolong the blood circulation time of paclitaxel, but also preferentially target the drug to tumor cells [20, 21]. Sialic acid is one such active targeting moiety that has the potential benefit of directing the nanoparticles towards breast cancer cells [22]. Sialic acid is an endogenous electro-negative charged monosaccharide that has demonstrated the efficient capability to improve the blood circulation time of nanoparticulate system and is biocompatible, non-toxic, non-immunogenic and biodegradable. Sialic acid preferentially binds to selectins (E-selectins/P-selectins) which are over expressed on the surface of the breast cancer cells. Thus, surface decorated sialic acid nanoparticles will enable us to direct our nano-delivery system towards breast cancer [22, 23].

Even though, paclitaxel is effective alone, it is prescribed in combination with other chemotherapeutic drugs for better breast cancer treatment. But, an augmented risk of toxicity is always there by combining different anti-cancer drugs, as they come along with their associated adverse-side effects too, like cardiotoxicity due to doxorubicin [24], neurotoxicity and bone marrow suppression due to docetaxel [25], neutropenia due to cyclophosphamide [25]. Likewise, other anticancer agents such as mitoxantrone, cisplatin, 5-fluorouracil, etc also possess non-specific toxic effects. However, this alerts the need of a new nontoxic compound in combination with paclitaxel which enhances its therapeutic efficacy and fundamentally assists the clinical management.

One such drug could be clotrimazole (CLZ), which other than being an antifungal is reported to preferentially inhibit tumor progression while avoiding non-cancerous cells [26]. The underlying mechanism of anti-proliferating effect of CLZ lie within its capability to inhibit 6-phosphofructo-1-kinase (PKF) and hexokinase (HK). PFK and HK are major glycolytic regulatory enzymes that are engaged actively in cancer biology. Another beneficial characteristic of CLZ is its potential to inhibit cell cycle at G-1 and M-phases, that will further aid the effectiveness of paclitaxel [26, 27].

Preferably, nano-delivery systems with cancer targeting capabilities will provide us with a higher therapeutic effect to toxicity ratio. Anti-cancer agents can be targeted towards cancer individually or in combination, encapsulated within biocompatible and biodegradable polymer. Numerous polymeric biomaterials have appeared during the advancement in nanotechnology for drug delivery applications, of which biodegradable polymers have an upper hand by virtue of their biocompatibility and controlled drug release [28, 29].

These approaches would allow the delivery of anti-cancer drugs directly to the desired site without obstructing their chemical rectitude, and thus up surging the availability of drug[29]. Moreover, polymeric nano-delivery system would enable us to encapsulate multiple drugs, which aided with surface modification would facilitate us with several advantages like selectivity, specificity and reduced dose [29, 30]. Such a co-delivery system would afford several advantages like, synergistically enhanced therapeutics, minimal drug resistance and controlled drug release, that would significantly improve the spectrum of cancer therapeutics [31, 32].

1.2 Scope and outline of the thesis

Combination chemotherapy plays an imperative role in the management breast cancer, wherein the different standard anti-cancer agents having different mechanism of action are combine together. Major limitation of chemotherapeutic agent is its associated side effects and combination of these agents would further increase this problem situation. Hence, to address these issues, rationally engineered nano carries systems that could encapsulate desired drug combination and release them in controlled manner would be an ideal approach.

Present thesis describes the novel approach to deliver drug combination at desired site by employing targeted nano-drug delivery system.

Chapter-1 gives the over view of breast cancer, epidemiology of breast cancer, types of breast cancer and available breast cancer treatments. Detailed description of chemotherapeutic drug; Paclitaxel and its associated adversities. Need of combination chemotherapy and potential of Clotrimazole to be used as cytotoxic agent against breast cancer. Overview of different approved drug combination to treat breast cancer. Use of nanotechnology in breast cancer treatment, passive targeting approaches and active targeting approaches followed by advantages of nanotechnology. Types of nano-carries with special emphasis on polymeric nanoparticles. Over view of Sialic acid and Polycaprolactone.

Chapter-2 describes the effect of paclitaxel and clotrimazole combination on breast cancer. Physical mixture of PAX and CLZ was analyzed for any possible chemical interaction through Fourier transform infrared spectroscopy (FTIR). Cytotoxic evaluation of drug combination (at reduced doses of PAX + CLZ) against breast cancer cells. CompuSyn Software showing synergistic action of selected concentration of drug combination. Oxidative and nitrogen stress alterations in breast cancer cells as an effect of drug combination was analyzed followed by investigation of drug combination effect on genotoxicity and glucose uptake studies.

Chapter-3 discusses the method used to fabricate SA surface functionalized NPs by exploiting carbodiimide chemical reaction. Surface morphological investigation (SEM), particle size zeta potential was determined. To confirm the SA functionalization on the surface on polymeric nanoparticles FTIR, UV and XRD analysis were performed. Further the photoluminescence study of SA-rhodamine-loaded NPs to represent cell specificity was performed. *In-vitro* drug release studies were carried out to demonstrate the effect of SA-surface functionalization. Lastly, the comparative cytotoxic studies were performed with drug-loaded-NPs on breast cancer cells and normal epithelial cells.

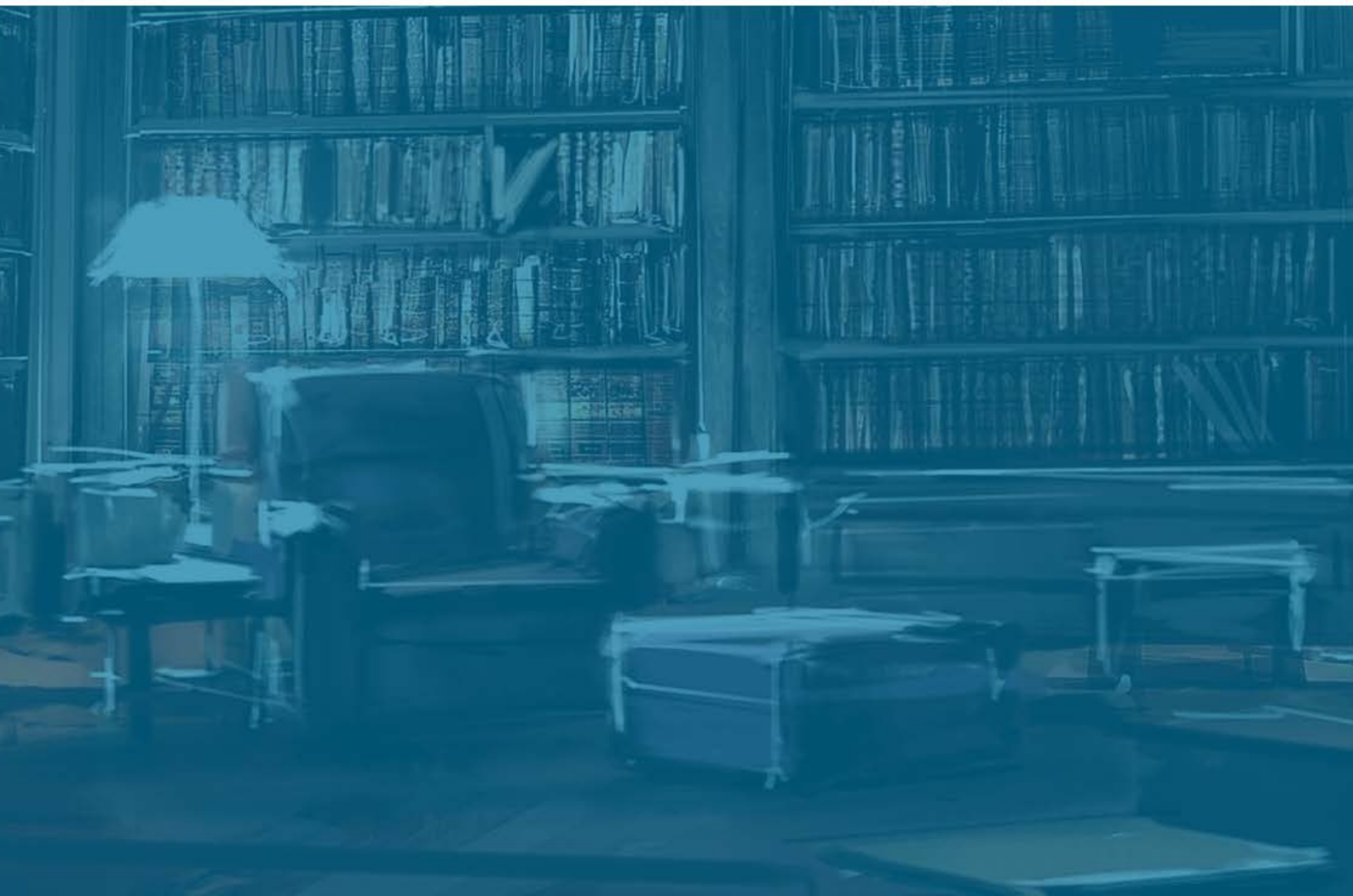
Chapter-4 deal with the optimization of different variable that are responsible for the success and failure of nano-delivery system. Independent variables were optimized through Response Surface Methodology (RSM). This chapter also discusses the Box Behnken design (BBD) generated 3D surface plot was analyzed to study the effect of variable on Particle Size and % Entrapment Efficiency of NPs. Desirability plot was also examined using Design Expert software.

Lastly, Chapter-5 elaborates the fabrication of NPs using optimized variable concentration followed by characterization of fabricated -NPs. *In-vitro* drug release studies of encapsulated dual drug (PAX+CLZ) were performed at two different pH (6.8 and 7.4 pH). AO/EtBr live dead staining was further performed to represent the effect of formulated nanoparticles. Further this chapter describes the cell specific uptake studies of formulated NPs.



CHAPTER-1

REVIEW OF LITERATURE



1.1 Breast cancer

Breast cancer is disease condition where the cells of breast tissue changes their normal cellular functioning (or mutate) and continuously proliferate by avoiding apoptosis (programmed cell death). Abnormally growing cells generally assemble themselves in cluster to form tumor. Tumor recognized as malignant (or cancerous), when the abnormal cells invade to other regions of breast. Likewise, when cancerous cells spread form the breast to other part of body through lymphatic system or through bloodstream is known as metastatic breast cancer [33, 34].

1.2 Epidemiology of Breast cancer

1.2.1 Worldwide Scenario:

Globally breast cancer is the second most common cancer accounting for 25% of the cases amongst all other forms of cancer (Figure.1.1). It is also the most frequently diagnosed cancer in women with estimated cases of 1.67 million in 2012 [35]. Report suggests that under developed nations had more number of breast cancer cases (8,83,000) than developed nations (7,94,000) as estimated in 2012. In context of mortality, breast cancer is the 5th most lethal among all cancers accounting for 5,22,000 deaths annually. However, in women, breast cancer is most lethal cancer in under developed regions accounting for 324,000 deaths i.e. 14.3% of total cancer mortality, whereas, second leading cause of mortality in developed accounting for 198,000 deaths i.e. 15.4% of total cancer mortality [2, 3, 6] .

Because of advancements in breast cancer management, the mortality rate has significantly declined in develop nations with 6 deaths per 100,000 cases in eastern Asia, as compared to that of 20 in 100, 000 in under developed regions like western Africa.

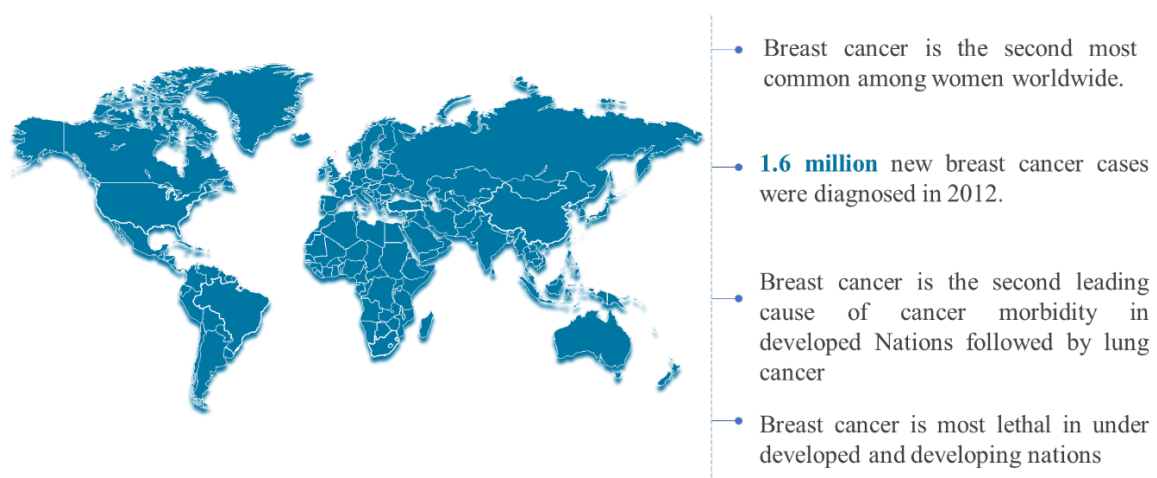


Figure 1.1 Breast cancer incidence World wide

Similarly, high economic-communities, like America (North) and Europe (Western), have witnessed considerable reduction in breast cancer mortality whereas persistent efforts are required in developing and under developed nations to overcome this hurdle [34, 35].

1.2.2 India

In India, breast cancer has surpassed the cervical cancer and has become a leading cause of cancer morbidity and mortality in Indian women (Figure 1.2). Likewise, 32 % of cancer cases are of breast cancer in India, wherein 1.28 lakh new breast cancer cases were estimated in 2012 and the incidence of breast cancer is projected to go up to 1.9 lakh by 2020. As per the Globocan-2012 report, there is an increase in the incidence of breast cancer by 11.54% from 2008-2012, in India. Whereas 13.82% rise was witnessed in mortality rate due to breast cancer during the same time period. The upsurge in morbidity is attributive to inaccessibility of breast cancer screening facilities, lack of awareness among women, diagnosis of ailment at more advanced or even at last stages and inappropriate medical amenities [36-38].

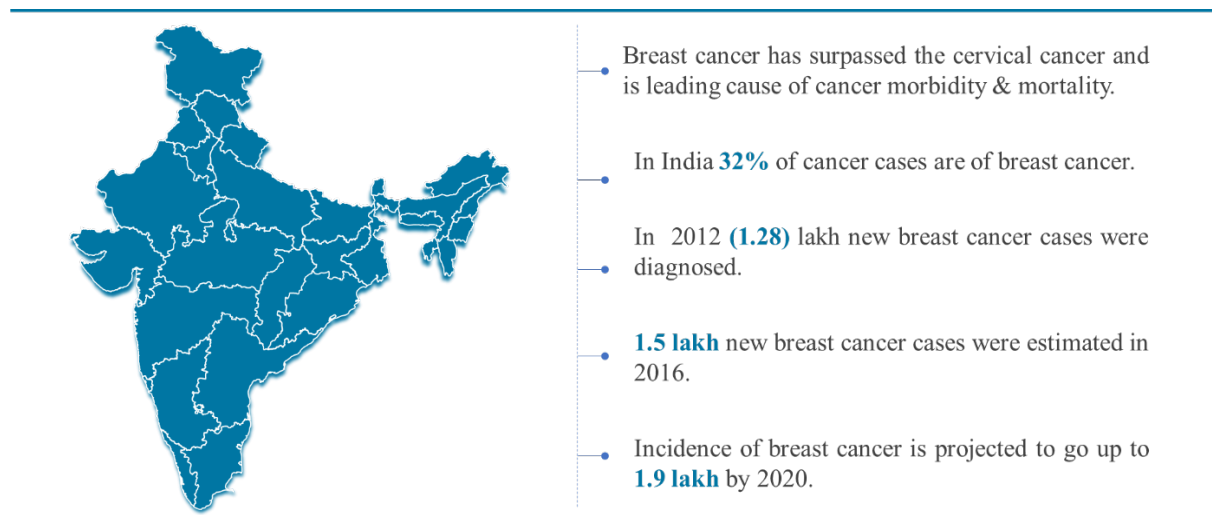


Figure 1.2 Breast cancer incidence in India

1.3 Types of Breast Cancer

Breast cancer can initiate for any part of the breast, like ducts, lobules and in rare cases in-between the breast tissue (Figure 1.3). Based on the invasiveness of breast cancer, it can be classified as: non-invasive and invasive carcinoma [39].

1.3.1 Ductal Carcinoma In-Situ (DCIS)

This is non-invasive type of breast cancer where abnormal cells start proliferating inside the milk ducts but, only confined to the local region of duct and don't affect the normal surrounding tissues. DCIS do not possess life threatening conditions but if not taken into consideration on time will eventually increases the menace of invasive breast cancer in near future. Even though

after successful treatment of DCIS, there is always a higher possibility of getting breast cancer later on and this phenomenon is also called as breast cancer recurrence. The chances of recurrence are upto 30% and the symptoms can be visible within 5 to 10 years after initial treatment. Over a period of time the incidence of DCIS has increased significantly and possible reasons behind this is that, women are more aware about their health and getting mammography that increases the possibility of early detection.

1.3.2 Lobular Carcinoma In-Situ (LCIS)

Non-invasive form of cancer where abnormal cell grows inside the breast lobules without invading the surrounding areas. Women diagnosed with LCIS are likely to have invasive breast cancer in future. LCIS is most-often diagnosed before menopause, generally between the ages of 40s-50s.

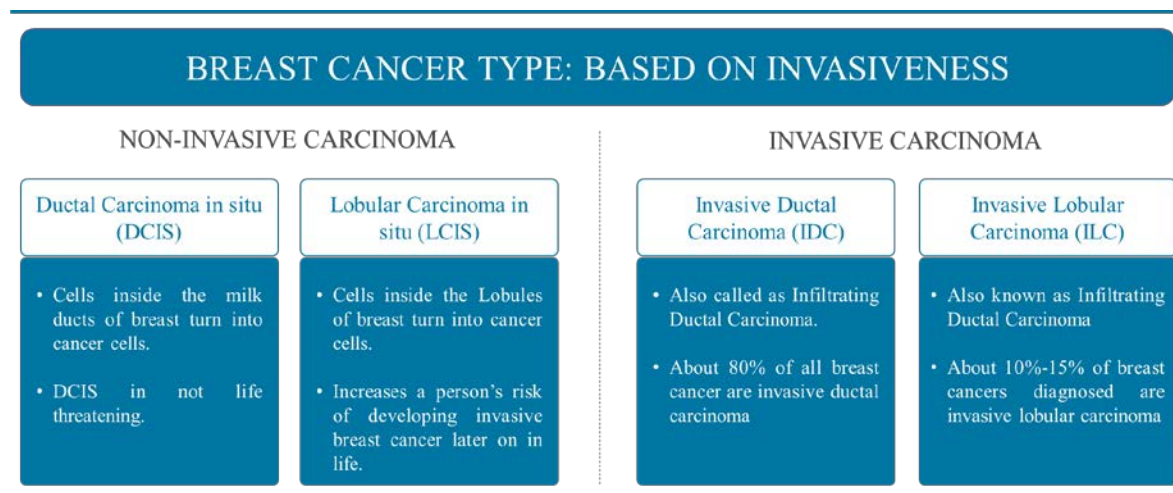


Figure 1.3 Type of Breast cancer based on Invasiveness

1.3.3 Invasive Ductal carcinoma (IDC)

IDC is most common type of breast cancer and is also recognized as infiltrating ductal carcinoma. Around 80% cases of breast cancer diagnosed are of IDC. It is the condition where cancer cells migrate from the cellular wall of milk duct and invade to the surrounding area of the breast. If not monitored-on time, IDC has the potential to spread into the lymph nodes and from there it may advance to the other distinct part of the body. IDC is more frequent in older women and in rare cases it affects men too.

1.3.4 Invasive Lobular carcinoma (ILC)

Invasive lobular carcinoma is the second most common form of breast cancer and also acknowledged as infiltrating lobular carcinoma. Around 10 % of breast cancer are of ILC type.

It is situation where abnormal cells migrate from the lobules of the breast to the surrounding tissue inside the breast. Over time ILC may proliferate further that holds the capacity to spread to the lymphatic system of the body and possibly infiltrate to other parts of the body.

1.4 Breast cancer classification: based Molecular subtype

More suitable approach to identify or classify breast cancer on a routine basis is based on the evaluation of biological markers that are majorly responsible for it. These include absence or presence of hormone mainly progesterone or estrogen receptors (HR+/HR-) and level of growth promoting protein primarily human epidermal growth factor receptors-2 (HER2+/HER2-) [40, 41].

There are primarily four main intrinsic molecular subtypes as described below (Figure 1.4):

1.4.1 Luminal-A subtype: Type of breast cancer which possess progesterone receptors (PR+) and estrogen receptors (ER+) but there is an absence of HER2 (HER2-) and Ki-67 protein (indicator of the aggressively multiplying cells). These carcinomas tend to proliferate slowly and are less aggressive in contrast to other molecular subtypes of breast cancer. 74% of cases in women diagnosed with breast cancer are of Luminal- A subtype and have the most promising prognosis [41].

MOLECULAR SUBTYPE OF BREAST CANCER				
Type	ER	PR	HER2	Occurrence Rate
Luminal A	+	+	-	74 %
Luminal B	+	+	+	12%
HER2 Positive	-	-	+	10%
Triple negative	-	-	-	4%

ER: Estrogen Receptor
 PR: Progesterone Receptor
 HER2: Human Epidermal growth factor Receptor 2

Figure 1.4 Overview of molecular subtype of breast cancer

1.4.2 Luminal-B subtype: Type of breast cancer that express ER+, PR+, HER2+ and further defined by the high levels of Ki-67 protein. Around 10 % of breast cancer diagnosed in women are Luminal- B subtype of cancer and is more aggressive form of cancer in comparison to Luminal-A subtype [41].

1.4.3 Triple negative subtype: This type of breast cancer is also recognized as basal-like subtype and around 12% of breast cancer in women are triple negative as because they are hormone receptor negative (ER-, PR-) and HER2 negative. This type of cancer is more common in black women than in white women and those with BRCA-1 gene mutations. This type of cancers has poor short-term prognosis in contrast to other subtype of breast cancer as because, till date there is not any specific targeted therapy available of this type of breast cancer.

1.4.4 HER2-enriched subtype: Near about 4% of breast cancer are HER2-enriched subtype, where hormone receptors are negative but HER2 positive. These types of cancers have the tendency to proliferate at very high frequency and are more aggressive in comparison to another subtype of breast cancer. However, with an advancement in targeted drug approach, now its little convenient to treat HER2 subtype of breast cancer [41].

1.5 Other Rare Breast Cancers

1.5.1 Tubular carcinoma in Breast: This is the invasive form of breast cancer that originates from the breast's milk duct and invades into the surrounding tissue. Tubular carcinomas are typically small in size (around 1cm or less) that appears like tubular structure. These types of carcinomas are less aggressive and do responds to cancer treatment. Reports suggests that tubular carcinoma is generally diagnosed in women at early 50s [42].

1.5.2 Medullary carcinoma in Breast: It is a rare subtype of invasive ductal carcinoma that account approximately 3-5 % of breast cancer. Shape and appearance of this tumor resemble the medulla in brain, therefore recognized medullary breast carcinoma. Medullary carcinoma most commonly found in the women with BRCA-1 mutation, diagnosed at any age, but women those are at their late 40s and early 50s are at higher risk. This carcinoma is slow growing that does not proliferate outside the breast to lymphatic system, hence easy to treat in comparison to other breast cancer [42].

1.5.3 Mucinous carcinoma in Breast: It is also acknowledged as colloid carcinoma and is a form of invasive ductal carcinoma which is very rare. Mucinous carcinoma can be diagnosed any age of women, but it affects the women after menopause and on an average woman at late 60s and early 70s. This type of cancer can be treated well as it is not aggressive in nature and has not evaded to other parts of the breast [42].

1.5.4 Papillary carcinoma in Breast: It is the rare form of invasive carcinoma that account for less than 1- 2% of total breast cancer incidences. It has a small finger like projections with

clear border line of the abnormal cells and have fast growing capabilities. This type of cancer is generally found in older women [42].

1.5.5 Cribriform carcinoma in Breast: This is the rare and unusual form of breast cancer, wherein the abnormal cells invade into the breast connective tissue called as stroma. Nest like formation appears in between the duct and the lobules of the breast and it is not easy to identify as because cells exhibit normal breast cell morphology [42].

1.5.6 Paget's Disease of the Nipple: Rare form of breast carcinoma where abnormal cells get accumulated around or inside the nipple. This type of cancer initially affects the ductal region of the nipple and then proliferate to the surface of nipple and the areolar region of the breast causing itchiness and inflammation [42].

1.5.7 Phyllodes tumors in Breast: Rare type of breast cancer that accounts only or less than 1% of overall incidences of breast cancer. Phyllodes is a Greek terminology for leaf like structure, herein tumors cells proliferation resembles the structure of leaf. This type of carcinoma has the tendency to grow fast and rarely invades to other part of the breast [42].

1.5.8 Male breast cancer: Breast cancer in male is a rare form of epidemic disorder. Very few cases have been reported or available for research. High estrogen level is mainly responsible for this type of cancer and having a strong family history of genetic mutation in BRCA-1 and BRCA-2 genes [43].

1.6 Metastatic breast cancer

Metastatic breast cancer also recognized as fourth stage cancer, where the cells separate themselves from the site of origin (breast) and invades to other parts of the body, most frequently to bones, brain, liver or lungs. This stage is also known as "De-novo-metastatic" breast cancer. Lymphatic system and bloodstream confer the outbreak of cancer cells to other organs. Approximately 30% breast cancer cases enter the metastatic stage. Metastatic breast cancer is an overwhelming situation when diagnosed, but under proper medical supervision and treatment, this condition can be improved considerably [44].

1.7 Breast cancer treatment

Treatment choices for breast cancer can be put together by the patient and the medical specialist after thoroughly discussing the stage and other biological features of the breast cancer. Point that should be taken into consideration before starting treatments are; age preferences of the patient, overall risk analysis during the treatment, associated drawback and benefits, last but

not least long-term side effects. The available standards treatment options for breast cancer may be sub-divided: local treatment and systemic treatment as represented in Figure 1.5 [45].

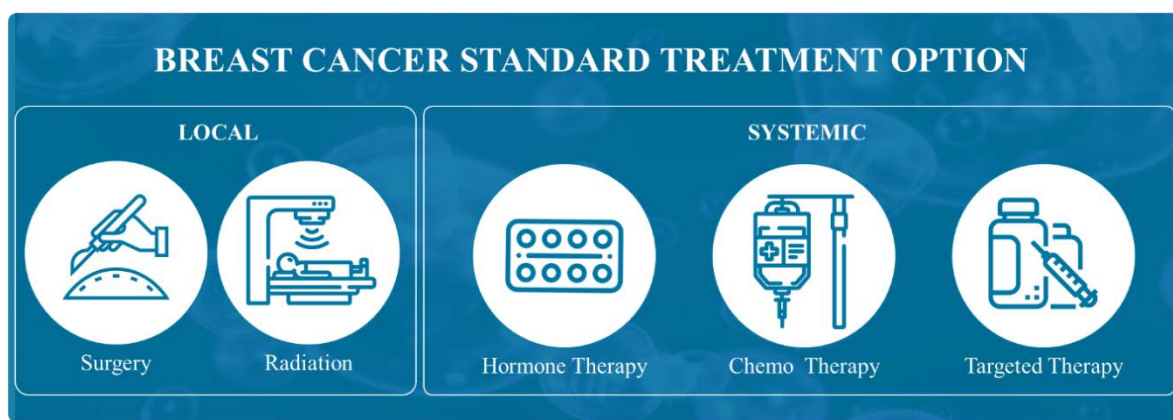


Figure 1.5 Schematic representation of the available options for the breast cancer treatment.

1.7.1 Localized

Treatment that specifically targets the desired organ (tumor tissue) with minimal effect on other organs of the body: Local treatment for breast carcinoma comprises of the following strategies:

1.7.1.1 Surgery

First line attack against breast cancer is surgical removal of the organ and is recommended for those patients having tumor size up to or less than 4 cm.

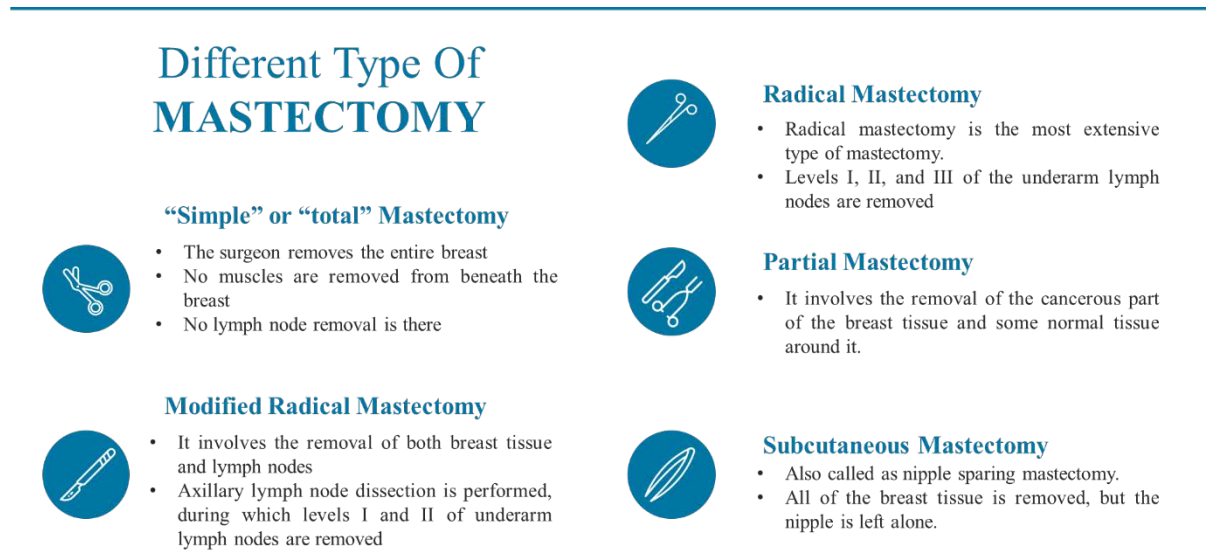


Figure 1.6 Schematic representation of various types of Mastectomy available for breast cancer treatment.

Main aim of the breast cancer surgery is to eradicate the tumor from the local region of breast. Lumpectomy also recognized as breast conserving surgery that involve the removal of tumor along with the rim of surrounding normal tissues. Mastectomy is more refined surgical method to confiscate tumor as because the supporting muscles under the breast are not removed. There are five different type of mastectomy as described in the Figure 1.6. Surgical treatment of breast cancer are generally followed by radiotherapy or chemotherapy [45].

1.7.1.2 Radiation therapy

Radiation therapy is local targeted treatment, intended to eradicate residual tumor cells that might be left after surgical removal of breast cancer (Figure 1.7). This therapy is painless treatment of breast cancer but exposure to radiation itself may lead to discomfort over the time. Five days per week is usually the treatment duration that may extend up to 7 weeks [46].

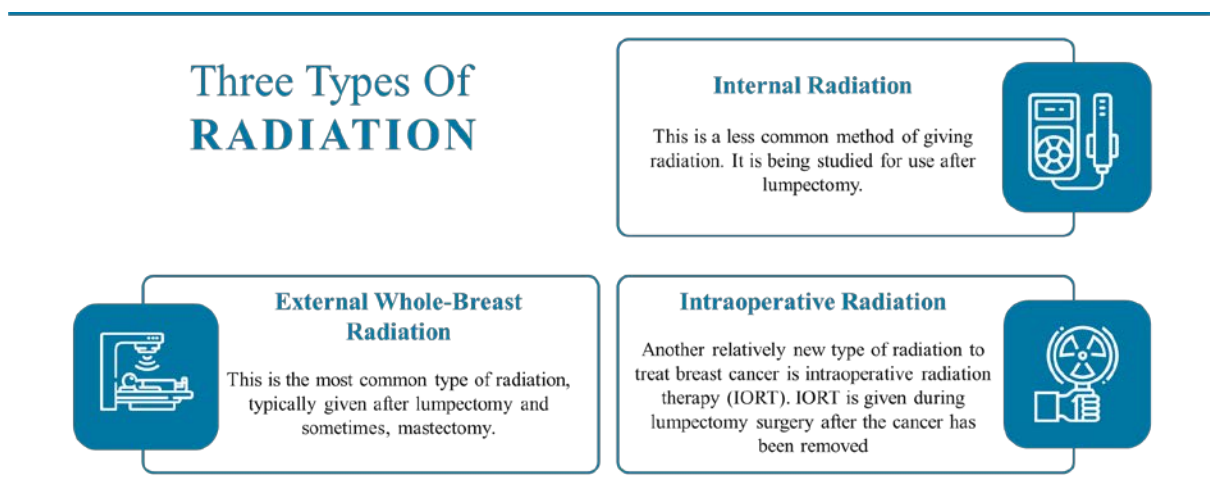


Figure 1.7 Schematic representation of different types of radiation therapy available for breast cancer.

To dealt with the more aggressive breast cancer radiation therapy is give two time a day upto 1 week of the initial therapy. Most of the associated side effects are temporary that usually subsides after discontinuation of radiation therapy. There will be no loss hair through this treatment until or unless radiations applied to head region. Local area receiving radiation may get inflammation or may get tan, for that dermatological treatments are available. Radiation therapy significantly reduces the risk of breast cancer returning [46].

1.7.2 Systemic treatment

Systemic therapy includes the administration of anti-cancer drug either through oral cavity in the form of tablet and capsule or injected directly into the blood stream. Here, the drug treatment will not be restricted to one region, rather it will be distributed to every organ of the

patient and affects all part of the body. Different type of systemic treatment that given before and after surgical removal of the breast cancer are described in the Figure 1.8:

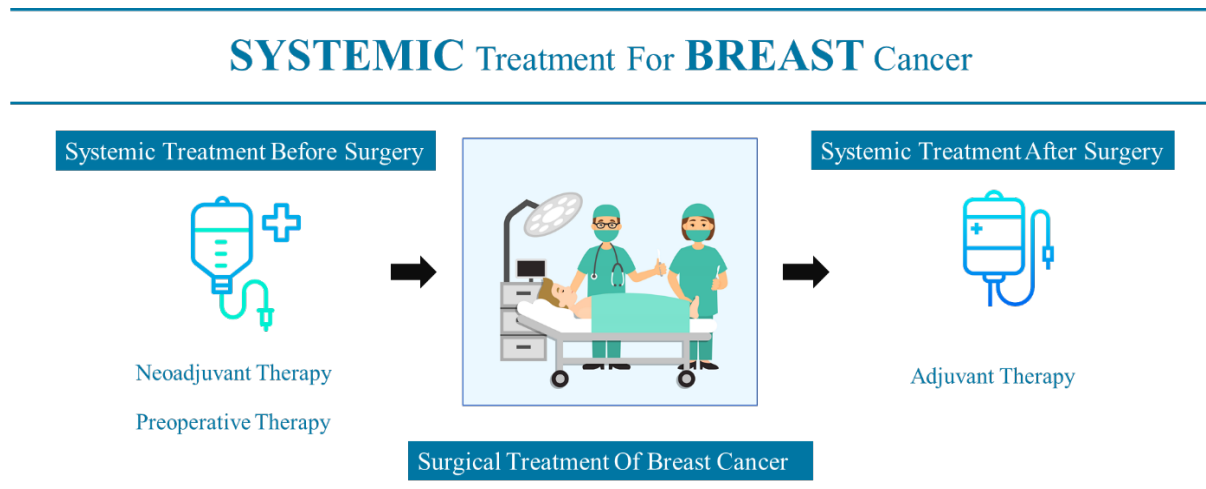


Figure 1.8 Schematic presentation of systemic treatment given before and after surgery.

Systemic treatment for breast cancer mainly includes chemotherapy, hormonal therapy and targeted therapy [47]:

1.7.2.1 Chemotherapy

It is usually given through intravenous injection or administered through oral cavity. Chemotherapy treatment includes anti-cancer agents that abolish the cancer cells in the body, comprising the cells at site of origin (breast tissues) and other cancer cells that may have migrated to other part of the body. In many incidences, combination of two or more chemotherapeutic drugs are administered to treat breast cancer. Selection of proper chemotherapeutic treatment is depended on numerous factors, like size and area of the tumor, involvement of the lymphatic system, level of hormone receptor mainly estrogen and progesterone receptor [48].

1.7.2.2 Hormone therapy

Hormonal therapy is also recognized as endocrine therapy and primarily aimed to eradicate the hormonal influence in cancer progression. This type of treatment is effective against hormone receptor positive breast cancer that works through two mechanisms [49]:

1. By decreasing the level of estrogen in the patient body.
2. By restricting the estrogen action leading to breast cancer cells proliferation.

Hormonal therapy is also beneficial to reduce the size of tumor and slow down the proliferation rate of metastatic hormone receptor positive breast cancer [49]. There are different types of hormonal therapeutic drugs available to deal with increasing risk of breast cancer like;

- **Aromatase inhibitor (AI):** block the over production or stops the biological synthesis of estrogen in postmenopausal women. (Anastrozole, Exemestane, Letrozole)
- **Selective estrogen receptor modulator (SERMs):** Restricts the action of estrogen receptors in breast cancer. (Raloxifene, Tamoxifen, Toremifene)
- **Estrogen receptor down-regulator (ERDs):** Stops the effect of estrogen in breast tissue by decreasing the estrogen receptor number. (Fulvestrant)

1.7.2.3 Targeted therapy

Targeted therapy also acknowledged as molecular targeted therapy and is one of the major modalities of medical treatment for breast cancer (Figure 1.9). This treatment specifically targets the important biological characteristics of the breast cancer. Most frequently applied to target HER2 and vascular endothelial growth factor (VEGF) protein that play a vivacious role in cancer development and generate resistance against anti-cancer drugs. Targeted cancer therapies are anticipated to be more accurate than conventional treatments of breast cancer and are less destructive to healthy cells. Some of the frequently used therapeutic strategies are targeting HER2 and VEGF protein that play a vital role in cancer progression and generating resistance against chemotherapy [50].

1.8 Chemotherapy: mainstay for breast cancer treatment

Chemotherapy or Chemo is a procedure where we deal with the problem of cancer by using tumor killing drugs that may be given intravenously or by mouth. Chemotherapeutic medicines are employed to stop cancer proliferation and to prevent migration of cell to other part of body. Chemotherapy is either administered intravenously or through oral route [51].

Chemotherapy given to patient before surgery is also acknowledged as neoadjuvant chemotherapy. This practice is generally performed to reduce the extensive efforts required during surgical removal of breast cancer and simultaneously it reduces the size of the tumor too. By giving neoadjuvant chemotherapy, doctor monitors the response of tumor to the administered anti-cancer drug and ensure its use or suggest other chemotherapeutic medicine [51].

TARGETED Therapies For Breast Cancer Treatment



Figure 1.9 Different types of targeted therapeutic agents employed to treat breast cancer.

Chemotherapy administered to the patient after surgical removal of breast cancer is also recognized as adjuvant chemotherapy. This strategy is generally employed to execute cancerous cells which might have been left behind. If the trailing cancer cells are not checked, they might lead to formation of new tumor cells colony either in same organ (Breast) or in other part of the body. Adjuvant chemotherapy ensures less chances of breast cancer reoccurrence in near future [52].

1.9 Chemotherapy for more aggressive and advanced breast cancer

Advanced breast cancer is the stage where tumor cells are not confined to one place, but in spite they start spreading from the site of origin (Breast) to other distinct part of the body. To treat these type of cancers, different categories of cytotoxic drugs are usually prescribed either alone or in combination [52]. Chemotherapeutics drugs that are administered in breast cancer has been listed in Figure 1.10.

CHEMOTHERAPY For Breast Cancer

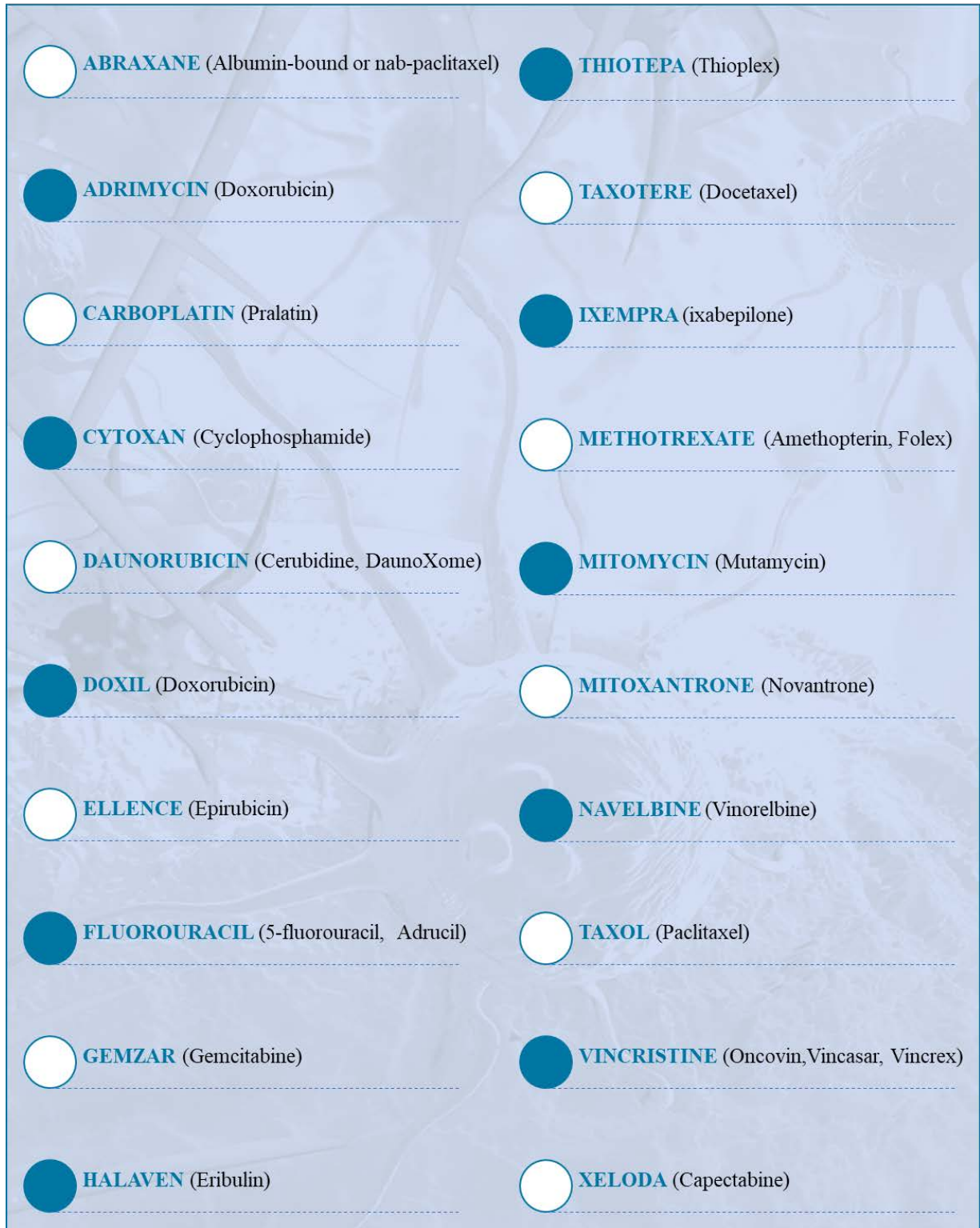


Figure 1.10 Different types chemotherapeutic agents employed to treat breast cancer.

1.10 Taxanes

Taxanes are diterpenoid which are biologically synthesized in plant of the genus *Taxus* possessing chemotherapeutic potential[53]. Taxane family comprises of docetaxel (brand name: Taxotere) and paclitaxel, having brand name Taxol. Paclitaxel is a naturally occurring alkaloid also known anti-microtubule agent that possess profound antitumor activity[54]. Discovered late in 1967s in U.S. National Cancer Institute where Monroe E. Wall and Mansukh C. Wani extracted it from the bark of the pacific yew tree, *taxus brevifolia* (Taxol). Bristol-Myers Squibb an American based pharmaceutical industry sold paclitaxel under the trademark of Taxol® [54]. Abraxis BioScience a global pharmaceutical industry having its headquarters in Los Angeles, United States of America, has developed the nano delivery system of paclitaxel bounded to albumin with name of Abraxane® (Got U.S. Food and Drug Administration approval in 2005)[55]. Paclitaxel is widely prescribed to treat patients with ovarian, breast, lungs, head and neck cancer [56]. Chemical structure of Paclitaxel and its physiochemical properties are represented in Figure 1.11.

1.11 Paclitaxel and its mechanism of action

Paclitaxel is potent anti-cancer medicine that interferes with the standard functioning of microtubule growth by stabilizing the structure and protecting the disassembly of microtubules. Microtubules are made up of small building block known as tubulin, paclitaxel specifically bind to β -subunit of the tubulin building block. By the virtue of which, paclitaxel-microtubule multifaceted structure lost the ability to disassemble, there by disrupting the normal cell division, that further halt cell progression [57].

1.11.1 Associated side of Paclitaxel

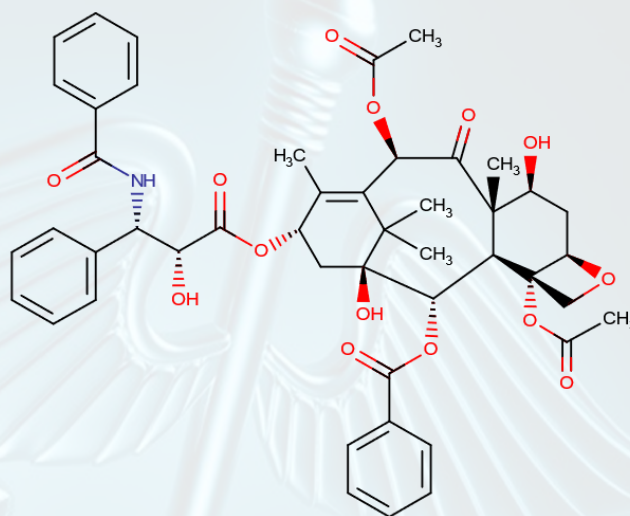
Exploitation of paclitaxel as an anti-cancer agent has articulated commendable success rate as single chemotherapeutic agent. Administration of paclitaxel to patients had witnessed some serious and minor associated adverse effects [57, 58].

Some of the commonly reported side effects are reported as below:

- Reduction in white blood cell count, that further increases the risk towards general infection.
- Loss of hairs (mostly head region is affected)
- Difficulty is breathing as the red blood cells count also decline partially.
- Reduced physical activity and alertness.

Drug Profile of PACLITAXEL

Chemical Structure



IUPAC Name:

5 β ,20-Epoxy-1,2 α ,4,7 β ,10 β ,13 α -hexahydroxytax-11-en-9-one
4,10-diacetate 2-benzoate 13-ester with (2R,3S)-N-benzoyl-3-phenylisoserine

CAS Number

33069-62-4

Molecular Formula

C₄₇H₅₁NO₁₄

Molecular Weight

853 Da

Description

Paclitaxel is crystalline powder with white to off white crystals.

Solubility

Practically insoluble in water, soluble in methanol and freely soluble in methylene chloride

Partition Coefficient

3.62

Melting Point

216-217 °C

Storage

Store the drug between 20-25 °C in light resistant container.

Figure 1.11 Brief description of Paclitaxel

- Persistent pain in joints and muscles.
- Tingling sensation in hands and feet followed by numbness
- Blood pressure decline during the chemotherapy
- Soreness in mouth
- Patient reported mild diarrhea
- Feeling of vomiting

Some of the above-mentioned side-effects get reduces after the completion of therapy.

1.12 Chemotherapy combination

Presently, various chemotherapeutic medicines are prescribed to treat tumor progression and their selection is made on the bases of specific pathway which they follow to kill cancer cells. However, frequent administration of single therapeutic agent to patient may develop resistance towards its mode of action. Which may further restrict the accessibility of single chemotherapeutic agent and in that case higher dose is required, resulting in associated side-effects and non-specific killing of normal cells. In recent years combination of two or more than two chemotherapeutic compounds have been employed to rectify the associated problem of conventional single therapeutic agent. Combination therapy to treat breast cancer can be strategically implicated by co-delivering two or more than two chemotherapeutic compounds concurrently or in combination hormone therapy, immunotherapy and radiotherapy [31, 59]. With the combinations of two or more chemotherapeutic drugs at low doses, the associated side-effects of single chemotherapeutic agent can be minimized. Furthermore, synergistic effect can be seen, as different drugs act though separate mode of action [60].

1.12.1 Advantages of combinational strategies in cancer therapy

In-order to enhance the therapeutic efficacy of the chemotherapy it is important to establish an alternative approach that could provide a resolution to the problem involved with single chemotherapeutic drug. To address this concern, combination approach could be the solution for better treatment and to downturn the associated side effects of anti-cancer drug [61].

Combination therapy is well known to combat the limitation of the single drug treatment as:

1. It can modulate different signaling pathways.
2. It can overcome the toxicity and simultaneously augment the therapeutic efficacy of the chemotherapeutic agents
3. It can overcome the mechanism of drug resistance related to cancer treatment.

In recent years the application of combination therapy has been well used for the cancer treatment and its advantages applied to cancer therapy are illustrated below.

- Combination therapy enable us to exploit the primary potential benefit of synergism. When combination therapy is used the overall therapeutic effect of the drugs in combination found to be greater than the sum of the effect represented by the individual drug treatment. These benefits have driven drug discovery efforts toward the exploration of new combination therapeutics. Combination index isobologram analysis is used to denote the synergism of combinational effects of any chemotherapeutic agents with its maximum efficacy against cancer and minimum side effects towards normal cells. For instance, when celecoxib which is a cyclooxygenase-2 inhibitor combined with emodin exhibited the synergistic against cholangiocarcinoma by which caspase-3 and caspase 9 get activated. Likewise, gemcitabine/ paclitaxel in combination with mTOR inhibitor (RAD001) displayed synergistic activity against non-Hodgskin lymphoma cells [31, 60].
- The main reason for the failure of chemotherapeutic drug treatment is the capability of cancer cells to develop the resistance against single drug treatment. Over the period of time, different well-known mechanisms are there that contribute to MDR in cancer cells, of which the multi drug efflux pump is one. The major drug efflux pumps over expressed in human cancer are; multidrug resistance protein-1 (MRP-1), membrane P-glycoprotein (P-gp) and breast cancer resistance protein (BCRP), mainly responsible for the out flow of chemotherapeutic drugs from the tumor vicinity. In this regard, co-treatment with modulator inhibitor like P-gp inhibitors might be an important insinuation that can hinder with the MDR proteins overexpressed in cancer cells and there by reverse the MDR effect. In recent report, when third generation P-gp inhibitors like tariquidar and elacridar administered along with paclitaxel, significant rise in the concentration of paclitaxel was observed in the brain of nude mice. Results were the attributive effect of elacridar and tariquidar as they instigated downregulation of P-gp expressed on the surface of blood brain barrier. In another case, when zosuquidar co-administered with daunorubicin and cytarabine, boost in the anti-cancer effect was witnessed in the patient suffering from myeloid leukemia [61, 62].
- Recently, when gemcitabine and carboplatin were administered in combination to treat patient with metastatic ovarian cancer, anticancer activity of the combination was found significantly high. In another report, co-delivery of curcumin with paclitaxel synergistically increases the cytotoxic activity against Hela cells. This combination not only exhibited

improved anti-cancer effect but also reduces the paclitaxel dose, that further diminishes the risk of getting associated side effects of paclitaxel [63, 64].

1.13 Commonly employed combination therapy for cancer treatment

1.13.1 Radiotherapy along with chemotherapy

Currently, this strategy is one among the foremost promising treatment available for breast cancer. This strategy is well known to boost the life span of patient after breast cancer treatment when compared to radiation therapy alone. In early nineteen seventies, patients suffering from rectal cancer had exhibited profound cytotoxic effects when radiotherapy was given along with 5-fluorouracil and mitomycin-C. Likewise, combination of topotecan (chemotherapeutic drug) and radiation therapy exhibited the synergistic effects against glioblastoma multiforme and simultaneously improve the life expectancy of patient after treatment (reveled through clinical studies). Similarly, in Phase-II clinical trials, when prostate cancer patients were exposed to radiotherapy followed by precise-antigen targeted vaccine, tumor cells become more sensitive for vaccine [65].

1.13.2 Chemotherapy along with hormone therapy

Hormone therapy plays a crucial role in breast cancer treatment, aimed to down-regulate or block hormone receptors (estrogen and progesterone receptor). Estrogen is biosynthesized with help of an enzyme know as aromatase. When the normal functioning of this enzyme is disrupted there will be less or no production of estrogen, therefor facilitate breast cancer management. Likewise, by employing selective hormone receptor inhibitor such as tamoxifen, estrogen will not bind to its respective receptor and this may assist chemotherapeutic drug treatment [66].

1.13.3 Immunotherapy with chemotherapy

Cancer immunotherapy triggers the immune system of the patient to work more efficiently against progressing breast cancer. this helps in breast cancer management by; inhibiting the cancer proliferation, stop tumor cells from migrating or invading to other part of the body and by attacking the cancer cells. Combining chemotherapy with immunotherapy enable us to achieve profound cytotoxic activity [67].

1.13.4 Combination of multiple chemotherapeutic agents

Among the various treatments available for breast cancer, combination of different anti-cancer agents are well practiced and is current trend of research (Figure 1.12). Combination of distinct anti-cancer drugs were first employed in late nineteen forties against Hodgkin's disease and childhood leukemia. Studies has shown that, by combining methotrexate with mitomycin has

increased the anti-cancer activity of taxane significantly against breast cancer. Another study also supported this idea, where 5-fluorouracil and leucovorin were used in combination to treat colon cancer. Paclitaxel combination with carboplatin has also demonstrated the increase in cytotoxicity against lung carcinoma [68].

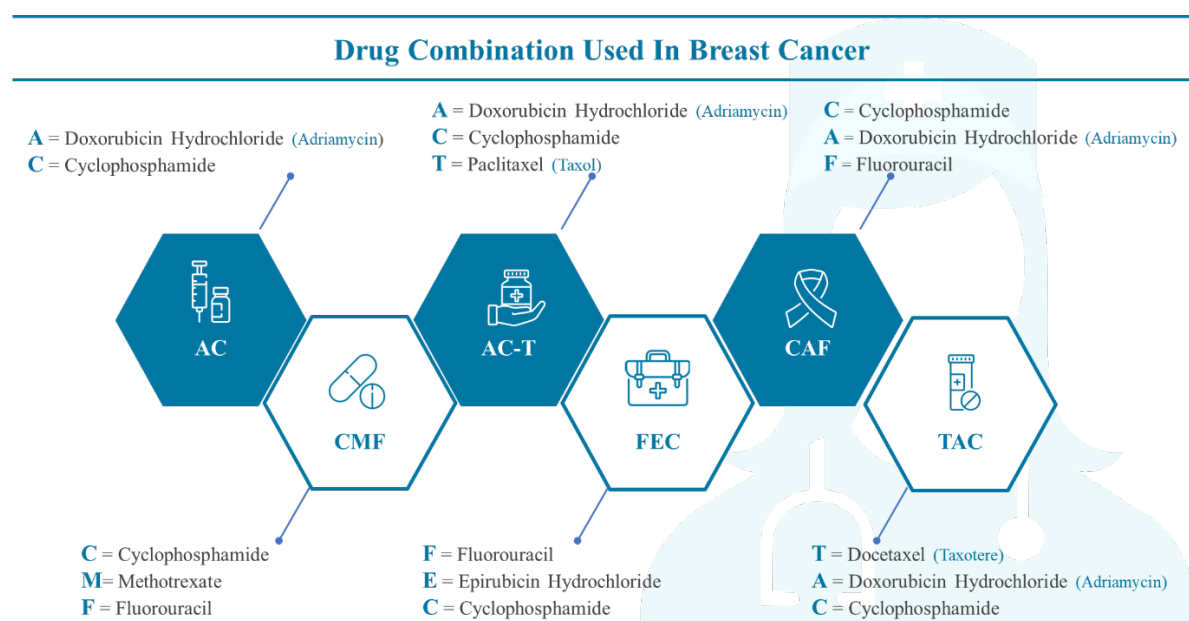


Figure 1.12 Different types of drug combination used for breast cancer treatment

1.14 Clotrimazole

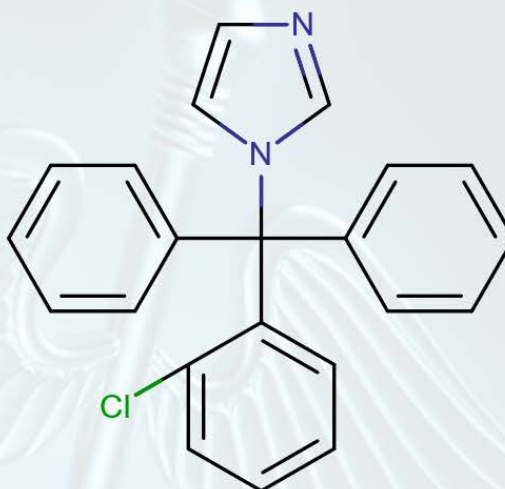
Clotrimazole belongs to azole derivative family, was synthesized in late 1960s by Karl Hienz Buchel (Bayer) and patented in 1972. Clotrimazole was first introduced in 1973 in German market with the brand name of Canesten. It is a broad spectrum anti-fungal compound that possess a unique potential to inhibit ergosterol, this is an integral component of the fungal cell membrane. Inhibition of ergosterol results in the disruption of enzyme system bound to fungal membrane and leads to loss of membrane integrity due to increased permeability, that eventually causes cell lysis. Brief description is given in Figure 1.13.

1.14.1 Mechanism of Action Against Tumor

There is always an increased energy demand in progression of cancer and /or required of cancer metastasis, to glucose is the primary source. Any disruption in glucose metabolism or its consumption bring cancer development to halt [69]. Hexokinase (HK) is an enzyme that plays a crucial role in glycolysis by phosphorylating it at first step. HK bind to outer membrane of

Drug Profile of CLOTRIMAZOLE

Chemical Structure



IUPAC Name:

1-[(2-chlorophenyl)-diphenylmethyl] imidazole

CAS Number

23593-75-1

Molecular Formula

$C_{22}H_{17}ClN_2$

Molecular Weight

344.842 g/mol

Description

Clotrimazole is white to pale yellow crystalline powder

Solubility

Practically insoluble in water, freely soluble in alcohol; soluble in polyethylene glycol 400 and slightly soluble in ether

Melting Point

154-156 °C

Storage

Store the drug between 20-25 °C in light resistant container.

Figure 1.13 Brief Description of clotrimazole

mitochondria through trans-membrane voltage-dependent anion channel and overexpressed on the cancer surface. Clotrimazole specifically interact with HK that leads to disruption in glycolytic flux in cancer, due to energy deprivation, cancer enters apoptotic phase. Report suggest that, when the clotrimazole is subjected to cervical cancer cells (HeLa), it specifically inhibited the HoK enzyme, that causes release of apoptotic proteins leading cell death [27]. Another report suggests, that clotrimazole cause decrease in ATP production as glycolysis was inhibited when the compound was studied against skin cancer cells (B16-F10 cells) [69].

Another cellular target for clotrimazole is phosphofructokinase (PKF) enzyme also involved in glycolysis [70]. There is significant upregulation of PPK on the surface of tumor in comparison to normal tissues and thus is a promising target for anti-cancer medicines. Study demonstrated that, when colon cancer (Caco-2) is treated with clotrimazole, noteworthy decline was observed with cancer cells in comparison to normal intestinal cells. Additionally, clotrimazole also inhibit Ca^{2+} activated potassium channel and restricts Ca^{2+} metabolism that further slowdown cancer cell proliferation [71]. Clotrimazole causes cell cycle arrest at G1 and M-Phase, inhibiting cancer progression [72, 73] . Another study demonstrate. that clotrimazole specifically obstruct human breast cancer proliferation whereas have little or no effect on normal human breast cell lines [74].

Above mentioned facts suggest that clotrimazole is a potential chemotherapeutic agent that specifically inhibit cancer cells.

1.15 Nanotechnology- chemotherapeutics

Chemotherapeutic medicine plays important role in the management of breast cancer, weather it is at initial stages or at more advanced stage. Even the most advance anti-cancer drug can not differentiate between abnormal cells and normal healthy cells when administers in body [75, 76].

This leads to non-specific distribution of the chemotherapeutic drug, resulting in systemic toxicity and associated adverse effects. Nanocarrier system provides us the suitable benefits to exploit the possibility to reduce systemic toxic effects and it is promising carrier system to acquire cancer targeted approach. Targeted nano-delivery system will have site specific targeting capabilities, it will maintain appropriate pharmacological level at targeted site for desired time period and thus possess superior qualities in comparison to conventional chemotherapeutic systems.

TARGETED NANO-DELIVERY SYSTEM



Figure 1.14 Schematic presentation of different approaches available for targeted nano-delivery system.

1.16 Nanoparticles Targeting Approaches

Nanoparticles tend to accumulate in the tumor cells by exploiting the special pathological features of the tumor. Based on the different targeting strategies nano-delivery systems can be divided into two categories; passive targeted nano-delivery system or active targeted nano-delivery system as represented in Figure 1.14 [21, 77].

1.16.1 Passive targeted nanocarrier system

Passive targeting is the approach where drug or designed nano-carrier system accumulates at the desired site by exploiting pharmacological and different physiochemical factors [78].

1.16.1.1 Targeting via Enhanced Permeability and Retention (EPR) effect

Nanoparticles get accumulated in tumor through enhanced permeation and retention (EPR) effect. This concept is based on two physiological factors:

- There is always an increased demand of oxygen and nutrient for cancer proliferation and to meet this demand tumor undergoes a physiological process called as angiogenesis (formation of new blood vessels from existing vessels). Architectural structure of newly formed vessels is usually abnormal, the endothelial cells are poorly aligned having wide gaps in between and become more permeable to macromolecules. In comparison to normal endothelium tissue, circulating nanoparticulate system becomes more permeable to malignant tumor and this phenomenon is called enhanced permeation effect [79].
- Lymphatic system is absent in aggressively growing tumor, due to which the accumulated nanoparticle will not be removed from the tumor, resulting in enhanced retention effect.

Collectively EPR effect facilitates targeting of nanoparticles to tumor vicinity and the concentration of drug may increase 10 -100 times in contrast to free drug [80].

1.16.1.2 Targeting via avoiding Reticuloendothelial system (RES)

Reticuloendothelial system of liver, spleen and other body parts cause removal of nanoparticulate system from the body, resulting in reduced blood circulation time. Nanoparticles are usually hydrophobic in nature and thus get detected by RES system that causes failure of the developed nano-delivery system. By increasing hydrophilic nature RES system can be avoided and this stealth property will increase the blood circulation time of drug. Integrating hydrophilic polymer on the surface of nanoparticle avoid RES detection, polyethylene glycol is hydrophilic polymer that form hydrophilic cloud around the nanoparticle resulting in increased circulation time period. With the help of EPR effect and avoiding RES, nanoparticles will generally accumulate in tumor by avoid normal tissue [81].

1.16.2 Active targeting

Active targeting is also recognized as ligand mediated targeting, comprising of strategic system that possess high binding affinity towards the receptors of the desired (cancer) site. Chemotherapeutic strategies with higher specificity, such as nano-targeted carrier systems are highly desirable. They not only tend to accumulate on the targeted site, but also have receptor mediated endocytosis that improves the delivery of drug molecules intercellularly. Various receptors have been explored for their potential to act as target moieties for breast cancer [17, 82, 83]. The most applicable receptors and their reported prevalence in breast tumors are listed in Figure 1.15.

Active targeting has been further classified as

- First order targeting approach: This involves the targeting of drug carrier system to the capillary bed of the desired target organ or tissue site. For example; liver, lungs, lymph, eyes, etc
- Second order targeting approach: Drug delivery to specific cells of the desired target is recognized as second order targeting of drug. For example; tumor cells of liver, breast, brain, etc.
- Third order targeting approach: This involves the targeting of the drug to intercellular site of desired cells, for example; mitochondrial drug targeting.

ACTIVE TARGETING MOITIES

TRANSFERRIN

- This is an iron-transporting serum glycoprotein that is efficiently taken binds to transferrin receptor.
- Transferrin receptor (TfR) is a transmembrane glycoprotein consisting of two 90 kDa subunits.
- A disulphide bridge links these subunits and each subunit can bind one transferrin (Tf) molecule

Example: Transferrin- conjugated lipid-coated PLGA nanoparticles encapsulated aromatase inhibitor for breast cancer cells

FOLIC ACID (FA)

- It has highly-efficient ligand that selectively binds to folate receptors overexpressed in tumour cells.
- This is nonimmunogenic and cost effective ligand possess high affinity towards cell-surface receptor.
- Targeting capabilities is due to efficient receptor-mediated endocytosis

Example: Poly-ethylene glycol-FA conjugated magnetic nanoparticles expresses efficient cellular uptake in breast cancer cells.

LECTINS

- Lectins are carbohydrate – binding proteins.
- Lectins have been investigated extensively to achieve targeted delivery of chemotherapeutics.
- Functionalization of lectins on the surface of nanoparticles enable site specific delivery system.

Example: lectin conjugated phthalocyanine-PEG gold nanoparticles for cancer specific delivery.

MODIFIED ALBUMIN

- Positively charged bovine serum albumin (CBSA) conjugated to long circulating nanoparticles has been successfully demonstrated as a promising targeting ligand for brain.
- CBSA has revealed a high accumulation profile and high specificity to brain endothelial cells compared to other organs such as the liver, heart, and lung.

Example: CBSA-conjugated PEGylated nanoparticles displayed enhanced endothelial cellular uptake of nanoparticulate system in brain.

PEPTIDES

Integrin targeted RGD-Peptide:

- RGD-peptide interact with α -integrins and β -integrins.
- Integrins are over expressed on the surface of tumor and these integrins help in formation of new blood vessels (angiogenesis).

Example: RGD- PEGylated Doxorubicin nanoparticles for breast cancer.

Other peptides

- Peptide targeting Luteinizing Hormone-release Hormone (LHRH)
- Peptides Targeting Epidermal Growth Factor (EGF).

Figure 1.15: Schematic presentation of active targeting approaches.

1.7 Sialic Acid

Sialic acid (SA)/poly-sialic-acid (PSA) an endogenous electro-negatively charged monosaccharide moiety present in higher animal. PSA is biocompatible, non-toxic, non-immunogenic and biodegradable [84]. SA mediated carrier system will fall under the second order targeted drug delivery system (as described earlier) [85].

Sialic Acid (SA) belongs to a class of neuraminic acid (*five-amido-3, five- dideoxy-D-glycero-D-galacto-nonulosonic acid*). Three are further main sub derivatives of SA (chemical structure represented in Figure 1.16:

- N-acetyl neuraminic-acid hydroxyalkyl (Neu5Gc)
- N-acetyl neuraminic-acid (Neu5Ac)
- 3-deoxy-D-glycero-D-galacto-nonyl-ketose (KDN)

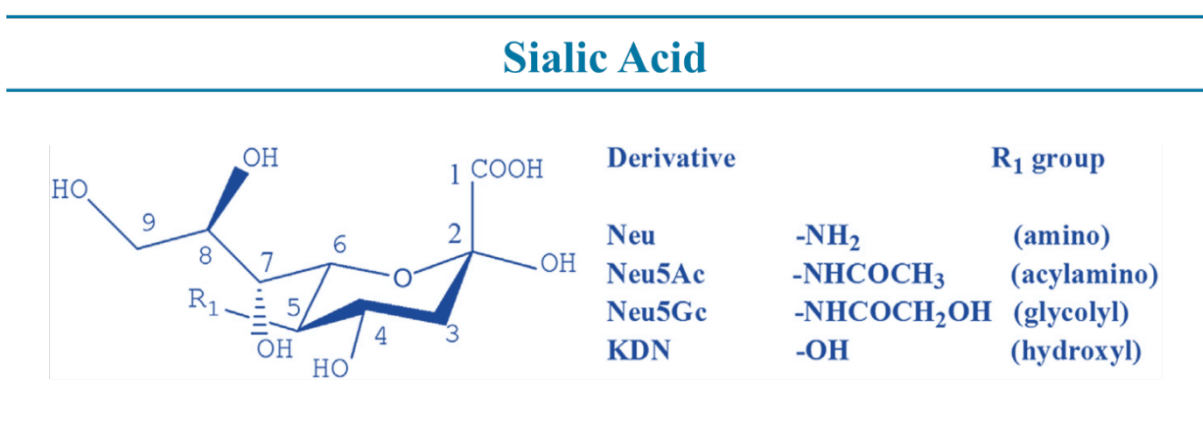


Figure 1.16 Chemical structure of Sialic acid and its derivatives. (Image courtesy: Zhang et al., 2014)

SA is negatively charged molecule, that produce attraction or repulsion in-between plasma protein and SA. Moreover, the negative charge further reconstructs the charge density at surface of cell, that regulates the transportation ability of transmembrane [86].

PSA conjugated NPs can transport drug directly into the vicinity of tumour through receptor-mediated endocytosis and increase the potency of drug [87]. Likewise, PSA conjugation to NPs will administer hydrophilicity and defend NPs from interacting with plasma proteins or macrophages, evading RES uptake and extending circulation half-life. Meanwhile, PSA degradation yields CO₂ and water that are non-toxic to living organisms. Apart from these, PSA can serve as targeting moiety for selectin (E-selectin/P-selectin) as these are overexpressed in the tumour vascular endothelial cells. Therefore PSA-modified-nanocarriers can be delivered to tumour cells more efficiently and consequently chemotherapeutic drugs can be targeted actively for cancer therapeutics [88].

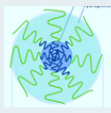
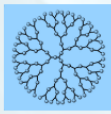

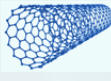

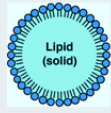

System	Structure	Characteristics
Polymeric micelles 	Hydrophobic core and hydrophilic shell are formed by assembling amphiphilic block copolymer	(a) Efficient carrier system for hydrophilic drug (b) Biodegradable, self-assembling, and biocompatible (c) Potential targeting (d) Functional modification Example: PEG-b-PLA- Paclitaxel-17-AAG-rapamycin polymeric micelles for breast cancer.
Dendrimers 	Synthetic polymer forming Nanosized branched structure with repeated units and regular pattern	(a) Uniformity in size, shape, and branch length (b) Tuned pharmacokinetics and biodistribution (c) Increased surface area, increased loading (d) Targeting is achieved Example: Methotrexate-retinoic acid-dendrimers
Liposomes 	Lipid bilayer membrane forming self-assembled closed colloidal structures	(a) Biocompatible (b) Longer duration of circulation (c) Amphiphilic Example: Transferrin conjugated –doxorubicin + verapamil liposomes
Carbon nanotubes 	Benzene ring forming carbon cylindrical structure	(a) Multi-functional Nano-system (b) Chemical modification possible (c) Water soluble and biocompatible Example: Folic acid conjugated Platinum base anticancer CNTs
NANOPARTICLES (NPs)		
Polymeric NPs 	Submicron colloidal system, where drug is dissolved, entrapped, encapsulated or attached to biodegradable ppolymer	(a) Biodegradable polymer is used (b) Drug is encapsulated inside NPs (c) Biocompatible (d) Tumour targeting capability Example: PLGA- NPs with vincristine + verapamil effective against MCF-7breast cancer cells
Solid Lipid NPs 	SLNs are made from solid lipids (lipids that are solid at room temperature and at body temperature) and stabilized by surfactants.	(a) Longer bioavailability (b) Biocompatible (d) Tumour specific delivery system can be achieved Example: Doxorubicin and paclitaxel SLNPs for colorectal cancer
Magnetic NPs 	Promising candidate possessing efficient capabilities to be employed in cancer therapeutics and diagnostics applications	(a) Excellent Surface functionalization capabilities (b) Magnet + drug dual delivery system (c) Biocompatible Example: Magnetic NPs conjugated with Her-2 antibody for breast cancer treatment

Figure 1.19: Brief description of different Nano delivery system available

Zheng et.al., has formulated the SA decorated selenium nanoparticles and examined the targeting capability of SA against HeLa cell line (human cervical carcinoma cells). His *in-vitro* investigation revealed that, SA functionalization had enhanced the cellular uptake in cancer and facilitates apoptosis [89, 90].

1.18 Different nanocarrier system

Combination of anti-cancer agents empower us to have better cancer treatment, but still there are issue that needs immediate attentions like, solubility problem with chemotherapeutic compound, rapid elimination of drug from the body, need of high dose in case if resistance is been developed, decreased accessibility of drug towards tumor and inappropriate bioavailability [91]. Thus, nano-technological based drug carrier systems have better resolution for the related complication of conventional chemotherapy [92]. Nanotechnology plays a vital role in development of novel cancer therapeutics by using various available nano-carries system such as, liposomes, polymeric micelle systems, dendrimers, carbon nanotubes and polymeric-drug conjugates based on combination therapy [93, 94]. These are briefly described in the Figure 1.19.

1.19 Polymeric nanoparticles

The term nanoparticles (NPs) is generalized term and is widely used to recognize the novel drug delivery systems that are submicron (less than 1 μm) in size or are colloidal systems generally made of polymers [95]. NPs is broad class that comprises of both vesicular systems (nano-capsules) and matrix system (nano-spheres), as represented in Figure 1.18 [94].

- **Nano-capsules** are the systems in which the drug the drug is confined to a cavity surrounded by unique polymeric membrane. These system generally possess larger size in comparison to nano-spheres of same polymeric composition. Likewise, degree of polymerization is also higher in nano-capsules [96].
- **Nano-spheres** are the systems in which the drug is dispersed through-out the polymeric matrix. These are smaller in size in comparison to nano-spheres of same polymeric composition. Similarly, degree of polymerization is also low [97].

1.19.1 Advantages of polymeric nanoparticles.

Nanoparticles possess several advantages in comparison to other available nano-carrier for drug-delivery system [97-99], for instance:

- Ease of manipulation with particle size and surface functionalization of polymeric NPs with the aim to acquire passive as well as active drug targeting.

- Drug release pattern from the polymeric-NPs can be controlled and sustained for desired period of time by selecting suitable polymer for NPs formulation, possessing distinct physicochemical properties.

Polymeric Nanoparticle

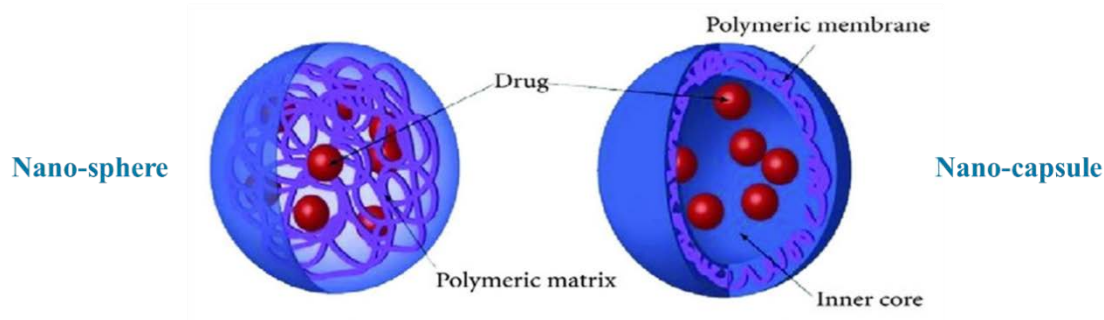


Figure 1.18 Different type of polymeric nanoparticles. (Image courtesy: Dadwal et.al., 2014)

- Larger surface area of NPs, these system own higher drug-loading capacity in contrast to other nano-carrier systems.
- Smaller size of polymeric NPs allows them to administer intravenously through injection in contrast to other colloidal nano systems, that tend to occlude both the capillaries and needles of injection.
- Due to small size of these NPs, they can easily pass through the sinusoidal spaces in the spleen and bone marrow in comparison to other carriers such as microspheres and liposomes.
- Selected polymeric composition to formulate NPs render them to acquire more stability unlike nano-emulsion systems and liposomes, that are fragile in nature.
- Polymeric-NPs increases the stability of encapsulated drug molecules and proteins.
- Polymeric NPs are much safer and more effective in targeted and site-specific drug delivery.

1.19.2 Selecting a Polymeric Drug Delivery

It ought to be noted that release of drug from any nano-carrier system is determined by the composite formation in-between polymer of choice and selected drug [100]. Typically, it relies upon the physicochemical properties of drug and rate of degradation of polymer. Biodegradable polymer are generally used to formulate polymeric NPs [100, 101]

Factors that should be recognized before proceeding to nano synthesis process

- Associated physicochemical properties of drug.
- Biodegradation and erosion behavior inside the body
- Desired site of action (Site- selectivity).
- Various challenges in drug delivery to desired area.
- Desired duration of drug release pattern associated with the drug.
- Drug loading capacity the selected nano-carrier system
- Preferred routes for administrating drugs.
- Selected polymer drug compatibility.
- Desired release kinetics of drug and degradation rate of polymer.

1.19.3 Types of polymer available for drug delivery

Polymers that are generally used in synthesis of nanoparticles can be broadly classified as natural and synthetic polymers [100] (Table1.1).

1.19.3.1 Natural polymers

Natural polymers or biopolymers are striking class of biodegradable polymers as they are extracted from natural sources. Natural polymers are easily available and relatively inexpensive [102]. These polymers possess certain demerits such as; *(i)* Poor bath to batch reproducibility of NPs, *(ii)* less environmental stability and *(iii)* related potential of antigenicity [103].

1.19.3.2 Synthetic polymers

As the name suggest these polymers are synthetically synthesized, that posses efficient degradation properties. Selection of these polymer for nano-formulation have certain benefits over natural polymer like [104, 105]; *(i)* ease of providing better stability to encapsulated drug, *(ii)* prolonged degradation time period, *(iii)* qualified for a number of chemical modification, etc

1.19.20 POLYCAPROLACTONE

Poly- ϵ -caprolactone (PCL) is a biocompatible, biodegradable and semi-crystalline polyester polymer possessing a very low glass transition temperature ($- 60\text{ }^{\circ}\text{C}$)[106]. Moreover, just because of its slow and gradual degrading nature, PCL is preferably suitable for the designing and development of controlled drug delivery systems [107]. It has been approved by Food and Drug Administration (FDA) for various biomedical application for instance, formulating various drug delivery carrier systems, biodegradable sutures, scaffolds, PCL-based nanofibers,

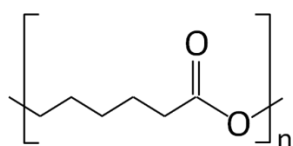
etc[108]. Chemical structure of PCL and some of its imperative associated physicochemical properties have been discussed in Figure 1.19.

Table 1. 1 Natural and Synthetic Polymers Used for the Preparation of Nanoparticles

<i>Natural polymers</i>	
Proteins	Polysaccharides
Gelatin	Alginate
Albumin	Dextran
Lectin	Chitosan
Legumin	Agarose
<i>Synthetic polymers</i>	
Pre-polymerised	Polymerized in process
Polylactides <i>(PLA)</i>	Poly (isobutylcyano acrylates) <i>(PICA)</i>
Polyglycolides <i>(PGA)</i>	Poly (butylcyano acrylates) <i>(PBCA)</i>
Poly(lactide co-glycolides) <i>(PLGA)</i>	Polyhexylcyano acrylate <i>(PHCA)</i>
Polycaprolactone <i>(PCL)</i>	Poly(methyl methacrylate) <i>(PMMA)</i>
	Copolmer of aminoalkylmethacrylate
	Methy methacrylate

Polycaprolactone

Chemical Structure:



IUPAC name	(1,7)-Polyoxepan-2-one
Systematic IUPAC name	Poly(hexano-6-lactone)
CAS Number	24980-41-4

Abbreviations	PCL
Chemical formula	$(C_6H_{10}O_2)_n$
Density	1.145 g/cm ³
Melting point	60 °C (140 °F)
Glass transition temperature	-60 °C
Biocompatible	
Biodegradable	

Ring-opening polymerization of ϵ -caprolactone, the main pathway to produce polycaprolactone

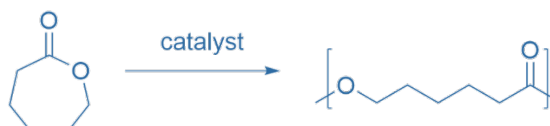


Figure 1. 19 Facts regarding PCL. (Image courtesy: Wikipedia)

1.20.1 Methods for preparation of PCL-NPs nanoparticles

Reis et.al., has described various methods that had been adopted to formulate polymeric (PCL) -NPs. However, in context to formulate drug loaded PCL-NPs, methods that are widely employed are;

- a) Solvent evaporation
- b) Nanoprecipitation
- c) Emulsification/solvent diffusion
- d) Dialysis

1.20.1.1 Solvent Evaporation Method

In this technique, polymer is dispersed in volatile solvents (chloroform, dichloromethane, etc.) to form polymeric emulsion system, stabilized by using suitable surfactant. Polymeric solution and drug solution are mixed together by using high-speed homogenizers or by ultrasonication [106] (Figure 1.20). The resulting emulsion is converted into nanoparticulates by evaporating the solvents by constantly stirring the mixture at moderate speed, followed by washing in order to remove unused polymer and surfactant [109, 110].

Solvent Evaporation

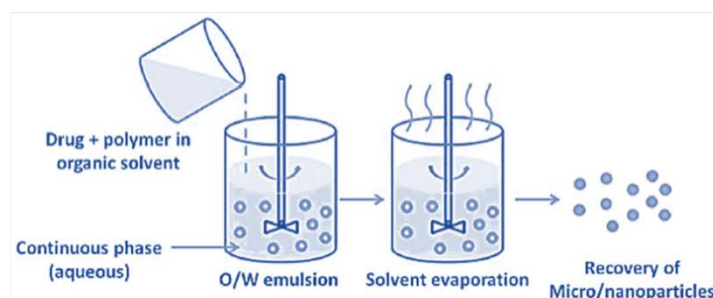


Figure 1. 20 Solvent evaporation technique to formulate polymeric-NPs. (*Image courtesy: Nagavarma et.al., 2012*)

R Li et.al., has demonstrated the o/w emulsion solvent evaporation method, to formulate Tetradrin-PCL-NPs. Aim of the study was to enhance the efficacy of drug and likewise to establish a robust method of evaluation of drug sensitivity against histo-culture drug response assay (HDRA). Approximately 300 nm drug (tetradrin)-loaded-PCL-NPs were formulated by using MPEG-PCL and PEG-PCL-PEG, followed by physicochemical characterization. Enhanced cellular uptake and improvement in cytotoxicity against LoVo cells were witnessed by employing this method [111, 112].

1.20.1.2 Nanoprecipitation method

It is also recognized as solvent displacement method. It includes the formation of precipitates of a selected biodegradable polymer from an organic solution. Eventually, organic solvent diffuses into aqueous medium in the absence or presence of a suitable stabilizing agent (surfactant-PVA) (Figure 1.21)

Chawla et.al., formulated Tamoxifen loaded-PCL-NPs of size range 250-300nm by employing this method [106].

Nanoprecipitation Technique

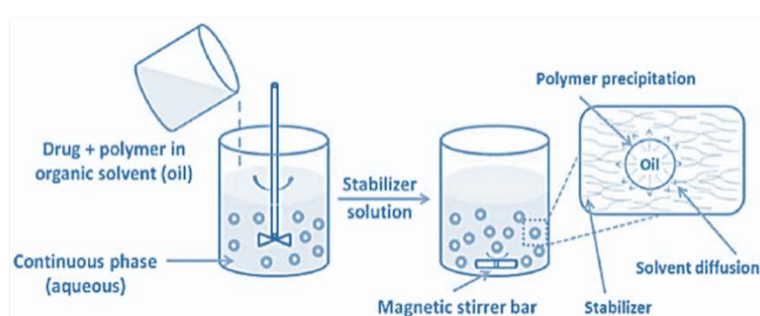


Figure 1. 21 Nanoprecipitation technique to formulate polymeric-NPs. (Image courtesy: Nagavarma et.al., 2012)

Objectives of the study was to formulate targeted drug delivery system of tamoxifen that should have controlled releasing pattern of drug. Resulting NPs possess zeta potential of 25mV, % EE of 66%. Significant cellular uptake of tamoxifen-NPs was noted in MCF-7 cell line after one hour signifying local accumulation of synthesized NPs [113].

1.20.1.3 Dialysis method

This technique offers a simple, uncomplicated and effective approach to formulate PCL-NPs having benefits of narrow particle size distribution [106]. Polymer is generally dissolved in a suitable organic solvent that is positioned inside a dialysis tube having appropriate molecular weight cut off. Dialysis is generally carried out against a non-miscible solvent with the previous polymeric miscible solvent. Solvent get displaced from inside (membrane compartment) to the surrounding solvent system, followed by the progressive accumulation of polymer due to a low solubility in outside solvent that results in homogenous NPs formation (Figure 1.22).

Pulkkinena et.al., has formulated Doxorubicin/paclitaxel PCL-NPs possessing approximate hydrodynamic diameter of 361nm. Resulting Doxorubicin/paclitaxel PCL-g-

PVA-NPs demonstrated controlled release upto 15 – 20 days in comparison to 1-2h of free drug release [114].

Dialysis Technique

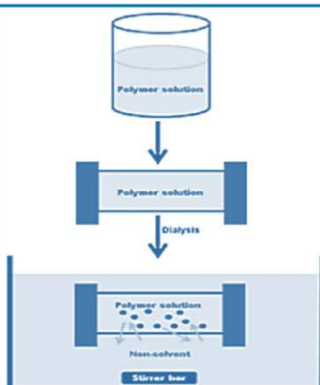


Figure 1. 22 Dialysis technique to formulate polymeric-NPs. (Image courtesy: Nagavarma et.al., 2012)

1.20.1.4 Emulsification/solvent diffusion (ESD) technique

This is a modified variant of solvent evaporation method. The biodegradable polymer is generally dissolved in a partly water-soluble solvent like propylene carbonate and further saturated with water to ensure the initial thermodynamic equilibrium of both liquids. This consequently produce nano-precipitated particulate system of the selected polymer[106]. Solvent is evaporated by constant stirring for upto 24h at room temperature, followed by washing with PBS, to remove unused polymer and free drug molecules (Figure 1.23).

Emulsification Diffusion Technique

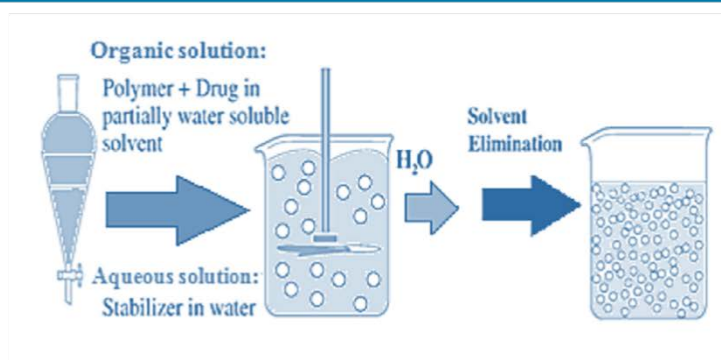


Figure 1. 23 Emulsification diffusion technique to formulate polymeric-NPs. (Image courtesy: Nagavarma et.al., 2012)

Bilensoy et.al., had synthesized Mitomycin-C (MC) loaded-PCL-NPs by aiming to have efficient targeted drug delivery system. The observed diameter of the NPs was in-between 180-

340 nm and the % EE was found to be with-in the range of 7% to 24%. Selective uptake of formulated NPs was observed with bladder cancer cells [115].

1.4 Aim and hypothesis of the thesis

AIM: To develop a targeted co-delivery system comprising paclitaxel (PAX) and clotrimazole (CLZ) as an anti-cancer agent, encapsulated with polycaprolactone (PCL) nanoparticles (NPs).

HYPOTHESIS:

CLZ will potentiate the cytotoxic effect of PAX in synergistic or additive manner

SA mediated NPs will be more specific to breast cancer cells

1.5 Specific objective of the thesis

Objective-1: To evaluate the effect of paclitaxel and clotrimazole combination against breast cancer cell line.

Objective-2: To formulate and characterize sialic acid conjugated nanoparticles.

Objective-3: To optimize drug loaded polymeric nanoparticles.

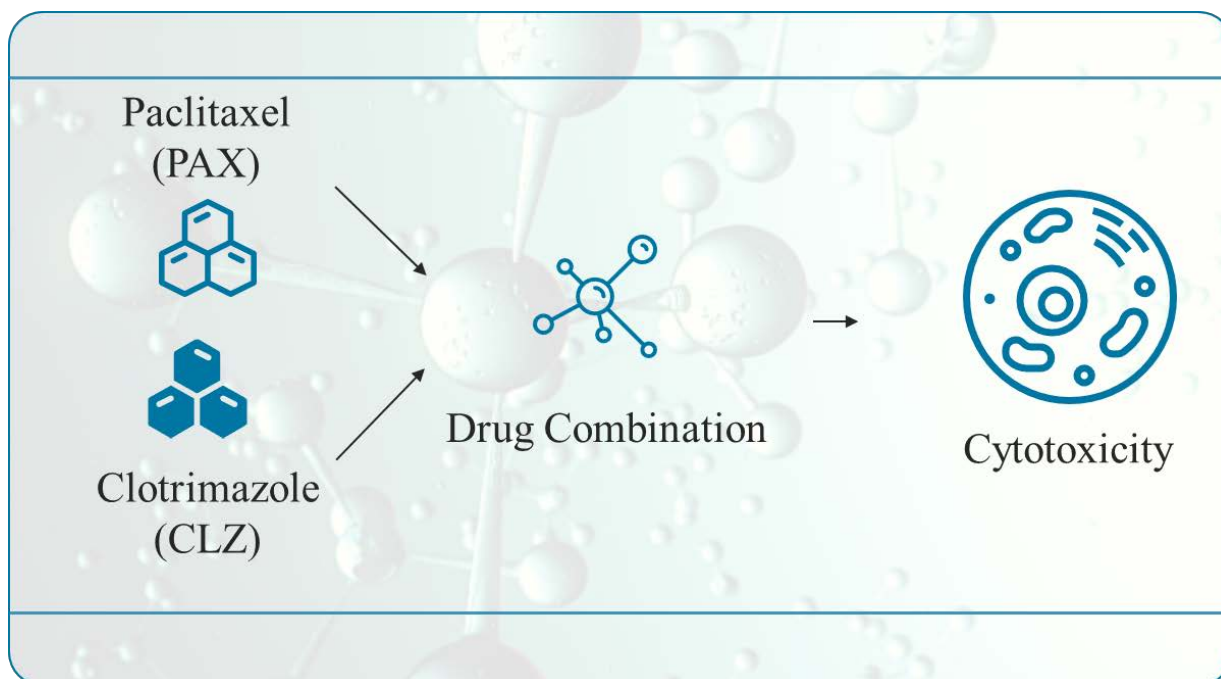
Objective-4: To synthesis sialic acid drug loaded nanoparticles and evaluation against breast cancer cell line.



CHAPTER-2

EFFECT OF PACLITAXEL AND CLOTRIMAZOLE COMBINATION ON BREAST CANCER

GRAPHICAL OVERVIEW OF CHAPTER



HIGHLIGHTS

- Physical mixture of PAX and CLZ was analysed for any possible chemical interaction through Fourier transform infrared spectroscopy (FTIR).
- Cytotoxic evaluation of drug combination (at reduced doses of PAX + CLZ) against breast cancer cells.
- CompuSyn Software showing synergistic action of selected concentration of drug combination.
- Investigation of oxidative and reactive nitrogen stress alterations in breast cancer cells as an effect of drug combination.
- Effect of drug combination on genotoxicity and glucose uptake studies.

2.1 INTRODUCTION

Breast cancer is the second leading cause of cancerous morbidity or mortality worldwide among women [3, 116]. The available treatments for breast cancer, surgical removal of breast tumour, radiation therapy, hormonal therapy, chemotherapy and use of different chemotherapeutic agent in combination [117]. Paclitaxel (PAX) is a potent anti-cancer agent, that belongs to the class of Taxan and possess specialized mechanism of cell killing i.e. by stabilizing microtubules during cell cycle. This leads to interference in cell-cycle advancement followed by programmed cell destruction. Despite being a potent chemotherapeutic agent, PAX is usually prescribed in combination with other chemotherapeutic agents [56, 118]. PAX is well known for its associated side effects and by combining PAX with other chemotherapeutic agent increases the risk factor of side effects even further [119, 120].

There is an always a great demand of such agent which possess high killing effect towards cancerous cells and likewise have minimal or no effect on normal dividing cells.

Evidences suggests that, Clotrimazole (CLZ), clinically used as an antifungal compound, is also effective against breast cancer cells whereas less effect towards normal cells. Reason reported for this effect is its capability to inhibit glycolysis by specifically acting on 6-phosphofructo-1-kinase (PKF) and hexokinase (HK) [121]. There is always an increased demand for energy in actively dividing cancer cells when compared to normal cells. Inhibition of key enzymes (PKF and HK) involved in glycolysis leads to energy deprivation that further leads to cell starvation and cell death [122]. CLZ inhibit cell-cycle progression at G-1 and M-phase, which is another outstanding feature of CLZ that can find its application in cancer therapeutics [122].

Keeping these facts in mind, the current chapter provides an evidence for the use of CLZ in combination with PAX. An attempt has been made to demonstrate whether low dose PAX and CLZ in combination possess any significant toxicity to breast cancer cells (MCF-7 and MDA-MB-231).

2.2 MATERIAL AND METHOD

2.2.1 Materials

PAX was procured as a gift sample from Samarth life science (Pvt. Ltd) – Himachal Pradesh, India. CLZ was obtained from Optimum Pharmaceuticals (Pvt. Ltd)- Himachal Pradesh, India. All the chemicals and reagents were acquired from Sigma Aldrich and used as such.

2.2.2 Fourier transform infrared spectroscopy (FTIR) analysis

The physical mixture of PAX and CLZ was investigated for the possible chemical functional group changes or interaction by FTIR (Agilent Technologies 630 Cary using Micro Lab software). Pinch of sample was placed on the sampling platform followed by lowering the upper nobe so that sample comes into the close contact with the sampling diamond. Spectra was determined by running the software and interpretation was made.

2.2.3 Cell lines maintenance and culturing

The MCF 7 and MDA MB 231 cells (breast cancer cell lines) were procured from NCCS Pune, India, whereas HEK293 cell line was obtained as gift from AMITY University, Noida (India). Dulbecco's modified Eagle's medium (DMEM; Invitrogen) was used to culture MCF 7 and HEK 293 cells, additionally complemented with 10% fetal bovine serum (FBS; Invitrogen), 1% antibiotics (penicillin-100 U/mL and Streptomycin 0.1mg/mL; Gibco) and 5% CO₂ sustained at 37°C. Leibovitz's specialized medium (L15; Himedia) was used to culture MDA MB 231 cells supplemented with all the essential component to monitor cell growth such as antibiotic (1%), FBS (10%) and the temperature was maintained at 37°C deprived of CO₂ atmosphere.

2.2.4 Cell cytotoxicity analysis and drug combination

MTT assay was employed to evaluate the anticancer effect of drug combination (PAX + CLZ) against MCF 7. Briefly, cells were subculture in 96-well cell culture plate at density of 1×10^4 which was further incubated at 37°C. Cells were subsequently treated with PAX; at different concentration ranging from 6.25 nM to 100 nM and likewise, 6.25 μM to 100 μM concentrations were used for CLZ. After 24h of cellular-drug interaction, culture medium was and carefully washed with phosphate buffer saline (PBS-7.4pH) twice. Afterwards, 20μl of MTT was added to each well treated with drug and further incubated at 37°C for 4h. Metabolically active cells converts MTT into insoluble formazan product, which was made soluble with help of DMSO (added 100 μl to each wells). Absorbance was measured at 570 nm (test wavelength) and 630 nm (reference wavelength) using a microplate reader; Bio-Rad. Percentage cell viability was estimated through following equation:

$$\% \text{ cell viability} = \left[\frac{(A)_{\text{Test}}}{(A)_{\text{Control}}} \times 100 \right] \quad (\text{Eq-1})$$

50 % inhibition (IC₅₀ value) was assessed by plotting graph between percent (%) cell viability and dose response curve. Mass-action law dependent on median-effect, a technique defined by Chou and Talaly [123], was used to examine interactions among PAX and CLZ at different concentration against MCF 7. Cellular drug interactions were inspected with the help of

COMPUSYN software [124, 125]. Values not exceeding IC₅₀ i.e for PAX (values not more than 50nM) and for CLZ (values less than 50µM) were subjected to computational simulation to generate combination index (CI). CI value have their own significance which depicts; CI > 1.45 (strong antagonism), CI=1.20-1.44 (antagonism), CI=1.10-1.19 (slight antagonism), CI=0.9-1.09 (additive), CI=0.85-0.89 (mild synergism), CI=0.70-0.84 (moderate synergism), CI=0.3-0.69 (synergism), [126]. For deep understanding FA-CI and FA-DRI plots were further investigated. Based on the detected values for CI, best suited drug combination of PAX and CLZ was nominated and cell viability was also evaluated for MDA MB 231 and HEK 293.

2.2.5 Microscopical evaluation cell death

2.2.5.1 Acridine orange (AO) and ethidium bromide (EtBr) staining to identify apoptosis

To examine the cellular morphological alterations as an effect of drug combination treatment in MCF 7 and MDA MB 231 cells, we conducted the AO/EtBr staining [127, 128]. Briefly, cells were subcultured in 6 well plate having density of 3×10^4 cells/well. Cells were further treated with selected drug combination of PAX (12.5 nM) and CLZ (25 µM) along with the individual drug concentration for 24 h. Cells were cautiously washed with phosphate buffer saline (PBS) followed by fixation by using 4% paraformaldehyde. 0.2% Triton-X-100 was use as permeabilizing agent. Cells were further incubated with, 100 µg/mL of AO (10 µL) along with 100 µg/mL of EtBr (10 µL) and finally the fluorescent microscopic images were captured with fluorescence microscope (Nikon Eclipse-Ti, Japan).

2.2.5.2 4'-6- diamidino-2-phenylindole (DAPI) and propidium iodide (PI) staining

Further to confirm the apoptotic effect of selected drug combination and to visualise the morphological changes phase contrast microscopic images were capture by using DAPI and PI as staining dye [129, 130]. To carry forward this study, breast cancer cells (MCF 7 and MDA MB 231) were subcultured in 6 well plate, comprising cell density of 3×10^4 cells/well. Cells were further treated with selected drug combination of PAX (12.5 nM) and CLZ (25 µM) along with the individual drug concentration for 24 h. Afterwards, the culture media was removed, cells were rinsed with PBS and further cells were incubated with 1 µg/ml of DAPI (5 µL) along with 10 µg/ml of PI (5 µL) for 5-min. Subsequently, fluorescent microscopic images were captured with fluorescence microscope (Nikon Eclipse-Ti, Japan).

2.2.6 Estimation of Reactive oxygen species (ROS)

To examine ROS production with respect to drug treatment, we calculated cell H₂O₂ generation through commercially accessible kit to evaluate H₂O₂ in *in-vitro* condition (PerXOquant™ Quantitative peroxide assay kits). Briefly, cultured cells were exposed to drug combination of

PAX (12.5 nM) and CLZ (25 μM) along with the individual drug concentration for 24 h. Afterwards supernatant (50 μl) was collected and transferred to new flat-bottom 96 well plate, working reagent (200 μl) was added to each well and the respective absorbances were recorded spectrophotometrically at 595 nm. Concentration of H₂O₂ was estimated through standard plot, made with known concentration of H₂O₂ ranging from 0 to 100μM. Percentage of H₂O₂ was assessed through following equation:

$$\text{Percentage H}_2\text{O}_2 \text{ level} = \frac{(\text{A}) \text{ of sample}}{(\text{A}) \text{ of control}} \times 100 \quad (\text{Eq-2})$$

2.2.7 Estimation of Reactive nitrogen species (RNS)

Nitric oxide is a potent RNS that leads to significant cellular damage[131]. Consequently, we evaluated the level of NO, after the drug was being exposed to breast cancer cells (MCF 7 and MDA MB 231) by using Griess reagent [132, 133]. Briefly, the cultured cells were exposed to drug combination of PAX (12.5 nM) and CLZ (25 μM) along with the individual drug concentration for 24 h. After the stipulated time for incubation, supernatant (75 μl) was collected and Griess reagent (150 μl) was subsequently introduced to each well. Absorbances was measured spectrophotometrically at 550 nm and the percentage of NO was calculated through following equation:

$$\text{Percentage NO level} = \frac{(\text{A}) \text{ of Sample}}{(\text{A}) \text{ of Control}} \times 100 \quad (\text{Eq-3})$$

2.2.8 Comet assay

Comet assay is also recognized as single cell gel electrophoresis, this is a highly sensitive, easy to conduct and widely employed method to identify genotoxicity or any damage to DNA [134, 135]. Briefly, prior to experiment, glass slide was coated with high melting agarose (1.5%). Cells exposed to drug were extracted from the culture plate and mixed with the 0.7 % low melting agarose (95 μl) at room temperature. Resulting mixture was poured on the previously made high melting agarose slide and instantly covered with glass coverslip in order to have uniform cellular layer. Slides were subjected to freshly prepared lysing buffer comprising 10-mM Tris, 100-mM EDTA, 2.5-M NaCl, 1% Triton-X-100, 10%-DMSO and pH was regulated to 10.2, and maintained at 4°C for 30 min. Afterwards, slides were exposed to electrophoresis (300 mA, 25 V for 30 min) at 4°C temperature under low light or dark conditions. Buffer for electrophoresis was freshly prepared which comprises of 300-mM NaOH and 1-mM EDTA. Slides were removed gently and further neutralized with the help of neutralizing buffer comprising 0.4-M Tris maintained at pH-7.5. 5 μg/ml of propidium iodide was used to stain

cells. Slides were washed two times with PBS and fluorescent microscopic images were captured (Nikon Eclipse-Ti, Japan). Acquired images were further examined through CaspLab software to calculate percentage of DNA in head and tail [136].

2.2.9 Glucose consumption

Fully grown breast cancer cells (MCF7 & MDA MB 231) were sub-cultured in 96 well cell culture plate with density of 1×10^4 cells/well. Cells were exposed to individual drug concentration PAX (12.5nM), and CLZ (25 μ M) along with respective combination of PAX + CLZ for upto 24 h at 37°C. Afterwards, the supernatant from each well was collected, difference in glucose levels (initial and after 24 h) were determined through Accu-Check Blood Glucose monitoring system, (Roche, Germany) and the data was represented graphically.

2.2.10 Statistics

Graph Pad Prism version 0.6 (Graph Pad Software, San Diego, CA, USA) was used to employ statistical analysis. One-way ANOVA was used to calculate statistical significance of data at * $p < 0.05$, ** $p < 0.01$ and *** $p < 0.001$. Results are represented as mean \pm SD.

2.3 RESULTS AND DISCUSSION

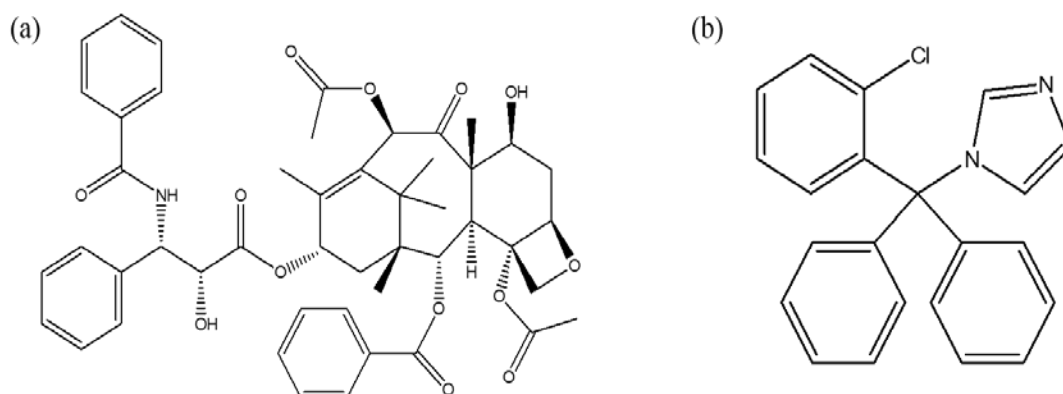


Figure 2.1. Chemical structure of (a) Paclitaxel [PAX] and (b) Clotrimazole [CLZ].

2.3.1. Physicochemical characterization of PAX/CLZ mixture

PAX is a well-known anti-cancer agent and CLZ also been reported to possess anti-tumour action without effecting normal cells. Physical mixture of PAX-CLZ was initially examined for possible chemical alterations by FTIR (Fourier transform infrared spectroscopy).

The FTIR spectra of PAX depicted its prominent and characteristic peaks at 3312/cm (O-H and N-H stretching), 2974/cm (C-H stretching), 1704/cm (COOH stretching) and 1248/cm (C-N stretching) (Fig.2a). For CLZ, characteristic IR peaks at 1495/cm and 1216/cm (C-N stretch) and 769/cm (C-Cl stretch) were observed (Fig. 2b). Representative band peaks of two drugs

appeared with no substantial interaction in the physical mixture of PAX-CLZ revealing stability of two compounds without any chemical interface (Fig.2c).

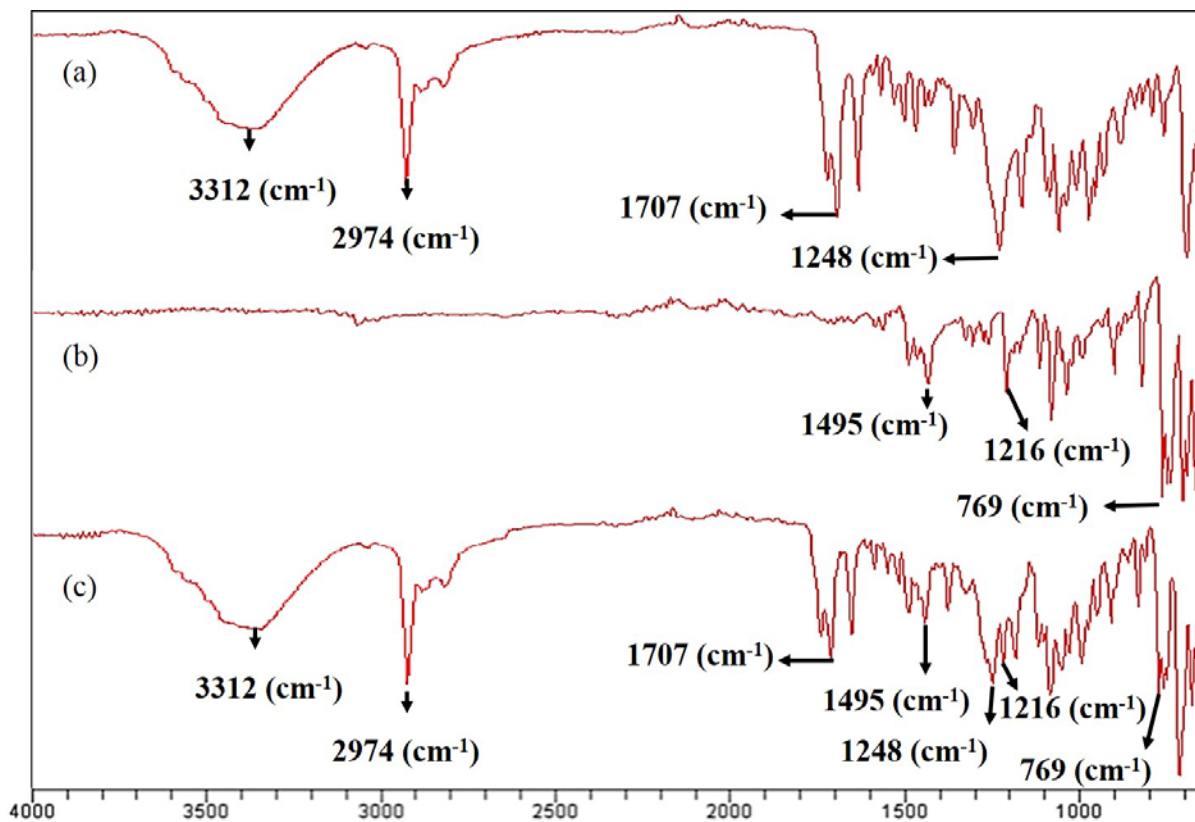


Figure 2.2. FTIR spectroscopic graphs of (a) Paclitaxel, (b) Clotrimazole and (c) physical mixture of PAX and CLZ.

2.3.2 Cell cytotoxicity analysis and selection of drug combination

The impact of drug exposure to MCF 7 cells was estimated through a widely used colorimetric technique, MTT exclusion assay. Cells were treated with different concentration of PAX and CLZ. Individually, both drugs displayed dose dependent cellular toxicity, with IC₅₀ values of 53.68-nM for PAX and 51.52- μ M for CLZ correspondingly (Fig. 2.3 a and b). Further, the combination of PAX and CLZ was evaluated by selecting the concentrations of drugs below observed IC₅₀ value. Combination of PAX (12.5-nM) and CLZ (25- μ M) exhibited 50%

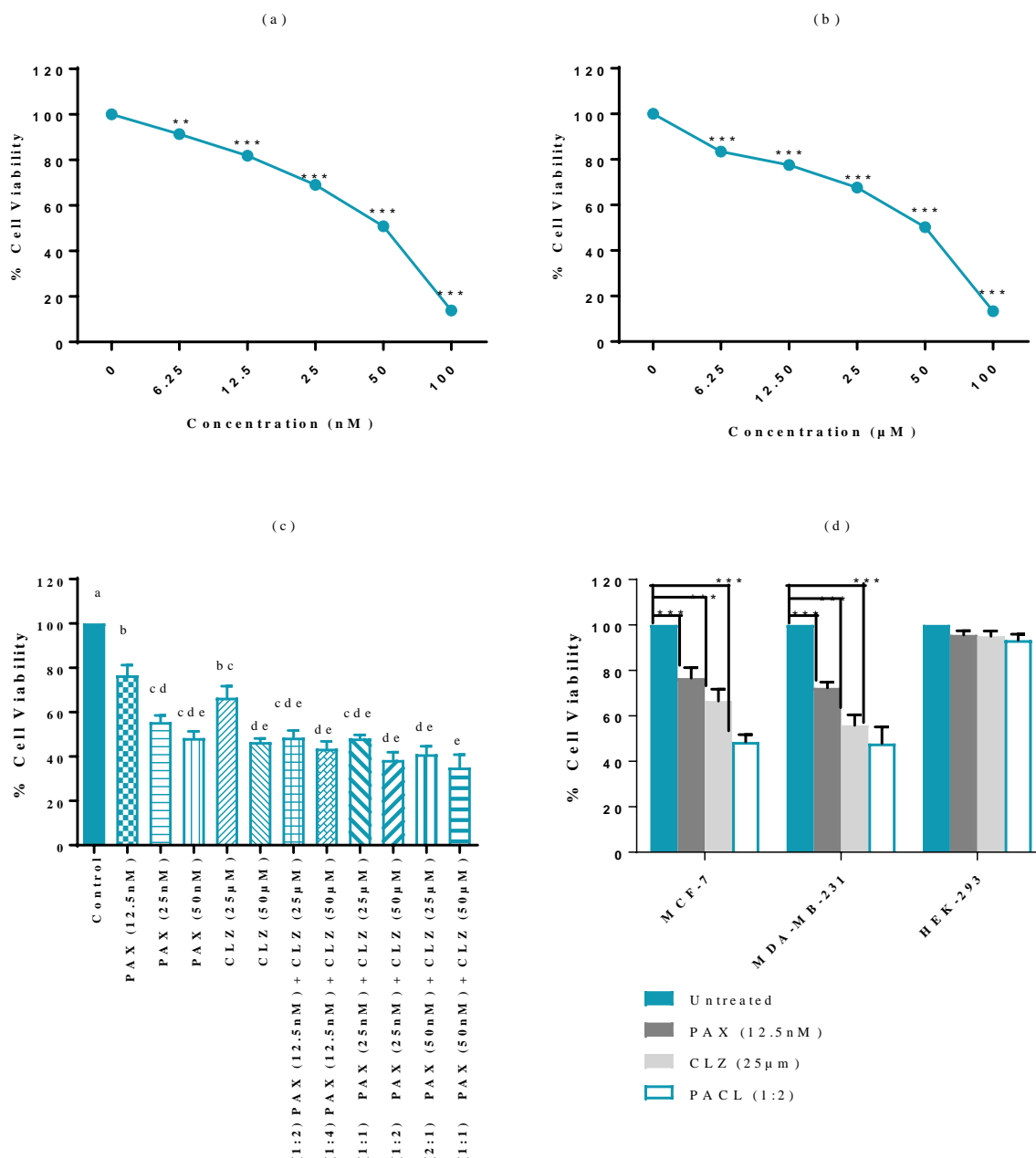


Figure. 2.3. Dose dependent effects of PAX and CLZ on viability of MCF-7 cells (a and b) in the form of percent cell viability relative to untreated control cells. Co-effect of selected PAX and CLZ doses in combination (c) and bars not sharing the same letters are significantly different with $p < 0.05$. Comparative analysis of selected combo on MCF-7, MDA-MB-231 and HEK-293 at 24h (d) and *** indicates $p < 0.001$ when compared with untreated group. All data is presented as mean \pm SEM of three independent experiments.

reduction in the viability of cells, whereas individually PAX (12.5-nM) demonstrated approximately 25% of reduction in cell viability and CLZ (25- μ M) exhibited 30% cell reduction. These results suggested that, combination of PAX and CLZ was more cytotoxic to cancer cells in comparison to single drug exposure.

Combination index (CI) values were determined from CompuSyn software, to depict whether the combination is having synergistic, additive, or antagonistic effect against breast cancer cells. Dose effect curve is graphically represented in Figure-2.4 (a), displaying drug (PAX + CLZ) interaction with MCF 7 cells.

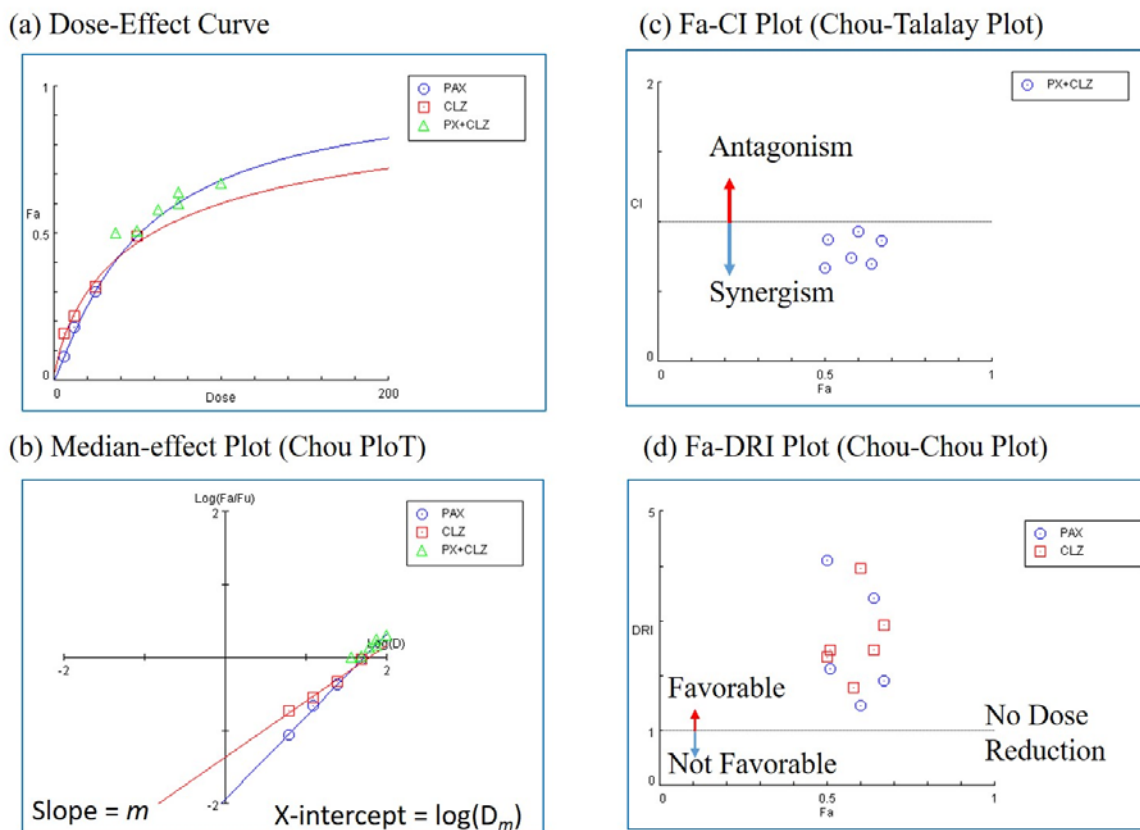


Figure. 2.4. Combination dose effect curve (a) as an outcome of PAX and CLZ interactions on MCF- & breast cancer cells, (b) mass-action algorithms derived from computerized simulations through CompuSyn showing media-effect plot (Chou Plot), (c) FA-CI plot (Chou-Talalay Plot) showing synergism interaction of PAX & CLZ and (d) FA-DRI Plot (Chou-Chou Plot) representing index of dose reduction.

Necessary fold percent decrease in dose of drug within combination to produce synergistic effect was suggested by Dose reduction index (DRI). If the DRI is greater than one, dose reduction is favourable, whereas DRI less than or equal to one signifies no dose reduction or un-favourable dose reduction. Figure-2.4. DRI is closely associated with CI values, however determination of CI value alone is efficient to authenticate synergism or antagonism [137]. CI value was found to be 0.66 suggesting that both the drugs were effective against cancer cells in a synergistic manner at reduced doses.

It should be stated that when the dose of a drug is decreased, associated toxicity also tends to decline. Considering this fact and recognizing the outcomes revealed via FA-CI plot (Chou-

Talalay Plot), we here by selected PACL as drug combination comprising 12.5-nM of PAX and 25- μ M of CLZ for further experimental analysis. PACL was also explored for its anti-cancerous effect against another breast cancer cell line, MDA-MB-231 cells (Figure 2.3d). Furthermore, PACL exhibited no significant cytotoxic

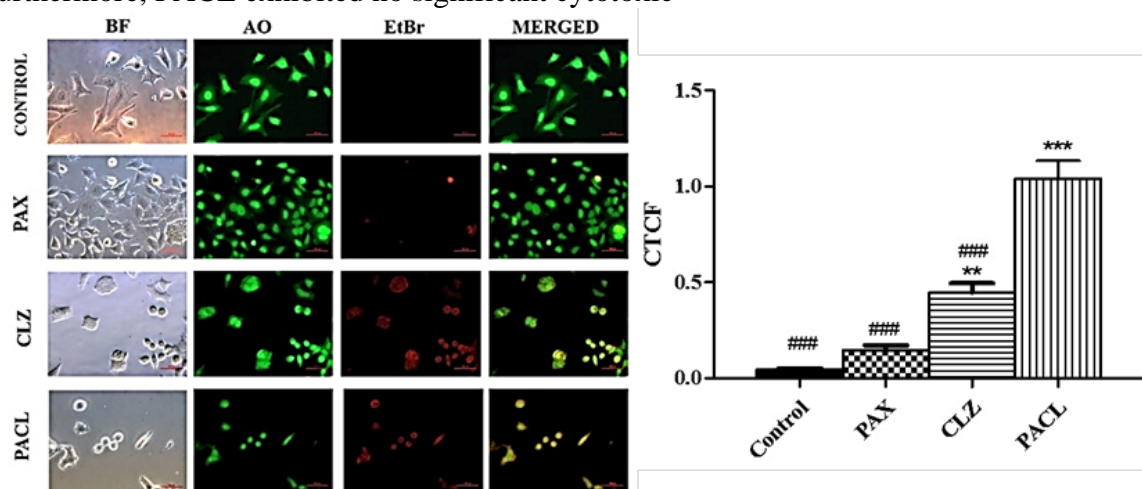


Figure 2.5. AO/EtBr staining of MCF-7 cells treated with PAX (12.5 nM), CLZ (25 μ M) and PACL (PAX 12.5 nM + CLZ 25 μ M). Cells were observed under fluorescent microscope at 200 X magnification and scale bar corresponds to 50 μ M. Graph characterizes the collective total cell fluorescence ratio for red fluorescence representing PI stained dead cells. * denotes $p < 0.05$, ** denotes $p < 0.01$ and *** denotes $p < 0.001$ when fluorescent intensity was compared with control group. Likewise ### denotes $p < 0.001$ when evaluated against combination treated cells. (CTCF: corrected total cell fluorescence).

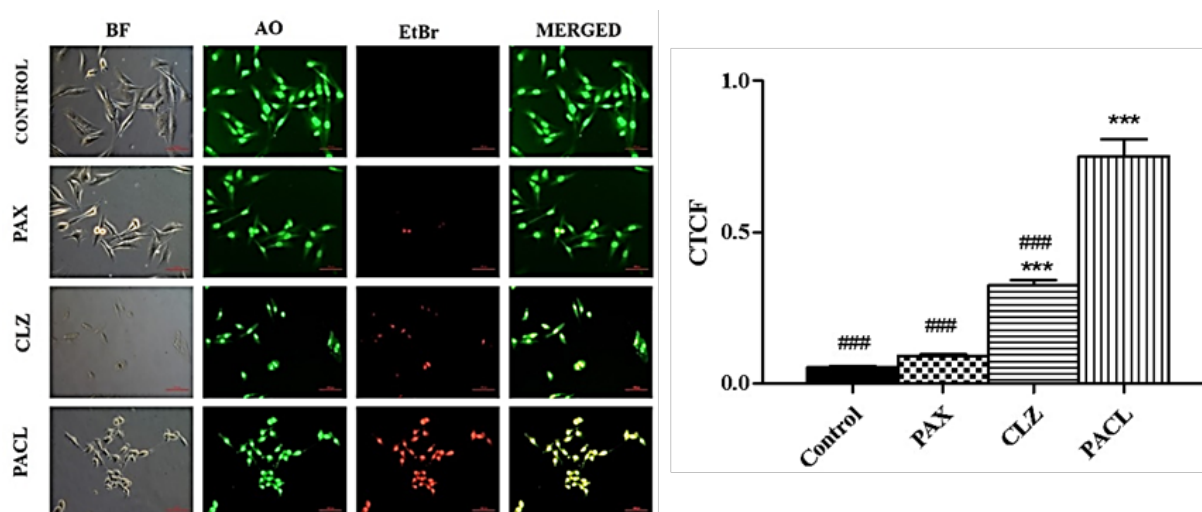


Figure 2.6. AO/EtBr staining MDA-MB 231 cells treated with PAX (12.5 nM), CLZ (25 μ M) and PACL (PAX 12.5 nM + CLZ 25 μ M). Cells were observed under fluorescent microscope at 200 X magnification and scale bar corresponds to 50 μ M. Graph characterizes the collective total cell fluorescence ratio for red fluorescence representing PI stained dead cells. * denotes $p < 0.05$, ** denotes $p < 0.01$ and *** denotes $p < 0.001$ when fluorescent intensity was compared with control group. Likewise ### denotes $p < 0.001$ when evaluated against combination treated cells. (CTCF: corrected total cell fluorescence).

effects on HEK-293 cells (normal epithelial cell line) as presented in Figure 2.3d. These results recommend that combination was effective against breast cancer cells were as less effective towards normal cells.

CompuSyn report and respective CI values for designed combination with their relevant statements are given in APPENDIX-Section-I.

2.3.3. Microscopical evaluation of cell death

2.3.3.1 Acridine orange (AO) and ethidium bromide (EtBr) staining to identify apoptosis

The nuclear morphological alteration in MDA MB 231 and MCF 7 cells were inspected through AO and EtBr, it is also acknowledged as live dead staining. Fluorescent microscopic images of drug treated, and un-treated cells were compared. AO stain both types of cells, live as well as dead cells and the stained cell exhibit green fluorescence when observed under a fluorescent microscope. Whereas, EtBr stains specifically cells with lost membrane integrity and cells demonstrate orange or red fluorescence. Corrected total cell fluorescence (CTCF) was calculated for the cells stained with EtBr (almost red fluorescent) representing apoptotic cells and the graph was plotted to draw a clear conclusion from the captured fluorescent images (Figure 2.5 and 2.6). PACL significantly augmented the fluorescent intensity in MCF 7 by 22.4-folds and MDA MB 231 by 13.8-folds in comparison to untreated cells.

Individual 12.5 nM concentration of PAX displayed 1.8-fold rise in the fluorescence intensity in MCF -7 and in MDA MB 231 by 1.51-fold when compared with control cells. Likewise, CLZ at 25 μ M concentration exhibited small increment in fluorescence intensity by 9.06 folds in MCF7 cells and by 4.9 folds in MDA MB 231 cells, as displayed in in (Figure 2.5 and 2.6). These observations revealed that the PACL has significantly greater cytotoxicity toward cancer cells.

2.3.3.2 4'-6- diamidino-2-phenyl-indole (DAPI) and propidium iodide (PI) staining

To further visualize cellular damage in MDA MB 231 and MCF 7 cells, dual staining was carried out by using DAPI and PI as a fluorescent dye. Bright blue fluorescence colour appeared in the nucleus of cell when DAPI was employed whereas PI displayed red fluorescent stain. DAPI specifically bind to the nucleus of the cell (live or dead), however, PI bind to necrotic and dead cells, as PI cannot migrate through the cellular wall of live cells. Cell treated with combination exhibited profound symptoms of apoptosis, such as cell shrinkage, condensation in chromatin, nucleus fragmentation and reduced cellular density in comparison to untreated cells (Figure 2.7 and 2.8). When the fluorescent intensity was calculated for PI stained dead

cells (through Image-J software), PACL displayed significant increase in the intensity in MDA MB 231 by 15 folds and in MCF 7 by 20 folds in contrast to untreated cells.

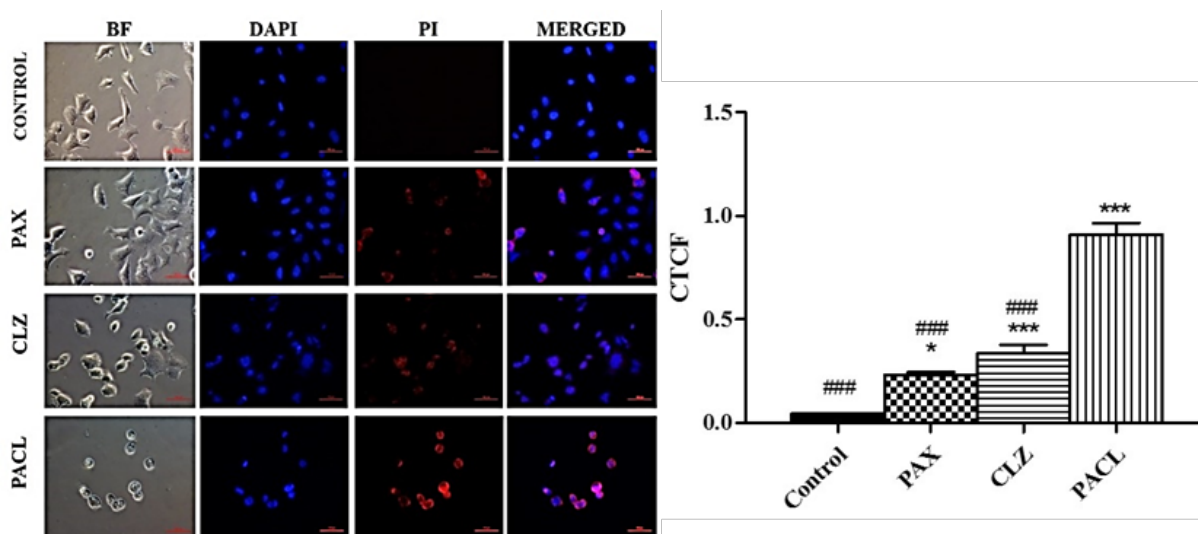


Figure 2.7. DAPI/PI staining of MCF-7 cells treated with PAX (12.5 nM), CLZ (25 μ M) and PACL (PAX 12.5 nM + CLZ 25 μ M). Cells were observed under fluorescent microscope at 200 X magnification and scale bar corresponds to 50 μ M. Graph characterizes the collective total cell fluorescence ratio for red fluorescence representing PI stained dead cells. * denotes $p < 0.05$, ** denotes $p < 0.01$ and *** denotes $p < 0.001$ when fluorescent intensity was compared with control group. Likewise, ### denotes $p < 0.001$ when evaluated against combination treated cells. (CTCF: corrected total cell fluorescence).

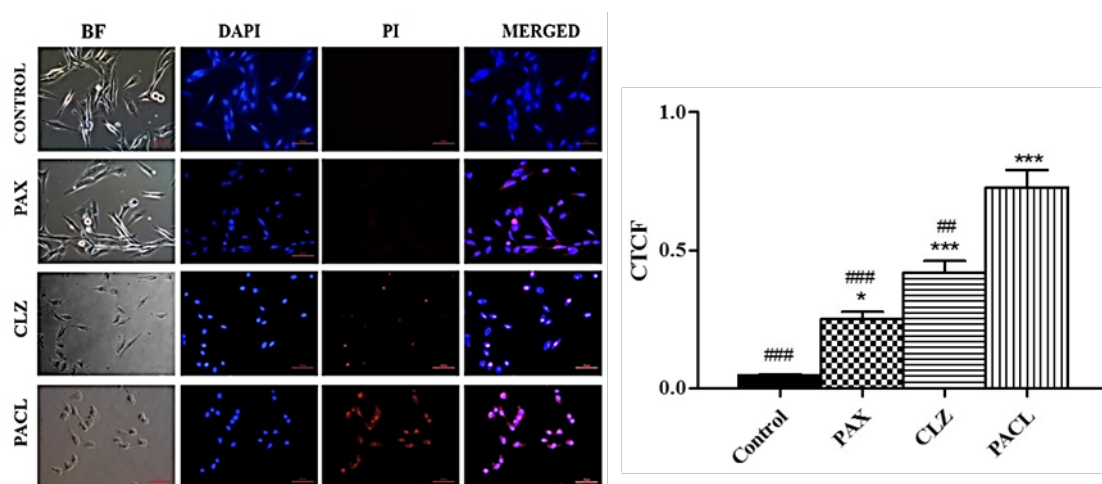


Figure 2.8. DAPI/PI staining of MDA-MB 231 treated with PAX (12.5 nM), CLZ (25 μ M) and PACL (PAX 12.5 nM + CLZ 25 μ M). Cells were observed under fluorescent microscope at 200 X magnification and scale bar corresponds to 50 μ M. Graph characterizes the collective total cell fluorescence ratio for red fluorescence representing PI stained dead cells. * denotes $p < 0.05$, ** denotes $p < 0.01$ and *** denotes $p < 0.001$ when fluorescent intensity was compared with control group. Likewise ### denotes $p < 0.001$ when evaluated against combination treated cells. (CTCF: corrected total cell fluorescence).

However, individual drug treatment of PAX (12.5nM) and CLZ (25µM) exhibited less significant rise in fluorescence intensity for PI (Figure 2.7 and 2.8). These observations verified that, PACL possess enhanced apoptotic effect against cancer cells in comparison to single drug treatment.

2.3.4 Estimation of Reactive oxygen species (ROS)

Subsequently, we estimated the drug induced generation of ROS. ROS is well known to cause serious damage to DNA, proteins and lipid membranes, disrupts normal functioning of cell and thus leads to apoptosis. [138]. We observed significant rise in the level of H₂O₂ with PACL approximately by 4.5 folds in both the cell lines MDA MB 231 and MCF 7, in comparison to untreated cells. Single drug treatment with PAX (12.5nM) exhibited no significant production of H₂O₂, for which MCF-7 exhibited only 1.4-folds of increase and likewise 1.9-folds increase was observed with MDA MB 231 cells. With CLZ at 25 µM concentration only 2.1 folds of rise was observed with MCF 7 and 2.7 folds was exhibited by MDA MB 231 cells (Figure 2.9). These observations suggested that drug combination synergistic induce apoptosis mediated cellular H₂O₂ generation.

2.3.5 Estimation of Reactive nitrogen species (RNS)

In the past decade, it has become evident that rise in the RNS concentration facilitates tumour inhibition and leads to cancer cell death [139, 140]. Thus, we determined the level of NO in the cells treated with drug and for PACL displayed remarkable increase by 2.4 folds in MDA MB 231 and 2.6 folds in MCF 7 cells. While, signal drug treatment unveiled small increase in the level of NO, where, PAX-12.5nM significantly produced 1.7 folds increase in the level of NO in MDA MB 231 and 1.5 increase in MCF 7. Likewise, MDA MB 231 and MCF 7 exhibited 1.9 and 1.7fold increase in the level of NO with CLZ (25 µM) in contrast to untreated cells as presented in Figure.2.9.

2.3.6 Comet assay

To investigate the damage to DNA as a result of drug treatment, comet assay was performed, where the applied electric field cause the migration of fragmented DNA [141]. Small fragments of DNA move faster and appears like a tail of comet, however unharmed DNA looks like intact spherical structure. Tail length signifies the damage to DNA, longer the length greater the damage [142]. Significantly greater DNA damage was detected with PACL treatment in comparison to single drug treatment. PACL induced 50% DNA damage in MCF 7 and 73% in

MDA MB 231 cells. Whereas, PAX (12.5nM) displayed 44% and 18% DNA damage in MDA MB 231 and MCF 7 cells while CLZ (25 μ M) exhibited 61% DNA damage in MDA MB 231

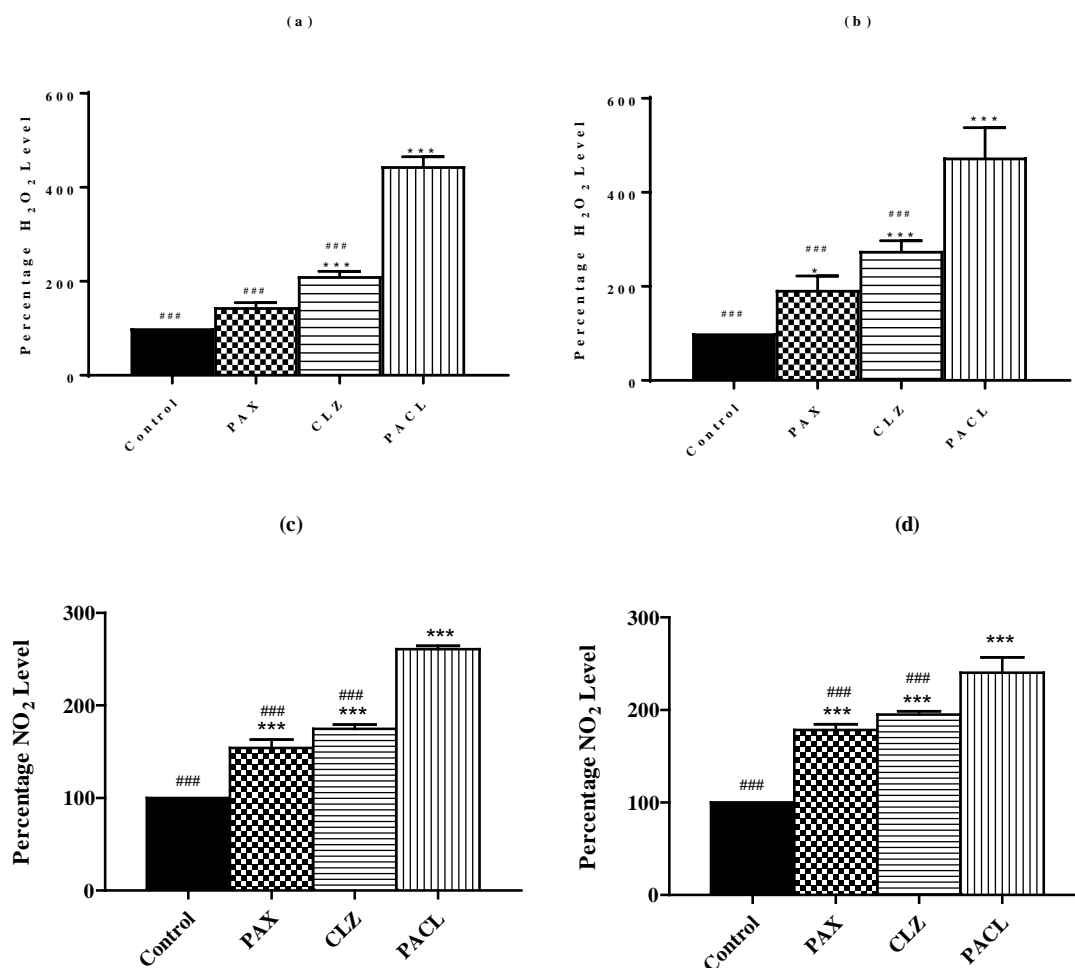


Figure 2.9. Percentage of H₂O₂ and NO level as an effect of PAX (12.5 nM), CLZ (25 μ M) and PACL (PAX 12.5 nM + CLZ 25 μ M) on MCF-7 (a and c) and MDA-MB-231 cells (b and d). Bars represents mean \pm SEM (n = 3). * indicates p<0.05, ** indicates p<0.01 and *** indicates p<0.001 when comparison made with control. Likewise, # indicates p<0.05, ## indicates p<0.01 and ### indicates p<0.001 in comparison to combination group for both cell lines (MCF-7 and MDA-MB-231).

and 34% in MCF 7 respectively (Figure 2.10). These findings confirm the synergistic activity of PACL against breast cancer cells in contrast to single drug treatment.

2.3.8. Glucose consumption

There is always an increased glucose requirement during tumour progression in contrast to normally growing cells and inhibition in glucose uptake leads to apoptosis [143]. Cellular glucose consumption was measured after the drug treatment, where we observed the 15% of glucose uptake in MCF 7 and approximately 20% of glucose was utilized by MDA MB 231 cells (Figure 2.11).

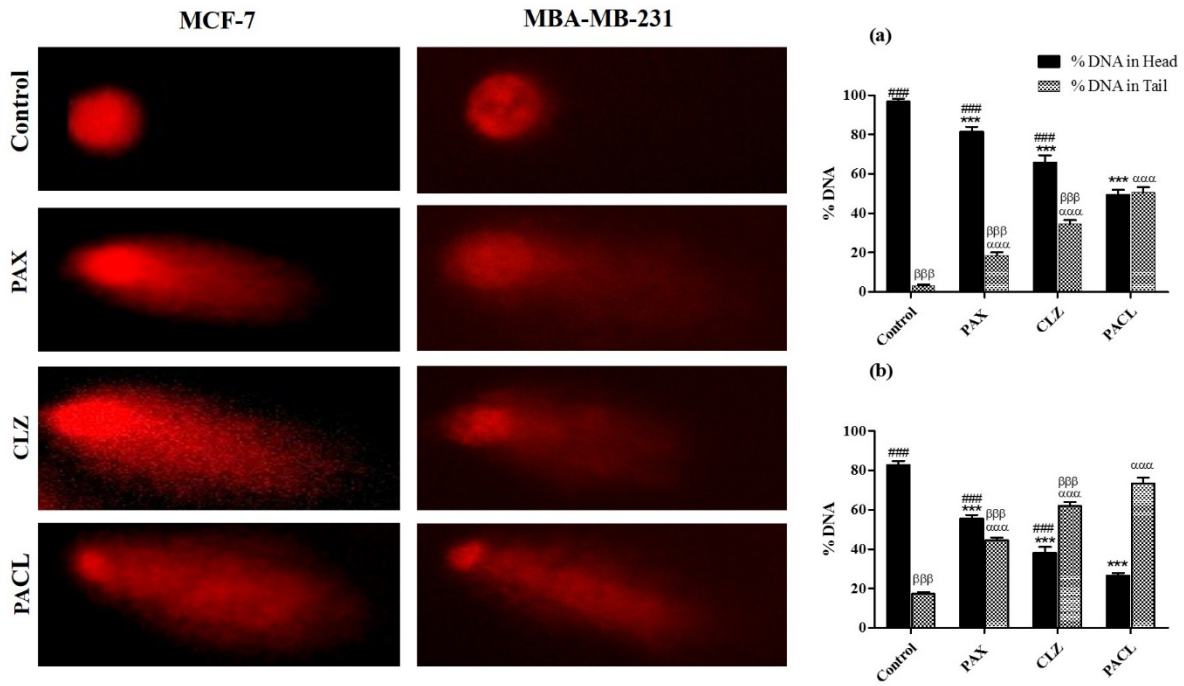


Figure 2.10. Genotoxic effect of PAX (12.5 nM), CLZ (25 μM) and PACL (PAX 12.5 nM + CLZ 25 μM) against MCF-7 and MDA-MB-231 cells. Graph represents the relative percentage of DNA in head and tail of MCF-7 (a) and MDA-MB-231(b) cells. *** specifies $p < 0.001$ when % DNA in head was compared with control and #### indicates $p < 0.001$ when % DNA in head compared with combination group. Likewise ααα denotes $p < 0.001$ when % DNA in tail was correlated with control and βββ denoted $p < 0.001$ when % DNA in tail was compared with combination treated cells for both cells (MCF-7 and MDA-MB-231).

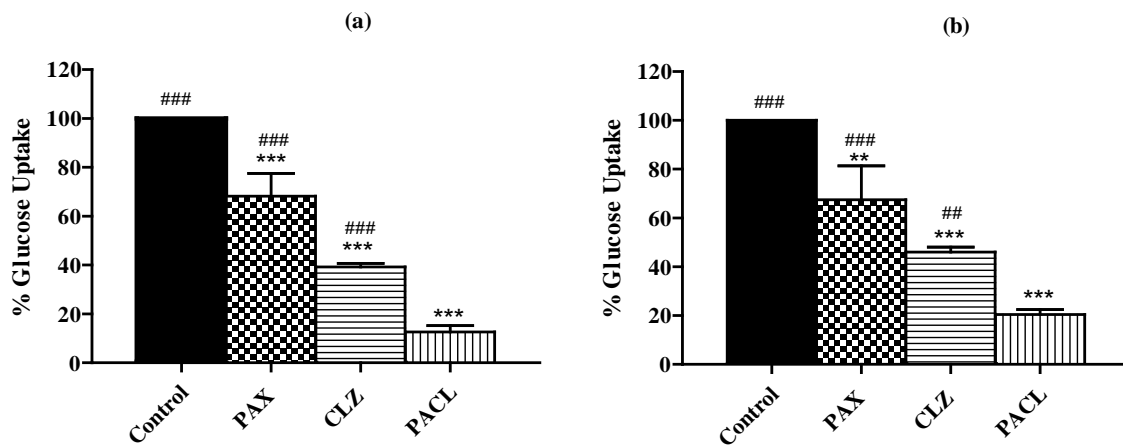


Figure 2.11. Glucose uptake in MCF-7 (a) and MDA-MB-231 (b) as an effect of PAX (12.5 nM), CLZ (25 μM) and PACL (PAX 12.5 nM + CLZ 25 μM). Presented bars denote mean ± SEM (n = 3). ** express $p < 0.01$ and *** express $p < 0.001$ when comparison made with control cells. Similarly, ## directs $p < 0.01$ and #### directs $p < 0.001$ when compared to combination treated cells.

While. Single drug treatment of PAX at 12.5 nM concentration exhibited 70% utilization of glucose in MCF 7 cells and 60 % in MDA MB 231 cells. Similarly, CLZ (25 μ M) displayed 50% of glucose uptake in MDA MB 231 and 45% in MCF 7 cells respectively. Presented data clearly displayed the synergistic inhibition in glucose uptake in cells treated with PACL.

2.4 SUMMARY POINTS

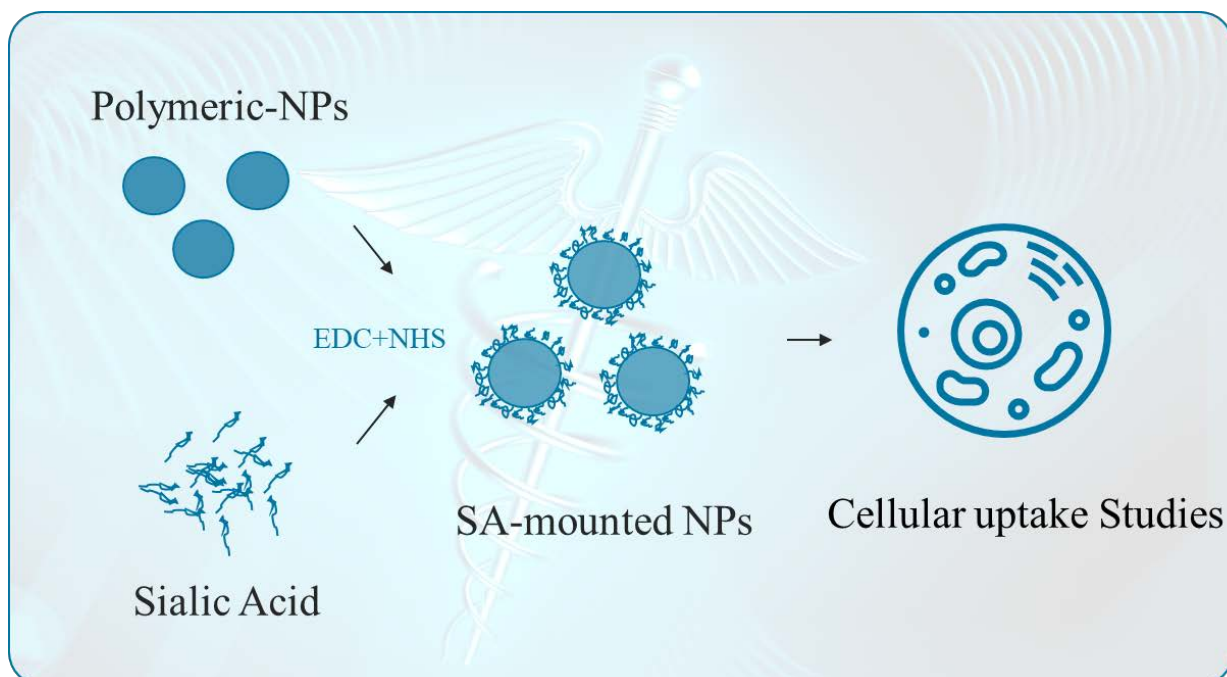
- Physical mixture of PAX and CLZ was found to be compatible as revealed from FTIR-spectral analysis, where no chemical interaction was detected.
- Cytotoxic studies displayed synergism between PAX and CLZ in combination at reduced concentration against breast cancer cell lines, that was further confirmed through CompuSyn Software analysis.
- Combination induced genotoxicity, increased oxidative & reactive nitrogen stress and glucose deprivation in breast cancer cells
- PAX and CLZ in combination possess minimal toxicity towards normal epithelial cells as revealed from HEK-293 cell line.



CHAPTER-3

FORMULATION AND CHARACTERIZATION OF SIALIC ACID CONJUGATED NANOPARTICLES.

GRAPHICAL OVERVIEW OF THE CHAPTER



HIGHLIGHTS

- Fabrication of SA surface functionalized NPs by exploiting carbodiimide chemical reaction.
- Surface morphological investigation (SEM) and particle size determination.
- Photoluminescence study of SA-rhodamine-loaded NPs to represent cell specificity
- *In-vitro* drug release studies to demonstrate the effect of surface functionalization of SA.
- Comparative cytotoxic studies of drug-loaded-NPs on breast cancer cells and normal epithelial cells

3.1 INTRODUCTION

Nanotechnology has provided intense scope of advancement in drug delivery to specific cells or tumour by employing nanoparticles, which is an integral part of cancer nanomedicine [144]. Polymeric nanoparticles (NPs) have drawn abundant attention over past 3 decades because of their distinguished features to encapsulate a variety of drugs, enhancing the stability of therapeutic agents and increasing the bio-distribution of active ingredients [145]. So far polyethylene-glycol (PEG) modified NPs are thought to be the milestone for various advancements in nanomedicine. As surface functionalized PEG-NPs has shown a dramatic reduction in surface protein adsorption through steric repulsion and hydrophilicity [146]. This permits the NPs to attain stealth modification, eventually by which NPs persist themselves within the bloodstream for a longer duration of time. The enhanced permeability and retention (EPR) effect describe the fact that tumour retain more polymeric NPs than the normal tissue and hence enable NPs to acquire passive targeting [22].

Regardless of the benefit of biodistribution obtained through PEGylation and EPR effect, majority of NPs are inevitably detected by reticuloendothelial system (RES), and thus, eradicated from the body by mononuclear phagocytes. To avoid RES uptake of NPs, active targeting can be explored to achieve spatial localization by deliberately homing NPs to desired tumour locations while eliminating off-target adverse effects in normal tissue [22].

Sialic acid (SA)/poly-sialic-acid (PSA) is an endogenous electro-negatively charged monosaccharide moiety present in higher animal. PSA can serve as a potential alternative to reduce or eliminate the drawbacks of passive targeted NPs, as PSA is biocompatible, non-toxic, non-immunogenic and biodegradable. PSA conjugated NPs can transport drug directly into the vicinity of tumour through receptor-mediated endocytosis and increase the potency of drug. Likewise, PSA conjugation to NPs will administer hydrophilicity and defend NPs from interacting with plasma proteins or macrophages, evading RES uptake and extending circulation half-life. Meanwhile, PSA degradation yields CO₂ and water that are non-toxic to living organisms. Apart from these, PSA can serve as targeting moiety for selectin (E-selectin/P-selectin) as these are overexpressed in the tumour vascular endothelial cells. Therefore PSA-modified-nanocarriers can be delivered to tumour cells more efficiently and consequently chemotherapeutic drugs can be targeted actively for cancer therapeutics [22, 89]. Literature suggests numerous techniques have been attempted to conjugate sialic acid to the surface of polymeric NPs. Notably, it always comes at the virtue of increased risk of toxicity

as attributive to the increased number of chemicals involved in the synthesis steps along with increased cost.

Carbodiimide crosslinking methodology is a successful and efficient technique to conjugate protein moiety on the surface of polymeric NPs. It possesses a special feature; zero-length cross-linking of reagent by establishing stable amide bond between carboxylic acid group and amine group and will benefit further by retaining the dimensions of NPs in nano scale. Additionally, it offers the benefit of low toxicity as *N*-(3-dimethylaminopropyl)-*N*'-ethylcarbodiimide (EDC), *N*-hydroxy succinimide (NHS) themselves are not involved in final cross-linked product.

The present study is focused on developing a simple technique to conjugate amine rich PSA moiety to the surface of poly-caprolactone (PCL)-NPs comprising of carboxylic group through carbodiimide (EDC+NHS) reaction to overcome passive transport drawbacks, enhance cancer targeting and cell-penetrating abilities of formulated NPs. Paclitaxel (PAX) is most frequently and widely prescribed chemotherapeutic agent for the treatment of breast carcinomas. It was used as a model drug for encapsulation and to demonstrate the efficiency of sialic acid mounted polymeric NPs.

3.2. MATERIALS AND METHODS

3.2.1 Materials

PCL (MW~ 14,000) was bought from Sigma-Aldrich (St. Louis), polyvinyl alcohol (PVA) was bought from Hi-media Laboratories. *N*-(3-dimethylaminopropyl)-*N*'-ethylcarbodiimide (EDC), 2-(*N*-morpholino) ethanesulfonic acid (MES), and *N*-hydroxy succinimide (NHS) were acquired from Sigma Aldrich. Like-wise Triton X-100, 3-(4,5-dimethylthiazol-2-yl)-2,5-diphenyltetrazolium bromide (MTT) was also obtained from Sigma Aldrich. Other reagents used in the study included acetone procured from Fischer Scientific and Trypsin- EDTA, fetal bovine serum (FBS), antibiotics- antimycotics, Dulbecco's modified Eagle's medium (DMEM) and Phosphate buffer saline (PBS) purchased from Gibco, Luria- Bertani (LB)-media was acquired from Merck Specialities Pvt. Ltd India. Water used for the experiments was purified using a Milli-Q Plus 185 water purification system (Millipore, Bedford, MA) with resistivity greater than 18 M Ω cm.

3.2.2 Preparation of PSA - PCL polymeric NPs

3.2.2.1 Fabrication of PCL-polymeric NPs

Polymeric NPs were fabricated by employing previously well-established protocol of single emulsion (o/w) method with slight modification [111]. Briefly, 100 mg PCL and 5 mg PAX

was dissolved in 2.5 ml dichloromethane (DCM). The solution was initially mixed with 5 ml of 5% w/v Poly-vinyl alcohol (PVA) under sonication (probe Oscar Ultrasonics-India) for 30 seconds at 17.5 W to obtain an o/w emulsion. The emulsion was further diluted with 15 ml of 1 % (w/v) PVA solution (aqueous based) followed by stirring at moderate speed for 3h to remove traces of DCM in the solution. The resulting admixture was washed at least thrice with ultrapure water followed by filtration (100 kDa Amicon filters). The procured NPs pellet was resuspended, freeze dried (AllicetFrost-80CNew Braswick) along with 3% mannitol and finally stored at 4°C. The Rhodamine (Rhd) loaded PCL-NPs were also fabricated by taking .01 mg/ml of Rhd for synthesis followed by the same procedure. Likewise, blank nanoparticles were fabricated by similar process.

3.2.2.2 Synthesis of PSA-PCL NPs

Sialic acid was mounted on PCL-NPs by exploiting carbodiimide reaction. Briefly, the lyophilised NPs were dispersed in carbodiimide solution (5 mM EDC and 10 mM NHS in 50 mM MES buffer, pH = 5.5) for 4h at room temperature. NPs were then rinsed twice with PBS using filter (100 kDa Amicron filter) to remove unreacted EDC and NHS. Carboxylic group activated NPs were incubated with PSA (50 mg in 10 ml of ultrapure water) for 4h at 37°C with gentle agitation. NPs were washed thrice ultrapure water to remove unconjugated sialic acid followed by lyophilization.

3.2.3 Particle size distribution and zeta potential analysis

Particle size, zeta potential and poly-dispersity index (PDI) analysis of formulated NPs were performed by using Malvern Zetasizer Instrument. Lyophilised NPs were resuspended in deionised-water, temperature was sustained at 25°C and the values were determined by taking measurements in triplicate.

3.2.4 Morphological analysis

Morphological inspection of the fabricated NPs was performed through scanning electron microscope (SEM-QUANTA 250, FEI Makers), moving electrons were made to incident on the sample particles placed inside the vacuum chamber while mounted on the metal stubs using double sided adhesive tape.

3.2.5 Fourier Transform Infrared (FTIR), Ultra violet (UV)-Visible Spectrophotometer analysis and X-Ray diffraction (XRD) analysis.

FTIR spectrum were determined (FTIR Instrument of Agilent Technologies 630 Cary using Micro Lab software) with the purpose to investigate the possible chemical functional group changes upon incorporation of sialic acid on PCL-NPs. To assure SA conjugation on NPs, we performed UV-Visible spectrophotometric analysis (Thermo-Scientific- Evolution-201). The

respective FTIR and UV spectrums were obtained through software and interpreted accordingly. Further, XRD pattern was investigated for conjugate (SA-PCL-NPs) as well as non-conjugated (PCL-NPs) nanoparticles. XRD graph was recorded at 2θ range of 0° - 80° , through D8-Advance of Bruker (Germany), Cu Ka radiation (45 kV, 40 mA).

3.2.6 Quantification of drug encapsulation and drug loading

To quantify the drug content of the designed NPs, lyophilised drug-encapsulated NPs were dissolved in acetonitrile. The resulting solution was mixed vigorously through vortex followed by incubation in shaking incubator for 3 h at 37°C in-order to remove acetonitrile from the solution. Amount of drug in the resulting solution was quantified through UV-absorption at specific wavelength of 229 nm (Thermo-Scientific- Evolution-201). The drug encapsulation efficiency and the drug loading was determined through following equations:

$$\text{Encapsulation Efficiency (\%)} = \frac{\text{Mass of encapsulated drug}}{\text{Mass of initial drug}} \times 100 \quad (1)$$

$$\text{Drug loading (\%)} = \frac{\text{Mass of encapsulated drug}}{\text{Mass of polymer used for encapsulation}} \times 100 \quad (2)$$

3.2.7 *In-vitro* drug release study

In-vitro drug release from NPs was evaluated by using a dialysis bag (molecular weight cut-off: 8,000-14,000). The PAX loaded NPs (20mg/2ml) were placed into the dialysis bag (dialysis membrane was pre-activated by soaking it in PBS for 24 h). Dialysis bag was immersed in 20 mL of PBS maintained at pH of 7.4 and 6.8 at 37°C with 100 rpm, containing 0.1% (v/v) Tween 80 (non-ionic surfactant). At designated time intervals, 1 mL release medium was removed and, subsequently, fresh medium (1ml) was added to maintain a sink condition. Afterwards, the content of PAX was quantified by UV spectrophotometer (wavelength 229 nm). The experiment was performed in triplicate and the resulting data was expressed in the form of percentage cumulative drug release.

3.2.8 Cell line and culture

MCF 7 and MDA MB 231 cell lines were procured from the NCCS, Pune, India and HEK-293 cell line was obtained as gift from AMITY University, Noida (India). The cells were seeded in tissue culture flask comprising growth medium solution (DMEM for MCF 7 and L-15 for MDA MB 231) accompanied by 10% FBS and 1% antibiotics (100 U/ml penicillin and 100 $\mu\text{g/ml}$ streptomycin). Cells were incubated and maintained at 37°C in a humidified atmospheric incubator supplemented with 5% CO_2 .

3.2.8.1 *In-vitro* cytotoxicity studies

The *in-vitro* cellular toxicity of formulated NPs was determined through standard MTT assay using human origin breast cancer cell line (MCF 7 and MDA MB 231) and normal cell lines

(HEK 293). Briefly, the cells were seeded (1×10^4 /well) in 96 well tissue culture plate for 24h prior to experiment. Formulated NPs were incubated with cells for different intervals (0, 6, 12, 24 and 48h). After incubation, 25 μ l of MTT (5 mg/ml) solution was added to each well and incubated further for 4h. Formazan thus produced by viable cells was dissolved by adding 200 μ L dimethyl sulfoxide (DMSO). The optical densities were recorded through a microplate reader (model-680, Bio-Rad) at 570 and 630 nm as test and reference wavelength subsequently. Cell viability percentage was calculated through following equation:

$$\text{Cell viability (\%)} = \frac{\text{OD (Test well)}}{\text{OD (reference well)}} \times 100 \quad (3)$$

All the results were assured by repeating the individual tests in triplicate for each time.

3.2.9 Photoluminescence spectrophotometric analysis for cellular uptake

To validate the cellular uptake of the synthesized NPs, the cells were seeded in 12 well plate (2×10^5 cells/well) prior to experiment for 24 h. After incubation cells were exposed to Rhd-PCL-NPs and SA-Rhd-PCL-NPs (10 mg/ml) for 3h followed by rinsing with PBS. Cell were harvested through trypsinization and extracted through DMSO (500 μ l). Supernatant was collected and further diluted by adding 2 mL of PBS. Samples were characterized through photoluminescence spectrophotometer (Perkin Elmer LS55 fluorescence) with an excitation sources from Xe lamp with in wavelength of 200-900 nm. Graphs were recoded, and intensity of the graphs exhibit the corresponding cellular uptake of NPs.

3.2.10 Fluorescent microscopic analysis of cellular uptake

To confirm and demonstrate the cancer cell specificity of formulated NPs, we performed the experiment by exposing cells (HEK 293, MCF 7 and MDA MB 231) to rhodamine loaded NPs. Cells were seeded in 12 well tissue culture plate with appropriate cell growth medium till the cells are 70% confluent. Prior to experiment, cell growth medium was removed, and the cells were exposed to PCL-Rhd-NPs and SA-PCL-Rhd-NPs upto 3h. Cells were washed with PBS twice and fixed with 4% paraformaldehyde solution for 15 min followed by washing with PBS. 5 μ L of DAPI (1 μ g/mL) was added to each well with the aim to visualize the nucleus of the cultured cells. Corresponding cellular images were captured by using fluorescent microscope (Nikon-ECLIPSE-Ti-U) and the inference was drawn by calculating fluorescent intensity through Image-J software.

3.2.11 Statistical analysis

Experiments were conducted in triplicate and results were articulated as mean \pm standard deviation. Statistical analysis was performed by using GraphPad Prism software (version 6) and comparisons between groups were carried out using one-way ANOVA.

3.3 RESULTS AND DISCUSSION

3.3.1 Characterization of synthesized nanoparticles

SEM analysis exhibited spherical morphology of synthesized PCL-NPs and SA-PCL-NPs (Fig.3.1a and b). Both the formulations were found to be in nano range. Size distribution of PCL-NPs and SA-PCL-NPs were 151.5 nm and 179.47 nm respectively (Fig.3.1c). Interestingly, we witnessed the increase in negative surface charge for SA-PCL-NPs in contrast to PCL-NPs that may be attributive to surface functionalization of sialic acid (Fig.3.1d).

Table 3.1: Formulation Table

Formulation	PCL (mg)	PVA	Drug (mg)	Conjugation	Entrapment Efficiency (%)
PCL-NPs	100	1%	-	-	-
SA-PCL-NPs	100	1%	-	SA	-
PCL+PAX-NPs	100	1%	PAX (5)	-	34.4 ± 2.3
SA-PCL+PAX-NPs	100	1%	PAX (5)	SA	

Mean ± SD; n = 3

FTIR-spectral interpretation was performed to check the surface modification of un-conjugated NPs (PCL-NPs). Characteristic peak for sialic acid were; O-H stretch was recognized at 3282cm⁻¹, strong amide peak was observed at 1644cm⁻¹ representing C=O and 1518cm⁻¹ depicts the N-H bending. PCL-NPs represents the specific C-H stretching at 2948cm⁻¹ and 1726cm⁻¹ exhibiting carboxylic acid C=O strong peak. FTIR spectra of SA-PCL-NPs displayed the SA acid peak at 3282, 1644 and 1518 cm⁻¹ representing the O-H, C=O and N-H peaks respectively and the characteristic peak of the PCL was also recorded (2948 and 1726cm⁻¹ representing C-H and C=O). FTIR-spectral analysis reveals the conjugation of SA on the surface of PCL-NPs Fig.3.2a

To further investigate the SA surface functionalization, UV-visible spectrophotometric analysis was performed. SA-PCL-NPs represents the strong peak at 281 nm, that corresponds to the protein absorption peak arising due to the aromatic ring presence. Whereas, protein peak was found to be absent in the PCL-NPs (Fig.3.2b) . These results verify the SA mounting on the surface of PCL-NPs.

XRD pattern of the PCL-NPs showed the major peaks specific for PCL at $2\theta = 21.5^\circ$ and 23.8° (Fig.2c), which can be assigned to (110) and (200) planes of PCL. After being conjugated with sialic acid, SA-PCL-NPs shows the crystalline characteristics of SA as evidenced from the presence of typical crystalline peaks and it was also noted that peaks in SA-PCL-NPs became slightly broader and weaker in contrast to PCL-NPs, implying low crystallinity (Fig.3.2c). FTIR analysis, UV-spectral investigation and XRD analysis assured the sialic acid mounting on the surface of the PCL-NPs.

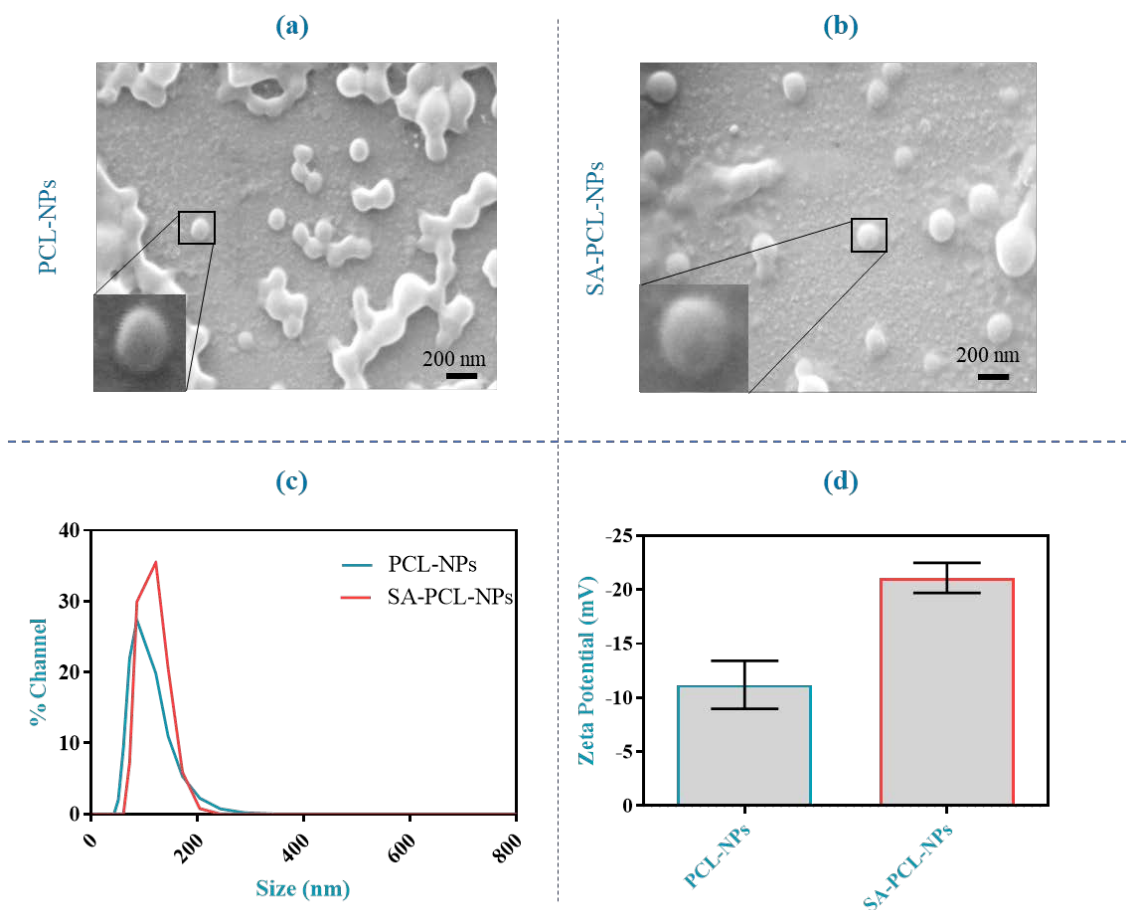


Figure 3.1: Surface morphological analysis through visualized through scanning electron microscopy for (a) un-conjugated NPs and (b) sialic acid conjugated NPs. (c) particle size distribution of distinct NPs and (d) zeta potential of the formulated NPs.

3.3.2 Drug encapsulation efficiency, loading and release

Drug encapsulation efficiency and drug loading was found to be 34.4% and 3.12% respectively (Table 3.1). *In-vitro* drug release studies was performed to investigate weather sialic acid funtionalization have any effect on releasing pattern of drug or not.

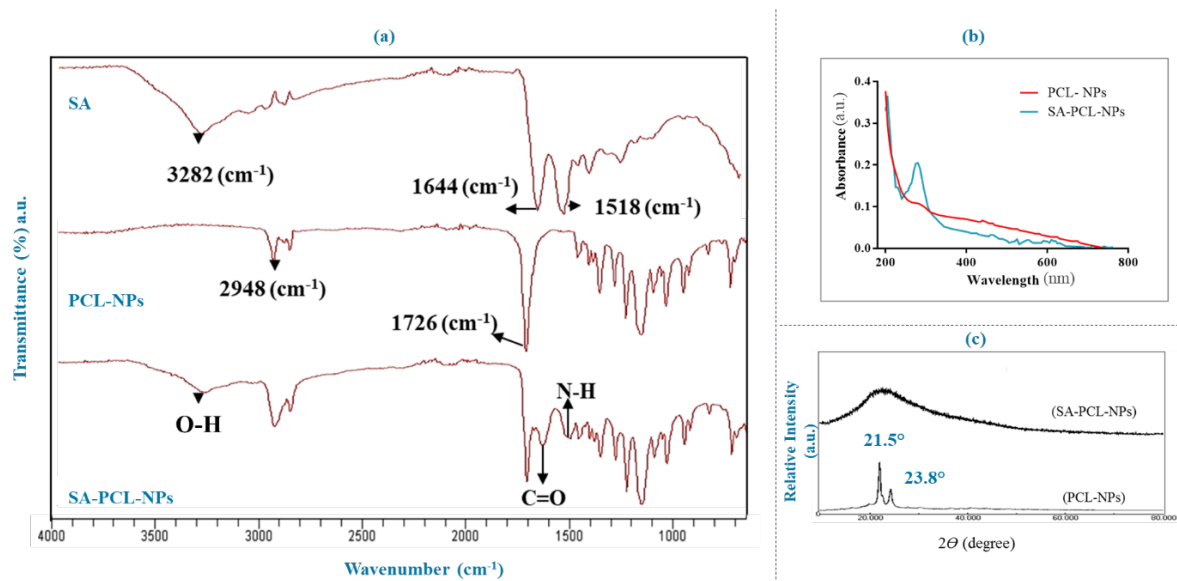


Figure 3.2: Presenting (a) Fourier-transform infrared spectroscopic graph of formulated NPs, UV (Ultraviolet-Visible) Spectroscopic Graph, (b) UV (Ultraviolet-Visible) Spectroscopic Graph and (c) **XRD** (X-Ray Diffraction) analysis of conjugated and un-conjugated nanoparticles.

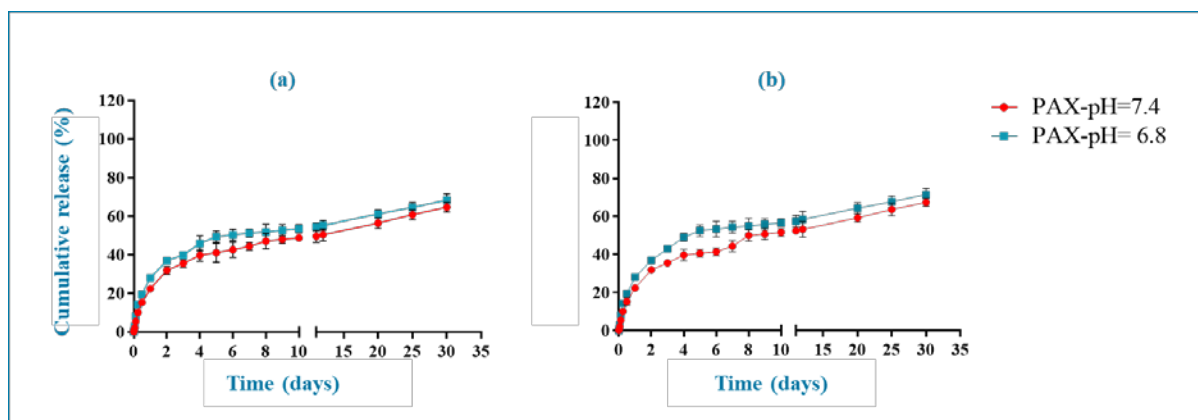


Figure 3.3: In-vitro drug release profile of PAX from (a) un-conjugated-PCL-NPs and (b) SA-conjugated-PCL-NPs at two different pH (6.8 and 7.4 pH). Data expressed as mean \pm standard deviation, n=3.

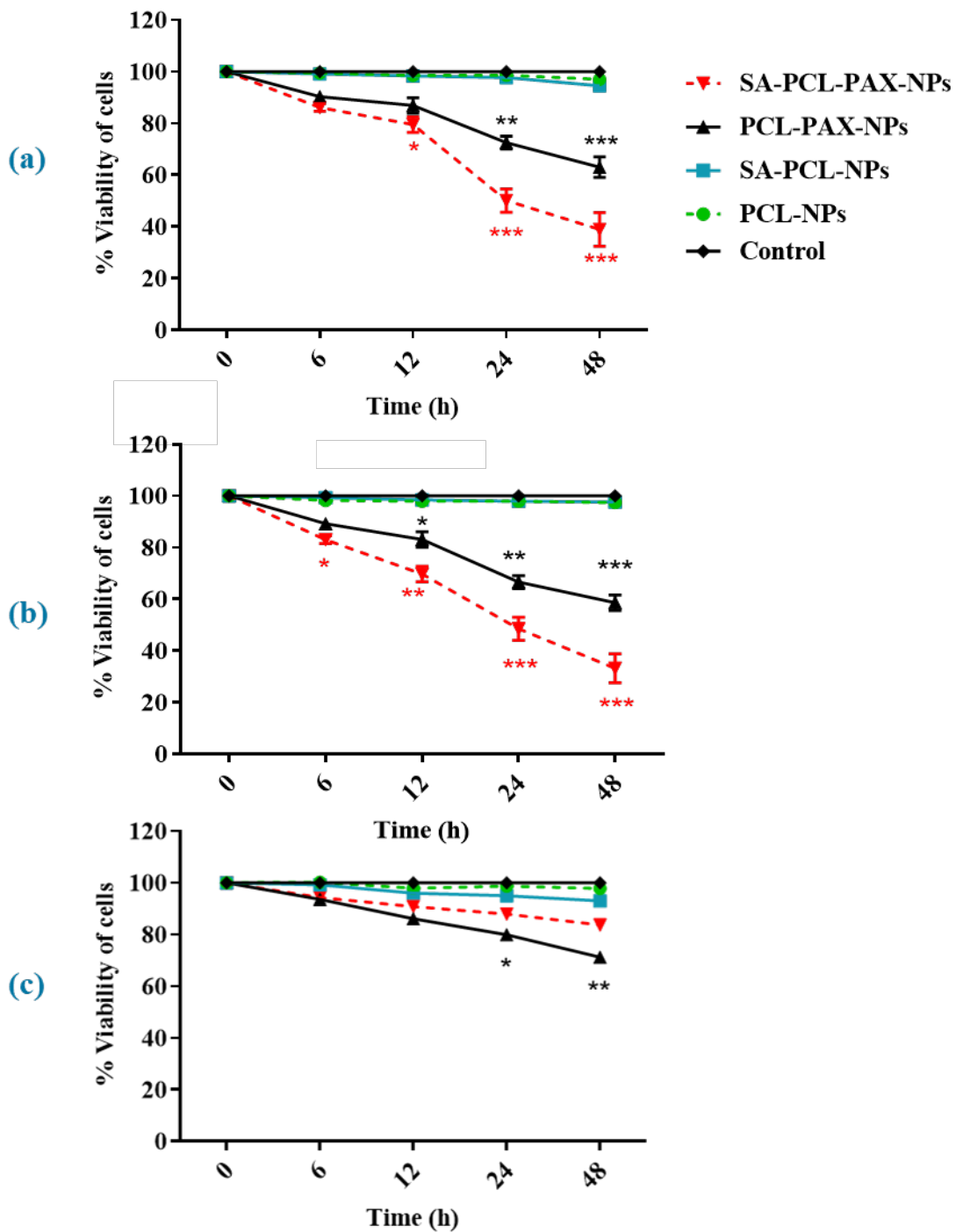


Figure 3.4: Time dependent cytotoxic effect of different formulation on breast cancer cells (a) MCF-7, (b) MDA-MB-231 and on normal cells (c). *** designates $p < 0.001$, ** designates $p < 0.01$ and * designates $p < 0.05$ when compared with untreated cells respectively.

Drug release profile for conjugated as well as non-conjugated NPs were examined at different pH conditions (7.4 and 6.8 pH), simulating the blood physiological pH and pH of endosomal compartments of breast, respectively. As represented in figure 3.3, initially, fast drug release

was witnessed followed by sustained drug release for both releasing media (7.4 and 6.8 pH). We observed no significant variation in drug release pattern with sialic acid modified NPs, suggesting that sialic acid functionalization have no effect on release pattern from NPs.

3.3.3 Cell cytotoxicity

MTT assay was conducted to evaluate the effect of drug loaded NPs (PCL-PAX-NPs and SA-PCL-PAX-NPs). Cells were incubated with fabricated nanoparticulates for different time periods ranging from 0 to 48h. PCL-NPs and SA-PCL-NPs did not display any sign of cell cytotoxicity in breast cancer cell lines (MCF 7 and MDA MB231) as well as in normal HEK 293 cells. These results hence provided us an evidence that SA conjugation have no effect on healthy epithelial cells and thus safe for further use. SA-PCL-PAX-NPs was found to be most cytotoxic in contrast to other drug loaded formulation and exhibited time dependent cytotoxicity against breast cancer cell lines. PCL-PAX-NPs also exhibited the cell toxicity in time dependent manner as displayed in Fig. 3.4. Uppermost cell killing capability was observed with sialic acid functionalized drug loaded NPs and this might be possibly because of sialic acid driven specific cancer cell uptake and avoiding normal cellular interaction.

3.3.4 Photoluminescence analysis.

To further reassure the SA specific cancer cell uptake, we replaced drug with Rhd, thus formulated Rhd-loaded NPs and these nanoparticulates were incubated with breast cancer cells and normal epithelial cells. More intense peak in graph corresponds to increased accumulation of nanoparticulates inside the cells. Interestingly, SA-PCL-Rhd-NPs exhibited the noteworthy rise in fluorescent intensity for both cancer cell lines (MCF 7 and MDA MB 231) when compared with PCL-Rhd-NPs, suggesting the greater interaction of Rhd-NPs with cancer cells.

Whereas, HEK 293 cells exhibited very less florescent intensity in comparison to breast cancer cells and this may be attributive to passive influx of the NPs. Results reveals that sialic acid functionalized NPs had successfully homed inside the cancer cells, signifying cancer cell specific uptake. Graph for blank and only Rhd-NPs were also recorded and represented in figure 3.5 for comparative analysis.

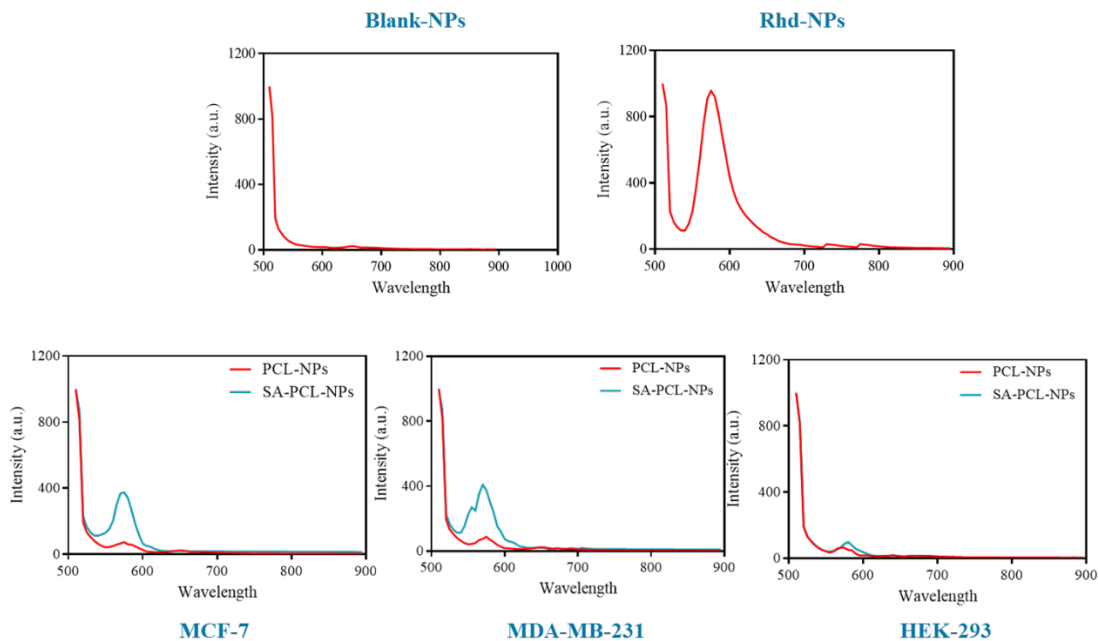


Figure 3.5. Representative photoluminescence graph showing effect of rhodamine loaded nanoparticles in different cell lines.

3.3.5 Microscopic analysis of cellular uptake

To validate the cell specific uptake, Rhd-NPs were formulated and exposed to normal (HEK 293) and cancerous (MCF 7 & MDA MB 231) cells. Fluorescent microscopic images were acquired and further studied to prove our previous results of SA mediated cancer cell targeting. As presented in Fig 3.6, HEK 293 cells exhibited no fluorescent intensity that signifies less or no cellular uptake of NPs. Whereas, both breast cancerous cell line displayed rise in the red fluorescent intensity, suggesting increased accumulation of Rhd-NPs in-side the cell. This was further confirmed through calculating corrected total cell fluorescence (CTCF) values (intensity calculated for Red fluorescence) exhibited that cancer cells were having intensity higher than that of normal cells.

Results suggests that NPs mounted with SA had represented higher cellular uptake in contrast to non-coated-NPs. It was also witnessed that SA facilitates the NPs uptake in cancer cells in comparison to normal cells.

Detailed images of Rhd-loaded- NPs for each cell lines (HEK 293, MCF 7 & MDA MB 231) has been represented in the APPENDIX- Section-II.

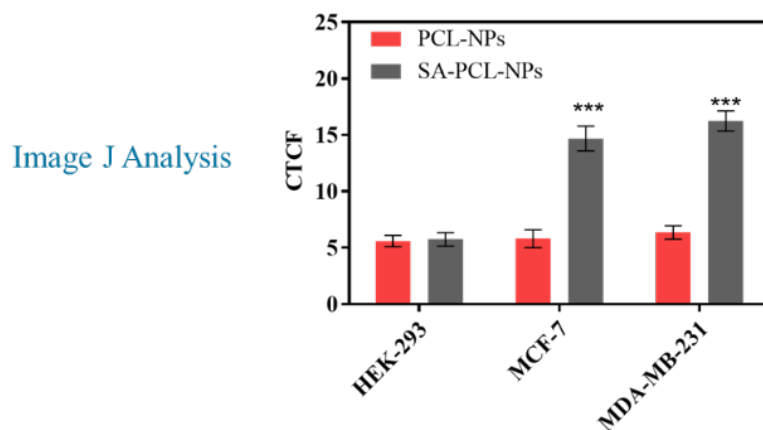
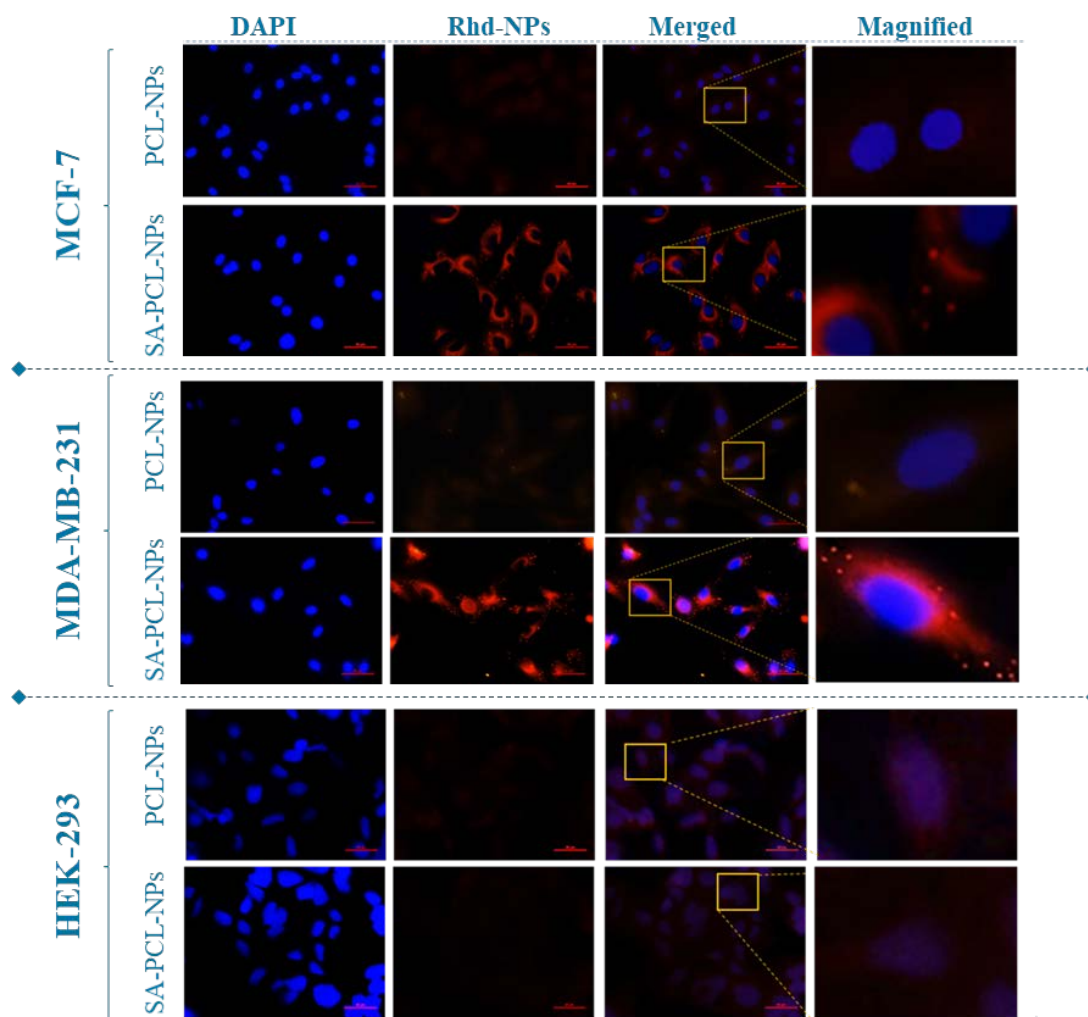


Figure 3.6: Fluorescent images representing the cellular uptake of rhodamine loaded nanoparticles in different cell lines. The scale bar of images corresponds to 50 μ M (200X). Graph represents the corrected total cell fluorescence (CTCF) for red fluorescence indicating dead EtBr stained cells. *** indicates $p < 0.001$ when fluorescent intensity compared with HEK-293.

3.5 SUMMARY POINTS

- A simple method for fabricating SA surface-functionalized PCL-NPs with improved cancer-targeting and cell-penetrating abilities has been confirmed in the presented chapter.
- Characterization revealed spherical & smooth surface morphology for formulated SA-conjugated as well as for un-conjugated nanoparticles.
- SA-rhodamine-loaded NPs exhibited tumour specificity as revealed from photoluminescence study and by performing fluorescent imaging.
- Drug loaded NPs also confirm our results that, SA-drug-loaded- NPs were more cytotoxic to breast cancer cell lines where as little or no cytotoxic effect was observed on normal cells.
- Our results indeed suggest that SA surface functionalized- NPs could be a decent active targeting approach to remove the limitation of passive targeting of nanomaterials and it also provide ample scope to develop novel chemotherapeutic for breast cancer.

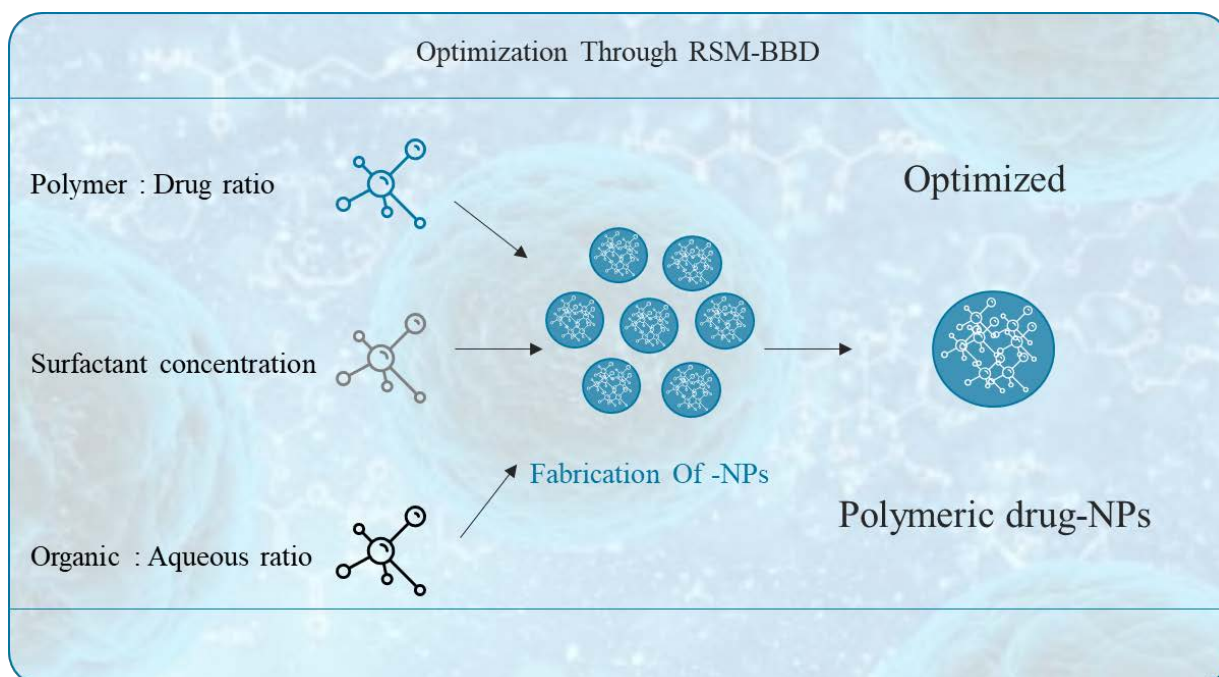


CHAPTER-4

OPTIMIZATION OF DRUG LOADED POLYMERIC NANOPARTICLES



GRAPHICAL OVER VIEW OF THE CHAPTER



HIGHLIGHTS

- Optimization of variable through Response Surface Methodology (RSM).
- Box Behnken design (BBD) generated 3D surface plot was analysed to study the effect of variable on Particle Size and % Entrapment Efficiency of NPs.
- Desirability plot was also examined using Design Expert software

4.1 INTRODUCTION

Nanoparticulate systems, less than 200 nm in diameter is generally considered to be ideal for drug delivery system to acquire an efficient targeting toward cancer [147]. Selection of optimal polymer to formulate nano- drug delivery system is the critical step that requires mind full efforts. The selected polymer must own respectable physiochemical properties through which, controlled drug release can be achieved. It should be biocompatible, biodegradable and upon degradation, it's by-product should not possess any threat to the human body [148]. Polycaprolactone (PCL) is one such polymer that fits ideally in all these parameters and is degraded through hydrolysis. PCL has been extensively explored for its distinct biomedical applications, among which the PCL nanoparticulate system has been exploited the most [149]. Formulating an effective nano-formulation system is greatly dependent on distinct variable involved during the stepwise synthesis of polymeric nanoparticles. Different process variables that play an important role are, stirring speed during NPs synthesis, working temperature, the polymer to drug ratio, concentration of the stabilizing agent, organic to aqueous volume ratio, etc [150, 151] .

General procedure to study the effect of variables that are mainly responsible for the synthesis of nanoparticle, is to change one variable at-a-time, which is a very complex method. This conventional approach of assessing single variable at a time is not cost-effective, it require more time to performe all the experiments and often leads to generation of misleading data [152, 153].

This problem can be resolved by using a systematic and more precise approach to evaluate the impact of the independent variable called as response surface methodology (RSM). It is a statistical method that generates the robust correlated design in between the reliant and self-reliant variables of nano-delivery system. RSM is capable of optimizing different variables at one time by progressively altering the variable and finally recommend the best experimental design available. Different steps involved in the RSM optimization are; performing the suggested experiments as per the design. Secondly, the selection of a mathematical model and finally, prediction of responses as per the selected model.

Full factorial design (FFD) is a type of RSM that is generally considered to study the effects of distinct variables. FFD has a major limitation, as the set of experiments are large in number and more over it is time-consuming process to conduct all these experiments to have the optimized procedure. Central composite design (CCD), Plackett barman design, and Box-

Behnken design (BBD) are the other optimizing designs. Among these, BBD is most suitable, as it requires a minimum set of experiments in comparison to CCD and FDD [154, 155].

BBD is an incomplete block design that efficiently optimizes significant variable by two level-factorial design. In comparison to the CCD method, BBD is considered as the most robust technique to evaluate quadratic response surface.

In the present chapter, we have discussed box-behnken design method of RSM to optimize polymeric nano-formulation. Where the polycaprolactone (PCL) was used as the polymeric base for nanoparticles synthesis and the variables that were optimized are polymer to drug ratio, surfactant concentration and organic to aqueous ratio[156, 157].

4.2 MATERIAL AND METHODS

4.2.1 Materials

PCL (MW~ 14,000) was purchased from Sigma-Aldrich (St. Louis), polyvinyl alcohol (PVA, MW: 70,000-1,00,000) was bought from Hi-media Laboratories Pvt. Ltd. Water used in all experiments was purified using a Milli-Q Plus 185 water purification system (Millipore, Bedford, MA) with resistivity greater than 18 M Ω cm. All other reagents and chemical used were of analytical grade.

4.2.2 Fabrication of PCL-polymeric NPs

Polymeric NPs were fabricated by employing previously well-established protocol of single emulsion (o/w) method with slight modification. Briefly, PCL and 5 mg PAX was dissolved in 2.5 ml dichloromethane (DCM). The solution was initially mixed with 5 ml of poly-vinyl alcohol (PVA) under sonication (probe -Oscar-ultrasonics India) for 30 seconds at 17.5 W to obtain an o/w emulsion. The emulsion was further diluted with 15 ml of 1 % (w/v) PVA solution (aqueous based) followed by stirring at moderate speed for 3h to remove traces of DCM in the solution. The resulting admixture was washed at least thrice with ultrapure water followed by filtration (100 kDa Amicon filters). The procured NPs pellet was resuspended, freeze-dried (AllicutFrost-80CNew Braswick) along with 3% mannitol and finally stored at 4°C.

4.2.3 Particle size distribution analysis

Particle size analysis of different formulated NPs was performed by using Malvern Zetasizer Instrument. Lyophilised NPs were resuspended in deionized-water, temperature was sustained at 25°C and the values were determined by taking measurements in triplicate

4.2.4 Quantification of drug encapsulation and drug loading

To determine the drug content of the designed NPs, lyophilized drug-encapsulated NPs were dissolved in acetonitrile. The resulting solution was mixed vigorously through vortex followed by incubation in shaking incubator for 3 h at 37°C in-order to remove acetonitrile from the solution. Amount of drug in the resulting solution was quantified through UV-absorption at specific wavelength of 229 nm (Thermo-Scientific- Evolution-201). The drug encapsulation efficiency was determined through following equations:

$$\text{Encapsulation Efficiency (\%)} = \frac{\text{Mass of encapsulated drug}}{\text{Mass of initial drug}} \times 100 \quad (1)$$

Table 4.1: Effect of polymer: drug ratio on particle size and % entrapment efficiency

Polymer : Drug Ratio (PCL:PAX)	PS(nm)	EE(%)
1:1	Not formed	Not formed
2:1	Not formed	Not formed
4:1	93.6 ± 4.14	33.3 ± 2.24
6:1	127.8 ± 3.64	37.56 ± 3.46
8:1	164.6 ± 5.16	41.02 ± 2.37
10:1	188.3 ± 4.46	46.70 ± 3.18
12:1	211.5 ± 8.21	53.39 ± 4.21
14:1	259.4 ± 7.76	57.57 ± 4.28

Mean ± SD; n = 3

Selected working range - - - - -

4.2.5 Preliminary investigation and identification of distinct variables

Based on the literature survey and preliminary investigation, independent variables that might affect the effectiveness of nano-formulation were identified. Polymer to drug ratio, concentration of surfactant (PVA) and organic phase to aqueous phase ratio was found to be the most critical independent variables responsible for the stability of nano-formulation. Further, the working range for each variable was selected by considering the facts, that the particle size should not exceed 200 nm in diameter and % EE should be greater than 40 %. The effects of selected variables on the PS and % EE were studied to calculate their optimal values

for optimization of formulation using RSM and finally optimized through Box Behnken Design.

Table 4.2: Effect of surfactant concentration on particle size and % entrapment efficiency

Surfactant Concentration (Polyvinyl Alcohol) (% w/v)	PS (nm)	EE(%)
0.25	394.2 ± 7.42	64.3 ± 2.94
0.50	229.4 ± 5.79	52.1 ± 3.45
1	181.7 ± 3.47	46.5 ± 2.46
1.5	204.6 ± 4.25	48.2 ± 3.37
2	244.1 ± 6.47	49.5 ± 3.13

Mean ± SD; n = 3

Selected working range - - - - -

Table 4.3: Effect of organic: aqueous Ratio on particle size and % entrapment efficiency

Organic : Aqueous Ratio (Dichloromethane: H ₂ O)	PS (nm)	EE (%)
1:1	246.5 ± 2.41	52.4 ± 1.87
1:2	203.6 ± 3.57	54.8 ± 1.41
1:3	197.5 ± 1.45	52.4 ± 1.54
1:4	207.6 ± 1.71	53.6 ± 1.92
1:5	250.6 ± 2.64	62.4 ± 2.47
1:6	323.4 ± 3.86	59.6 ± 2.47

Mean ± SD; n = 3

Selected working range - - - - -

4.2.6 Optimization of Nanoparticles using Box-Behnken response surface methodology

BBD was employed to investigate the effect of selected independent variables such as polymer to drug ratio, the concentration of surfactant (PVA) and organic to aqueous phase ratio. BBD generated total 15 set of experimental runs and all the resulting formulations were further

Table 4.4: Selected working range of variable of different formulation after conducting preliminary investigation.

Variable	Working Range
<i>Formulation variables</i>	
Polymer: Drug Ratio	6:1-10:1
Surfactant concentration	0.5% - 1.5%
Organic : Aqueous ratio	1:2 - 1:4
<i>Fixed process condition</i>	
Sonication	200 W (5s run & 2s off)
Homogenization	6h (1000rpm)
Temperature	Room temperature

Table 4.5: Sets of experimental runs suggested by Box-Behnken design and respective particle size analysis and %EE.

Code	X ₁	X ₂	X ₃	Y1	Y2
F1	10	1	4	184.4 ± 3.12	49.3 ± 3.21
F2	10	0.5	3	266.8 ± 4.05	64.6 ± 2.35
F3	8	1.5	4	176.4 ± 3.45	48.1 ± 2.34
F4	8	1	3	202.1 ± 4.14	42.4 ± 2.15
F5	8	0.5	2	262.2 ± 4.56	62.5 ± 2.74
F6	6	0.5	3	257.8 ± 4.75	43.4 ± 2.06
F7	6	1	2	224.7 ± 2.59	39.9 ± 1.87
F8	8	0.5	4	219.4 ± 3.61	55.3 ± 2.51
F9	8	1	3	208.4 ± 2.51	46.1 ± 2.31
F10	10	1	2	199.4 ± 3.45	40.1 ± 2.34
F11	10	1.5	3	197.6 ± 3.92	45.5 ± 3.27
F12	8	1	3	195.6 ± 2.67	42.1 ± 2.86
F13	6	1	4	213.9 ± 3.87	36.2 ± 2.17
F14	6	1.5	3	217.2 ± 3.16	34.4 ± 2.45
F15	8	1.5	2	214.2 ± 3.21	41.4 ± 1.65

X₁ = polymer : drug ratio

X₂ = surfactant concentration

Y₂ = Entrapment efficiency (%)

X₃ = aqueous : organic phase ratio

Y₁ = particle size (nm)

Mean ± SD; n = 3

investigated for PS distribution followed by % EE. Design-Expert software version-11 was used to generate optimized summary table through BBD.

4.2.7 Statistical analysis

Experiments were conducted in triplicates and results were articulated as a mean \pm standard deviation. Statistical analysis was performed by using GraphPad Prism software (version 6) and comparisons between groups were carried out using one-way ANOVA.

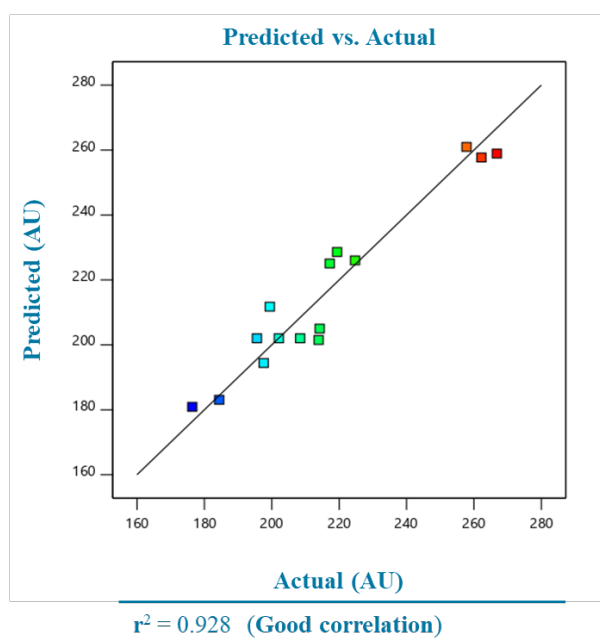


Figure 4.1 Predicated v/s actual pot for particles size of formulated NPs

4.3 RESULT AND DISCUSSION

4.3.1 Preliminary investigation

On the bases of literature, critical factors that could affect the quality of nanoparticles were selected. Preliminary investigation was carried out with the purpose to acquire appropriate working range for each factor. Certain facts were taken into consideration while optimization, such as particle size should not exceed 200 nm and entrapment efficiency of the nanoparticles should not be below 40%. Different formulations were subjected to particle size analysis and entrapment efficiency was determined as represent in Table 4.1-4.3.

Amount of polymer and drug content in formulation plays a significant role in design and development of nano-delivery system for which the selected working range was 6;1-10:1 (Table-4.4). PVA is an efficient surface stabilizing agent and is mainly responsible for the shape and size of the nanoparticulate system. It is an important variable in the fabrication of nanoparticles, as slight change in the concentration leads to considerable alteration in the size

[R]. Through preliminary studies we selected the working concentration of PVA in between 0.5% to 1.5% . Another critical factor is organic: aqueous ratio and the preferred working range was from 1:2 to 1:4.

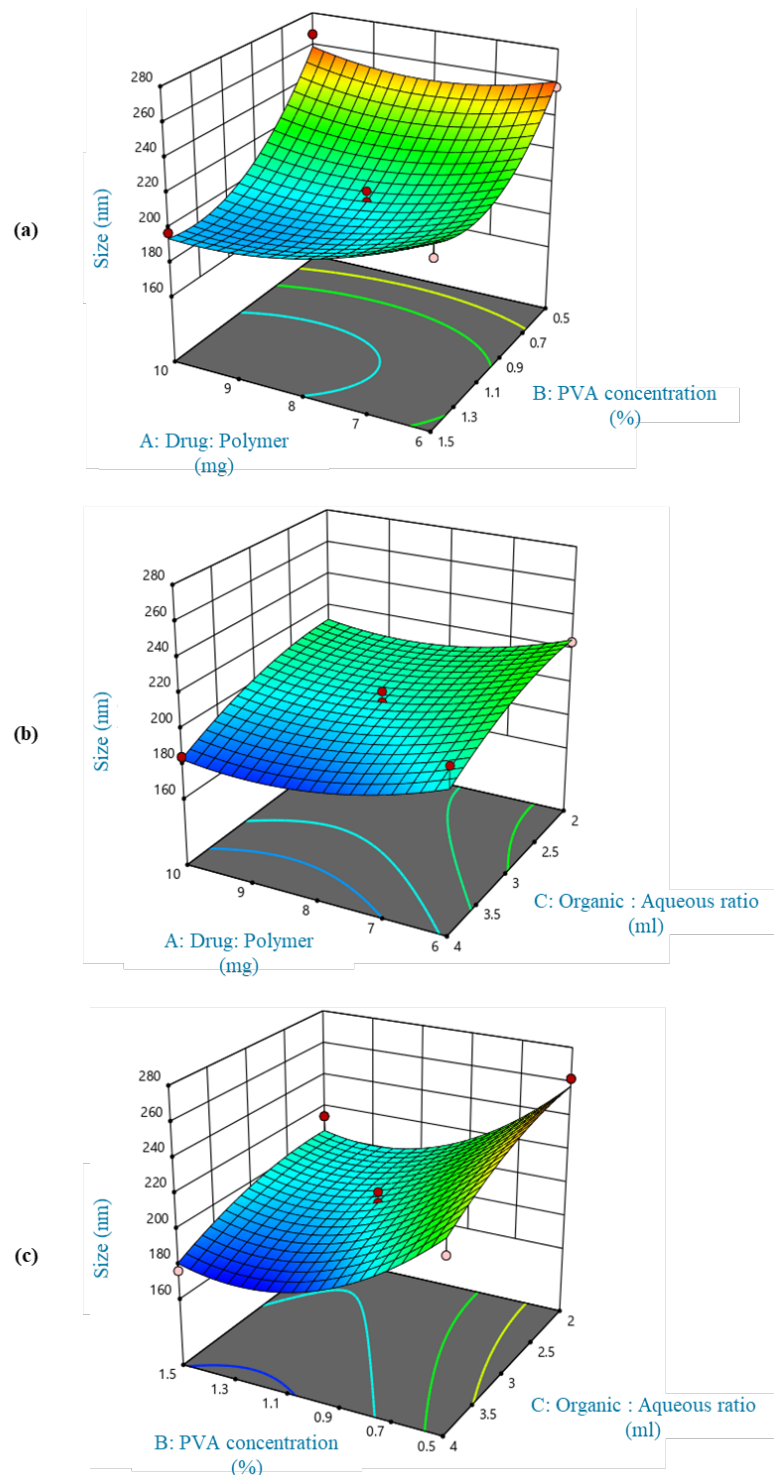


Figure 4.2. 3D-Response surface plots representing effects of variables on particles size, (a) polymer: drug ratio and surfactant concentration, (b) polymer: drug ratio and organic: aqueous ratio, (c) surfactant concentration and organic: aqueous ratio.

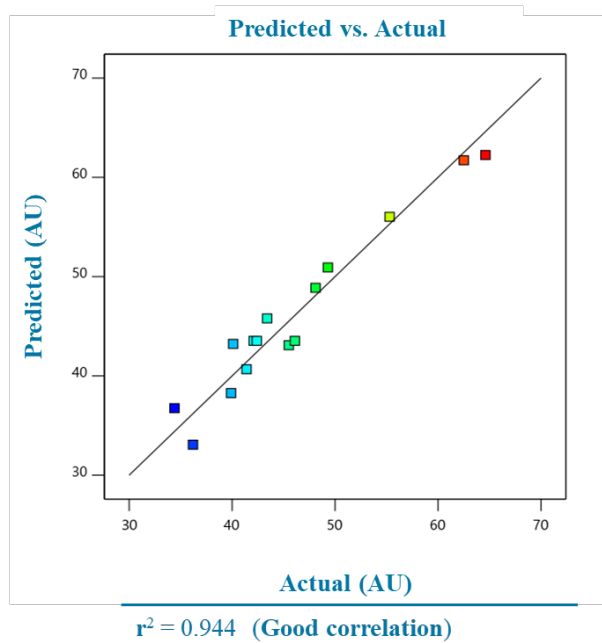


Figure 4.3 Predicated v/s actual pot for % entrapment efficiency of formulated NPs

4.3.2 Response surface methodology and Box-Behnken design

Total 15 sets of experimental runs were suggested by BBD method to optimize PAX loaded nano-formulation. All the experiments were conducted to optimize three independent variables (polymer: drug ratio, PVA concentration and organic: aqueous ratio). Resulting formulations were further characterized for particle size distribution and percentage entrapment efficiency as depicted in Table 4.5. Three-dimensional response surface plots were generated and further analyzed with the help of design expert software version-11.

4.3.3 Effect of variables on particle size (PS) studied through-BBD

Variation in PS was recorded from 176.4 nm (F3) to 266.8 nm (F2), shows that the combination of different variables affected the PS of nano-formulation. From the statistical analysis, we observed that the R^2 value for actual v/s predicted values of PS was 0.928, which signifies a good correlation between them. The results from ANOVA confirmed that the selected model terms were significant for the purpose to study the effect of selected variables on PS with p value < 0.05 as presented in Figure 4.1. The obtained results were further analyzed through 3D response surface graphical plot, where we observed that with the increase in polymer: drug ratio there was increase in PS of NPs. In case of polymer: drug ratio and aqueous: organic ratio, no prominent effect was observed from 3D surface plot. When surface plot for surfactant concentration and aqueous: organic phase was examined, a decline in PS was witnessed as represented in Figure 4.2.

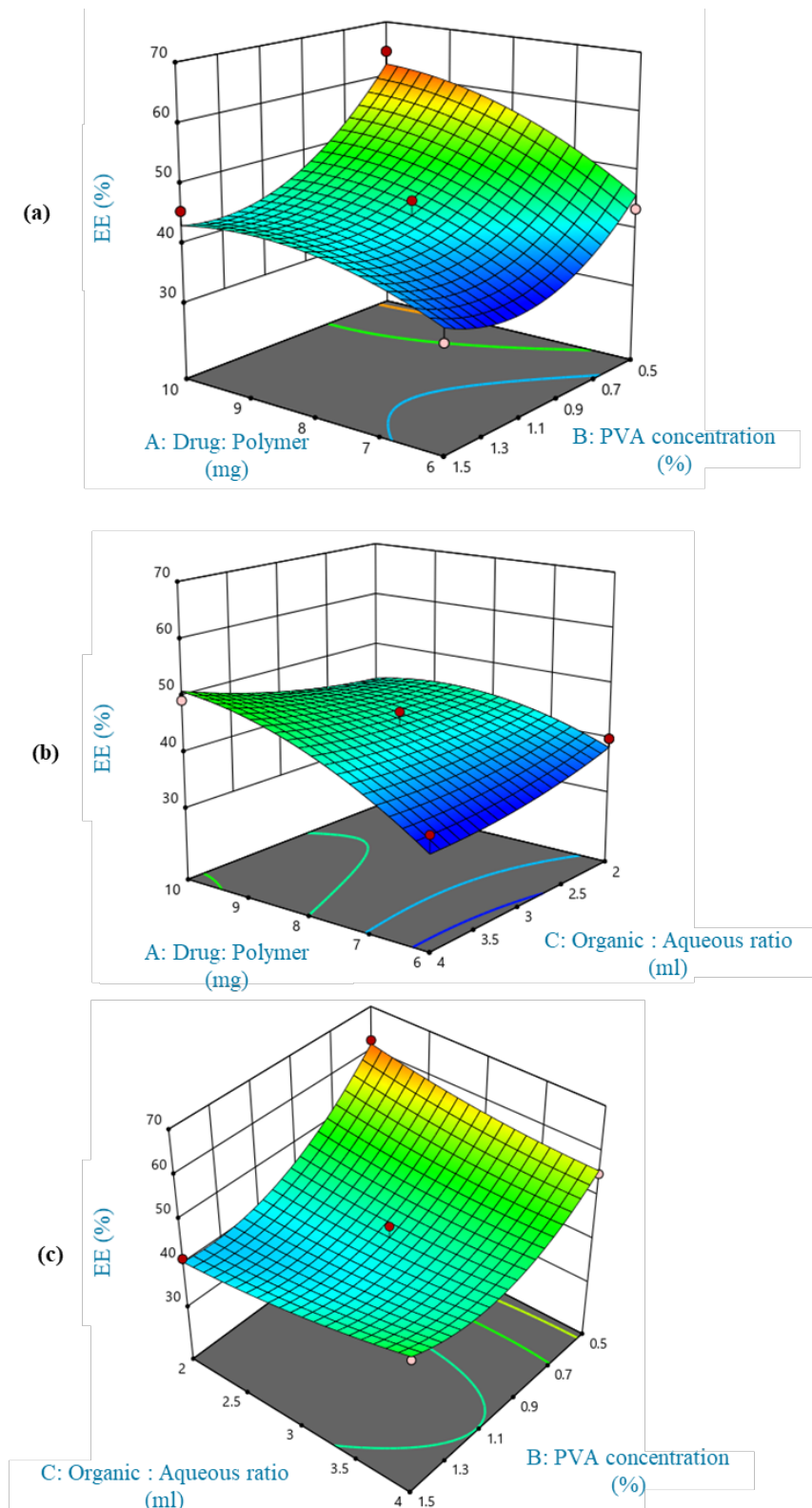


Figure 4.4. 3D-Response surface plots representing effects of variables on % entrapment efficiency, (a) polymer: drug ratio and surfactant concentration, (b) polymer: drug ratio and organic: aqueous ratio, (c) surfactant concentration and organic: aqueous ratio.

4.3.4 Effect of variables on entrapment efficiency (%EE) studied through (BBD)

The %EE for each formulation batch was recorded, that varied from 34.4% (F14) to 64.6% (F2) which further suggested that the various combinations of critical formulation variables affected the %EE of NPs. From statistical analysis R^2 value for actual v/s predicted values for %EE was found to be 0.94 which further indicates that there was a good correlation between predicted and actual values. Likewise, the result from ANOVA confirmed that the model was significant to study the effect of selected variables on %EE having p value < 0.05 (Figure 4.3). Polymer: drug ratio and surfactant concentration 3D surface plot revealed that, by increasing polymer: drug ratio there was a substantial increase in %EE. Likewise, when aqueous: organic phase was increased, %EE of the nano-formulation was also augmented as observed from 3D surface plot analysis. Whereas, rise in surfactant concentration reduced the % EE as exhibited by aqueous: organic and surfactant concentration 3D surface plot shown in Figure 4.4.

4.3.5 Optimization of variable through desirability plot

Desirability plot was also examined using Design Expert software, where the upper and lower desired values of response were selected ($PS < 200\text{nm}$ and $\%EE \geq 40$), and software generated the values of variables that would help to achieve the desired response. A composite desirability plot value of 0.924 was recorded, which predicts that if the formulation is prepared according to the optimized values of independent variables, the chance to obtain the desired value of response is 92.4% (Figure 4.5). The suitability of desirability plot was assessed by formulating nanoparticles as suggested by desirability plot and the resulting nano-formulation was further characterized for desired responses (PS and %EE). Comparative analysis was performed by measuring predicted and actual responses, where we witnessed slight increase in the particle size; from 178.7 (predicted) to $182.4 \pm 1.86\text{nm}$ (obtained). Likewise, small decline in % EE was witnessed by comparing predicted and actual response, that can be considered as optimized formulation as the responses were very close to each other.

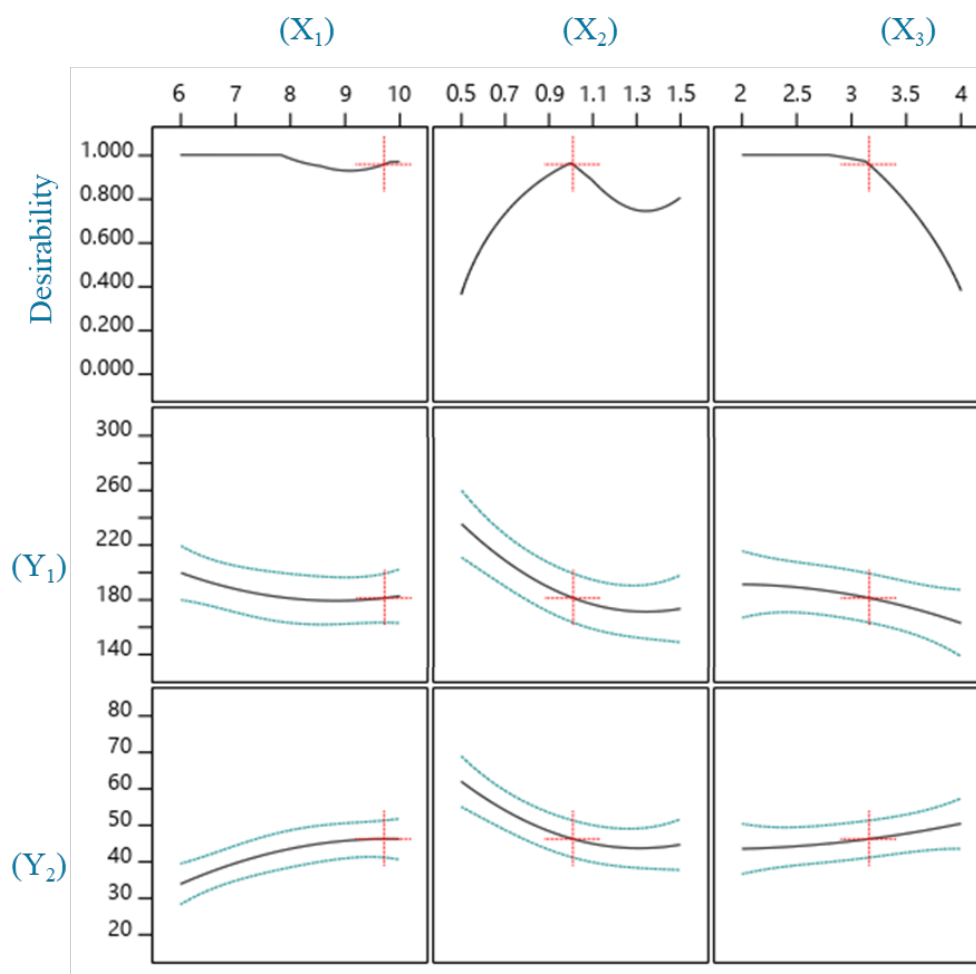


Figure 4.5 Obtained desirability plot for optimized nano-formulation

Table 4.6 Optimized value for the formulation as suggested by desirability plot along with actual obtained values of responses

Desired Responses		Desired Criteria
Particle size (nm)		200 max
Entrapment Efficiency (%)		40 % min

Independent Variable	Suggested	Normalized
Polymer: drug ratio (X_1)	9.72 :1	10:1
Surfactant Con. (X_2)	1.01 (%)	1%
Organic: aqueous phase ratio (X_3)	1 : 3.15	1:3

Responses	Predicted	Obtained
Particle Size (Y_1)	178.7 nm	182.4 \pm 1.86nm
Entrapment Efficiency (Y_2)	49.13 %	47.7 \pm 2.36 %

4.5 SUMMARY POINTS

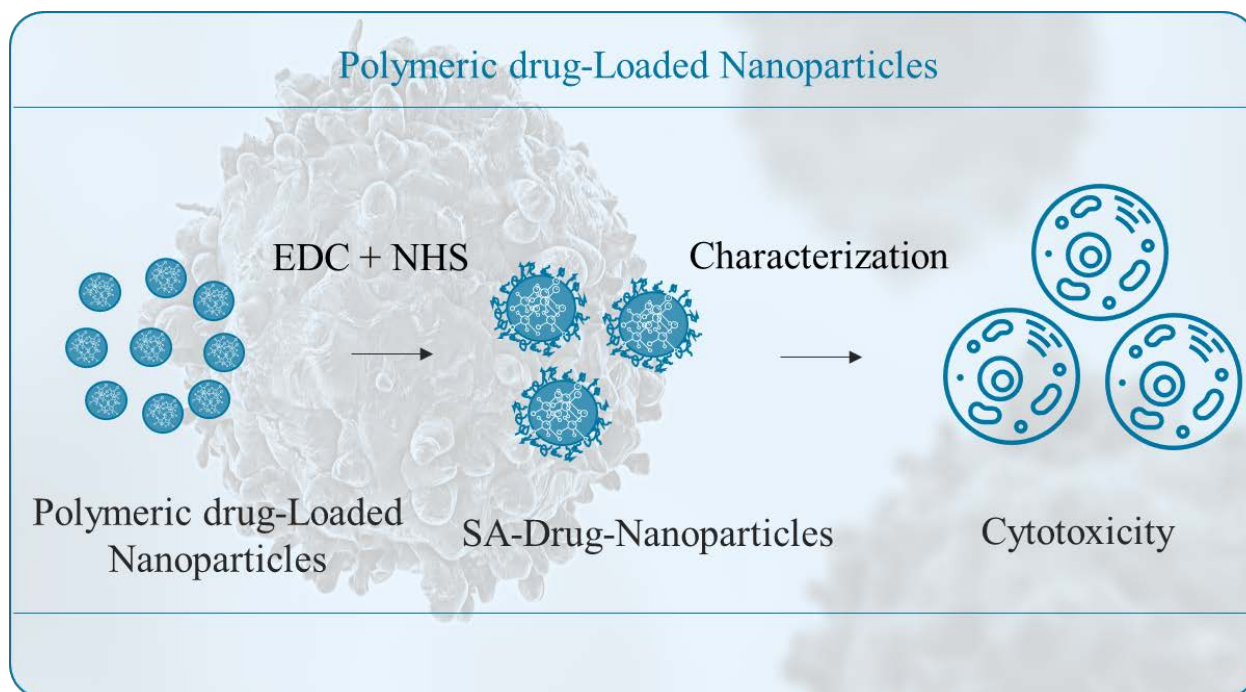
- Three different independent variables; polymer: drug ratios, concentration of surfactant (PVA) and organic phase: aqueous phase ratios were selected for further optimization as per preliminary investigation.
- Effect of variables were studied for particle size distribution and percentage entrapment efficiency through response surface methodology (RSM) by employing Box Behnken design (BBD).
- The obtained results demonstrated the establishment of a suitable and robust design to formulate nano-formulation and these optimized variable concentrations can be employed further for scale up formulation studies.



CHAPTER-5

SYNTHESIS OF SIALIC ACID DRUG
LOADED NANOPARTICLES AND ITS
EVALUATION AGAINST BREAST
CANCER CELL LINE

GRAPHICAL OVER VIEW OF THE CHAPTER



HIGHLIGHTS

- Fabrication of NPs using optimized variable concentration.
- Characterization of fabricated -NPs
- *In-vitro* drug release studies of encapsulated dual drug (PAX+CLZ)
- Cell specific uptake studies of formulated NPs

5.1 INTRODUCTION

As mentioned in the introduction of the thesis, PAX is the most commonly prescribed chemotherapeutic agent for the management of breast cancer. Patients receiving chemotherapy (PAX) generally struggle with the associated unfavorable effects within the form of decreased blood count, loss of hair, increased risk of infection, nausea, vomiting etc [158, 159]. To address such situations medical professionals, prefer combination of distinct anti-cancer agents, every so often at reduced dosages to have much safer and efficient treatment against breast cancer [14]. There are various chemotherapeutic agents that has been frequently employed in combination for breast cancer management, such as; AC (doxorubicin hydrochloride + cyclophosphamide), ACT (doxorubicin Hydrochloride (Adriamycin) + cyclophosphamide + paclitaxel (Taxol)), CAF (cyclophosphamide + doxorubicin hydrochloride (Adriamycin) + 5-fluorouracil), CMF (cyclophosphamide + methotrexate + 5-fluorouracil), FEC (fluorouracil + epirubicin hydrochloride + cyclophosphamide) and TAC (Docetaxel (Taxotere) + doxorubicin hydrochloride (Adriamycin) + cyclophosphamide). Although, these combination exhibits enhanced cytotoxicity against breast cancer at reduced dose, but still risk of associated side effects of these anti-cancer agents is still there.

Substituting the chemotherapeutic agent with another less toxic agent, that have specific cancer killing capabilities and is safe for normal cells, is an available alternative to overcome the associated side effects of chemotherapy. Literature suggests that Clotrimazole (CLZ) is an anti-fungal compound that possess anti-cancerous benefits specifically against breast cancer, whereas have minimal effect on normal cells.

In the present chapter we have discussed the cytotoxic effects of formulated Sialic Acid (SA)-drug loaded NPs against breast cancer cell lines. Wherein, the encapsulated drugs were PAX + CLZ in combination, SA was functionalized on the surface of NPs and employed as targeting moiety. Fabricated nano-particles were characterized for their surface morphology through SEM and functionalization of SA was confirmed through FTIR-spectroscopic analysis. Efforts have been made to study *in-vitro* drug release pattern from the formulated NPs, followed by cytotoxicity analysis through MTT assay. To confirm the effect of drug combination, fluorescent microscopic investigation was performed by staining cells with AO-EtBr staining dyes.

5.2 MATERIAL AND METHODS

5.2.1. Materials

PCL (MW 14,000) was bought from Sigma-Aldrich (St. Louis), polyvinyl alcohol (PVA, MW: 70,000-1,00,000) was bought from Hi-media Laboratories. EDC (*N*-(3-dimethylaminopropyl)-*N'*-ethylcarbodiimide), NHS (*N*-hydroxy-succinimide), MES (2-(*N*-morpholino)ethanesulfonic acid), Triton-X-100 and MTT (3-(4,5-dimethylthiazol-2-yl)-2,5-diphenyltetrazolium bromide) were acquired from Sigma Aldrich. Acetone was procured from Fischer Scientific and Trypsin- EDTA, FBS (fetal-bovine-serum), antibiotics- antimycotics, DMEM (Dulbecco's modified-Eagle's medium) and PBS (Phosphate buffer saline) was obtained from Gibco, Luria- Bertani (LB)-media was acquired from Merck Specialities Pvt. Ltd India. Water used for the experiments was purified utilizing a Milli-Q Plus 185 water purification system (Millipore, Bedford, MA).

5.2.2. Ingredient volume selection from previously optimized concentrations

Prior to experiment, all the essential ingredients of the formulation were quantified in such proportion, as they would match previously optimized concentration. As mentioned in Chapter-4, optimized organic: aqueous ratio (1:3) and surfactant concentration (1%), for that, 2ml of dichloromethane (DCM) was used as organic phase and 6ml of 1% polyvinyl alcohol (PVA) was used as aqueous phase. 500 mg of polycaprolactone (PCL) as polymer and 50 mg of drug was preferred to match optimized polymer to drug ratio.

25 μ g of PAX and 50mg of CLZ was further selected to comply with optimized drug combination of 12.5nM of PAX and 25 μ M of CLZ as specified in Chapter-2 (Figure.5.1).

5.2.3. Fabrication of drug loaded PCL-nanoparticles

Single emulsion (o/w) method was employed to fabricate dual-drug encapsulated nanoparticles with slight modification. Briefly, 500 mg PCL and 50 mg of drug (25 μ g of PAX and 50 mg of CLZ) was dissolved in 2 ml dichloromethane (DCM). The resulting solution was added to 6 ml of 1% w/v -PVA under sonication (probe Oscar-Ultrasonics India) for 30 seconds at 17.5 W to obtain an o/w emulsion. The emulsion was further diluted with 15 ml of 0.5 % (w/v) PVA solution (aqueous based) followed by stirring at moderate speed for 3h to remove traces of DCM in the solution. The resulting admixture was washed at least thrice with ultrapure water followed by filtration (100 kDa Amicon filters). The NPs pellet was resuspended, freeze dried (AllicetFrost-80CNew Braswick) along with 3% mannitol and finally stored at 4°C. Drug loaded PCL-NPs were synthesized by o/w emulsion and solvent evaporation technique.

Amount of drug	
PAX: CLZ	
<i>Optimized Conc.</i>	12.5 nM PAX+25 μ M CLZ
<i>Optimized ratio</i>	1:2000
<i>Selected</i>	25 μ g:50mg

Organic Phase : Aqueous Phase	
<i>Optimized</i>	1:3
<i>Selected</i>	2ml:6ml
Polymer : Drug ratio	
<i>Optimized</i>	10:1
<i>Selected</i>	500 mg : 50 mg
Surfactant concentration	
<i>Optimized</i>	1%
<i>Selected</i>	1% PVA

Figure 5.1 Optimized concentration of ingredients used for the current synthesis of NPs

5.2.4 Functionalization of Sialic Acid (SA) on PCL NPs

Sialic acid was mounted on PCL-NPs by exploiting carbodiimide reaction. Briefly, the lyophilised NPs were dispersed in carbodiimide solution (5 mM EDC and 10 mM NHS in 50 mM MES buffer, pH = 5.5) for 1 h at room temperature. NPs were then rinsed twice with PBS using filter (100 kDa Amicon filter) to remove unreacted EDC and NHS. Carboxylic group activated NPs were incubated for 4h at 37°C with gentle agitation. NPs were washed thrice using deionized water to remove unconjugated sialic acid followed by lyophilization.

5.2.5. Surface morphological investigation

Morphological examination of the fabricated NPs was performed through scanning electron microscope (SEM-QUANTA 250, FEI Makers), moving electrons were made incident on the sample particles placed inside the vacuum chamber while mounted on the metal stubs using double sided adhesive tape.

5.2.6. Fourier Transform Infrared (FTIR) analysis.

FTIR spectrum were determined (FTIR Instrument of Agilent Technologies 630 Cary using Micro Lab software) with the purpose to investigate the possible chemical functional group changes upon incorporation of sialic acid on PCL-NPs.

5.2.7. Particle size distribution and zeta potential analysis

Particle size, zeta potential and poly-dispersity index (PDI) analysis of formulated NPs were performed by using Malvern Zetasizer Instrument. Lyophilised NPs were resuspended in deionised-water, temperature was sustained at 25°C and the values were determined by taking measurements in triplicate.

5.2.8. Quantification of drug encapsulation and drug loading

To quantify the drug content of the designed NPs, lyophilised drug-encapsulated NPs were dissolved in acetonitrile. The resulting solution was mixed vigorously by using vortex followed by incubation in shaking incubator for 3 h at 37°C in-order to remove acetonitrile from the solution. Amount of drug in the resulting solution was quantified through UV-absorption at specific wavelength of 229 nm (Thermo-Scientific- Evolution-201). The drug encapsulation efficiency and the drug loading was determined through following equations:

$$\text{Encapsulation Efficiency (\%)} = \frac{\text{Mass of encapsulated drug}}{\text{Mass of initial drug}} \times 100 \quad (1)$$

5.2.9. In-vitro drug release study

In-vitro drug release from NPs was evaluated by using a dialysis bag (molecular weight cut-off: 8,000-14,000). The PAX loaded NPs (20mg/2ml) were placed into the dialysis bag (dialysis membrane was pre-activated by soaking it in PBS for 24 h). Dialysis bag was immersed in 20 mL of PBS maintained at a pH of 7.4 and 6.8 at 37°C, containing 0.1% (v/v) Tween 80 (non-ionic surfactant). At designated time intervals, 1 mL release medium was removed and subsequently, fresh medium (1ml) was added to maintain a sink condition. Afterwards, the content of PAX was quantified by UV spectrophotometer (wavelength 229 nm) using UV-Visible Spectrophotometer. The experiment was performed in triplicate and the resulting data was expressed in the form of percentage cumulative drug release.

5.2.10. Cell line and culture

MCF 7 and MDA MB 231 cell lines were procured from the NCCS, Pune, India and HEK-293 cell line was obtained as gift from AMITY University, Noida (India). The cells were seeded in tissue culture flask comprising growth medium solution (DMEM for MCF 7 and L-15 for MDA MB 231) accompanied by 10% FBS and 1% antibiotics (100 U/ml penicillin and 100 µg/ml streptomycin). Cells were incubated and maintained at 37°C in a humidified atmospheric incubator supplemented with 5% CO₂.

5.2.10.1. In-vitro cytotoxicity studies

The *in-vitro* cellular toxicity of formulated NPs was determined through standard MTT assay using human origin breast cancer cell line (MCF 7 and MDA MB 231) and normal cell line (HEK 293). Briefly, the cells were seeded (1×10^4 /well) in 96 well tissue culture plate for 24h

prior to experiment. Formulated NPs were incubated with cells for different intervals (0, 6, 12, 24 and 48h). After incubation, 25 μ l of MTT (5 mg/ml) solution was added to each well and incubated further for 4h. Formazan thus produced by viable cells was dissolved by adding 200 μ L dimethyl sulfoxide (DMSO). The optical densities (OD) were recorded through a microplate reader (model-680, Bio-Rad) at 570 and 630 nm as test and reference wavelength subsequently. Cell viability percentage was calculated through following equation:

$$\text{Cell viability (\%)} = \frac{\text{OD (Test well)}}{\text{OD (reference well)}} \times 100 \quad (3)$$

All the results were assured by repeating the individual tests in triplicate for each time.

Table 5.1: Formulation codes representing amount of ingredients used in different formulations

Formulation	PCL (mg)	PVA	Drug	PS (nm)		EE (%)	
				Unconjugated	SA-conjugated		
PCL-NPs	500	1%	-	184.4 \pm 2.8	187.4 \pm 1.3	-	
PAX-NPs	500	1%	D1	189.6 \pm 3.4	191.6 \pm 1.9	59.45 \pm 1.8	
CLZ-NPs	500	1%	D2	188.2 \pm 2.7	193.2 \pm 2.6	63.37 \pm 2.6	
PACL-NPs	500	1%	D1+D2	192.5 \pm 3.8	197.5 \pm 1.8	D1	D2
						50.91 \pm 1.8	47.54 \pm 3.1

D1 = Paclitaxel (12.5nM)

PCL = Polycaprolactone

PS = Particle Size

D2 = Clotrimazole (25 μ M)

PVA = Polyvinyl Alcohol

EE = Entrapment Efficiency

5.2.11. Acridine orange (AO) and ethidium bromide (EtBr) staining to identify apoptosis

AO/EtBr dual staining was carried out, to examine the nuclear morphological changes in MCF-7, MDA-MB-231 and HEK-293 cells as an effect of synthesized NPs [22].

Briefly, cells were subcultured in 6 well culturing plate having the density of 3×10^4 cells/well, that were further treated with synthesised NPs (PCL-NPs, PAX-NPs, CLZ-NPs and PACL-NPs) for 24 h. The cells were washed carefully through phosphate buffer saline (PBS) followed by fixation with 4% paraformaldehyde (10 min) at room temperature. Cells were further permeabilized with Triton X-100 (0.2%) for 10 min and incubated with 10- μ L of AO (1 mg/mL) and 10- μ L of EtBr (1 mg/mL). Corresponding cellular images were captured by using fluorescent microscope (Nikon-ECLIPSE-Ti-U) and the inference was drawn by calculating corrected total cell fluorescence (CTCF) intensity for each set of experiments through Image-J software.

5.2.12. Statistical analysis

Experiments were conducted in triplicates and results were articulated as mean \pm standard deviation. Statistical analysis was performed by using GraphPad Prism software (version 6) and comparisons between groups were carried out using one-way ANOVA.

5.3 RESULTS AND DISCUSSION

5.3.1. Scanning electron microscopy, particle size distribution and % entrapment efficiency.

Surface morphology plays a crucial role in the nano-delivery system as circular or sphere-shaped nanoparticles are preferred over other form of nanostructure. This is just because of the fact that, circular structure tend to accommodate more drug molecules inside its matrix system and its reduced surface area reduce the chances of interaction with macrophages while circulating in blood. Scanning electron microscopic (SEM) analysis revealed the spherical and smooth surface morphology of formulated NPs (Figure.5.2). The particles size distribution of all the formulations were found to be very close to the predicted size of nanoparticle by BBD method of RSM (desired size range- optimized in Chapter-4) i.e. having PS less than 200nm (Table 5.1). Interestingly, we witnessed slight increase in the size of conjugated NPs in contrast to un-conjugated NPs, where the presence of SA on the surface could be the attributing factor for this observation. Important point to mention, despite of SA functionalization the increase in size was within the desired range (<200 nm).

EE % was found to be $50.91 \pm 1.8\%$ for PAX and $47.54 \pm 3.1\%$ for CLZ respectively in SA-PACL-NPs (Table 5.1). Likewise, $59.45 \pm 1.8\%$ EE was calculated for SA-PAX-PCL-NPs and 63.37 ± 2.6 for SA-CLZ-PCL-NPs simultaneously.

5.3.2. Fourier-transform infrared spectroscopic analysis

The FTIR-spectral interpretation was performed to examine surface modification of PCL-NPs. Standard PCL FTIR pattern depicts the specific C-H stretching at 2948cm^{-1} and 1726cm^{-1} represents carboxylic acid C-O strong peak. (Figure 5.3). FTIR-pattern of drug combination (PAX+CLZ) revealed PAX characteristic peaks at 3312cm^{-1} , 2974cm^{-1} , 1704cm^{-1} and 1248cm^{-1} corresponding to O-H and N-H stretching, C-H stretching, COOH stretching and C-N stretching respectively. Likewise, distinctive peaks of C-N stretch at 1495cm^{-1} and 1216cm^{-1} and C-Cl stretch at 769cm^{-1} was noticed in CLZ. Drug combination of PAX+CLZ was found to be chemically compatible with each other, as no new prominent peak was observed with drug combination (detailed description of individual FTIR-graph for PAX and CLZ is mentioned in Chapter-2- Fig.2.2).

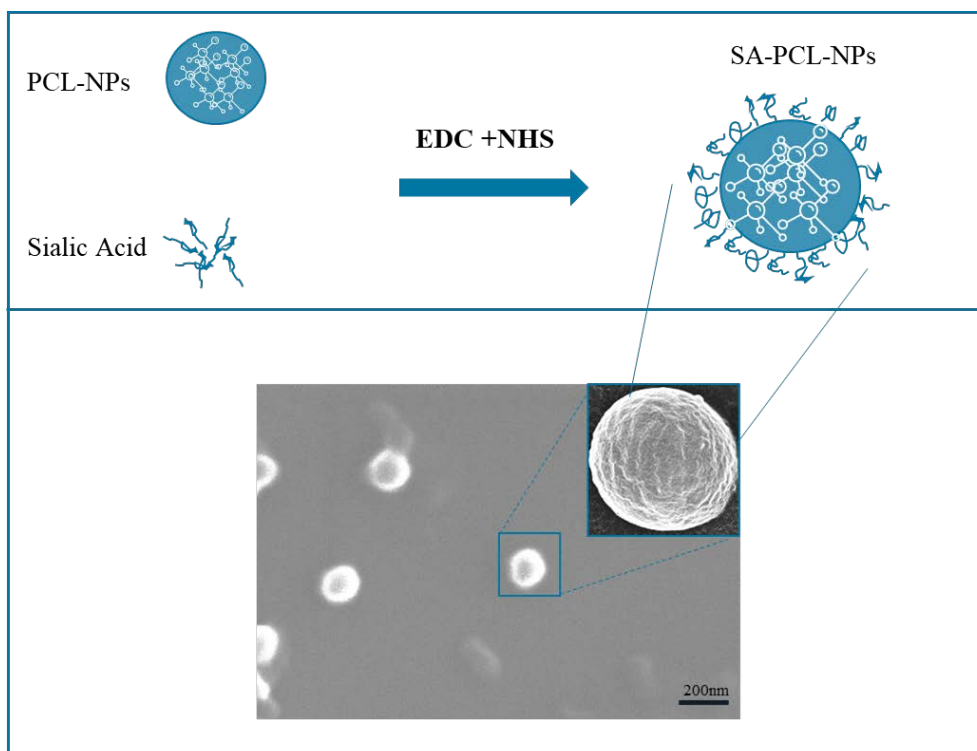


Figure 5.2. Schematic of sialic acid conjugated polymeric nanoparticles by exploiting EDC-NHS conjugation, where inset represents the surface morphology of SA-conjugated-PCL-NPs.

FTIR graph for PACL-Drug-NPs revealed characteristic peaks at 2948cm^{-1} and 1726cm^{-1} conforming C-H stretching and carboxylic acid C-O presence, moreover there was no associated peaks of drug combination. This signify that drug has been encapsulated inside the polymeric (PCL) matrix as revealed in Figure 5.3.

Observed characteristic FTIR peaks for SA were; O-H stretch at 3282cm^{-1} , 1644cm^{-1} representing C=O and 1518cm^{-1} depicts the N-H bending. FTIR spectra of SA-PACL-NPs exhibited the strong amide peaks at 3282 , 1644 and 1518cm^{-1} representing the O-H, C=O and N-H peaks respectively, suggesting SA conjugation on the surface of PCL-NPs.

5.3.3. *In-vitro* Drug release studies

Releasing pattern of the drug from nanomaterial is an imperative parameter, that distinguishes nano-delivery systems from conventional systems. *In-vitro* drug release studies were performed at two different pH; 6.8 pH (mimics the pH of breast cancer) and 7.4 pH (normal pH level of blood) [R]. Percentage cumulative drug release profile of PAX (Figure 5.4-a) form PACL-NPs reveals controlled drug release from the formulation having both the drug. Initially, burst release was observed, with approximately 20% of drug released within 24 h followed by a sustained release in both the pH conditions (6.8 and 7.4 pH). Likewise, CLZ also exhibited

initial burst release 25% within 24h followed by controlled drug release (Figure 5.4-b). However, we observed a slight increase in the drug release at lower pH, but overall drug release pattern was found to be in controlled proportion for both the compounds (PAX and CLZ). Drug release depicted in Figure 5.4 is specifically related to SA-PACL- NPs, as the main purpose was to demonstrate releasing pattern of drug from dual drug-encapsulated-NPs.

5.3.4. *In-vitro* cell cytotoxicity studies

The cellular cytotoxicity of synthesized NPs was studied through Mtt assay on MCF-7 and MDA-MB-231 breast cancer cell lines as well as on HEK-293 normal cell lines. Cells were incubated with formulated NPs (PCL-NPs, SA-PAX-NPs and SA-CLZ-NPs and SA-PACL-NPs) for different time periods (0 to 72h).

SA-PACL-NPs effectively inhibited MCF-7 cells, where 44 % of cell were viable at 24h and viability of cells were further declined to approximately 14% by 72h. Similarly, PCL-PACL-NPs exhibited percentage cell viability of 68 % at 24 h and 35 % by 72h. SA-PACL-NPs were found to most effective against MCF-7 in comparison to PCL-PACL-NPs, where the cellular growth inhibition was greatly influenced by the incubation period and time-dependent cytotoxic effects were observed. The apparent cause of the highest toxicity of SA-PACL-NPs towards MCF-7 might be due to SA driven cellular uptake.

Likewise, similar time-dependent results were witnessed with MDA-MB-231 cells, where approximately 38% of cells were viable at 24h with SA-PACL-NPs and the percentage rate gradually decreased to 8% by 72h. PCL-PACL-NPs exhibited 75 % of cellular viability at 24h and approximately 47% cells were viable by 72h. Here also, SA-PACL-NPs was found to be most toxic in comparison to other formulations.

However, the cytotoxicity of SA-PACL-NPs with normal cells (HEK-293) was found to be less. PACL-NPs also exhibited a decline in cell proliferation after 24 h, possibly because of passive intake of the NPs and another factor could be the slow dividing rate of the normal cells. PCL-NPs and SA-PCL-NPs did not exhibit any sign of cellular toxicity in breast cancer cells as well as in healthy normal cells. This further suggests that the selected protocol of synthesis yield biocompatible nanoparticles, as there was no decline in cell viability of HEK-293 cells. Detailed comparative graphical representation has been depicted in the APPENDIX-Section-III.

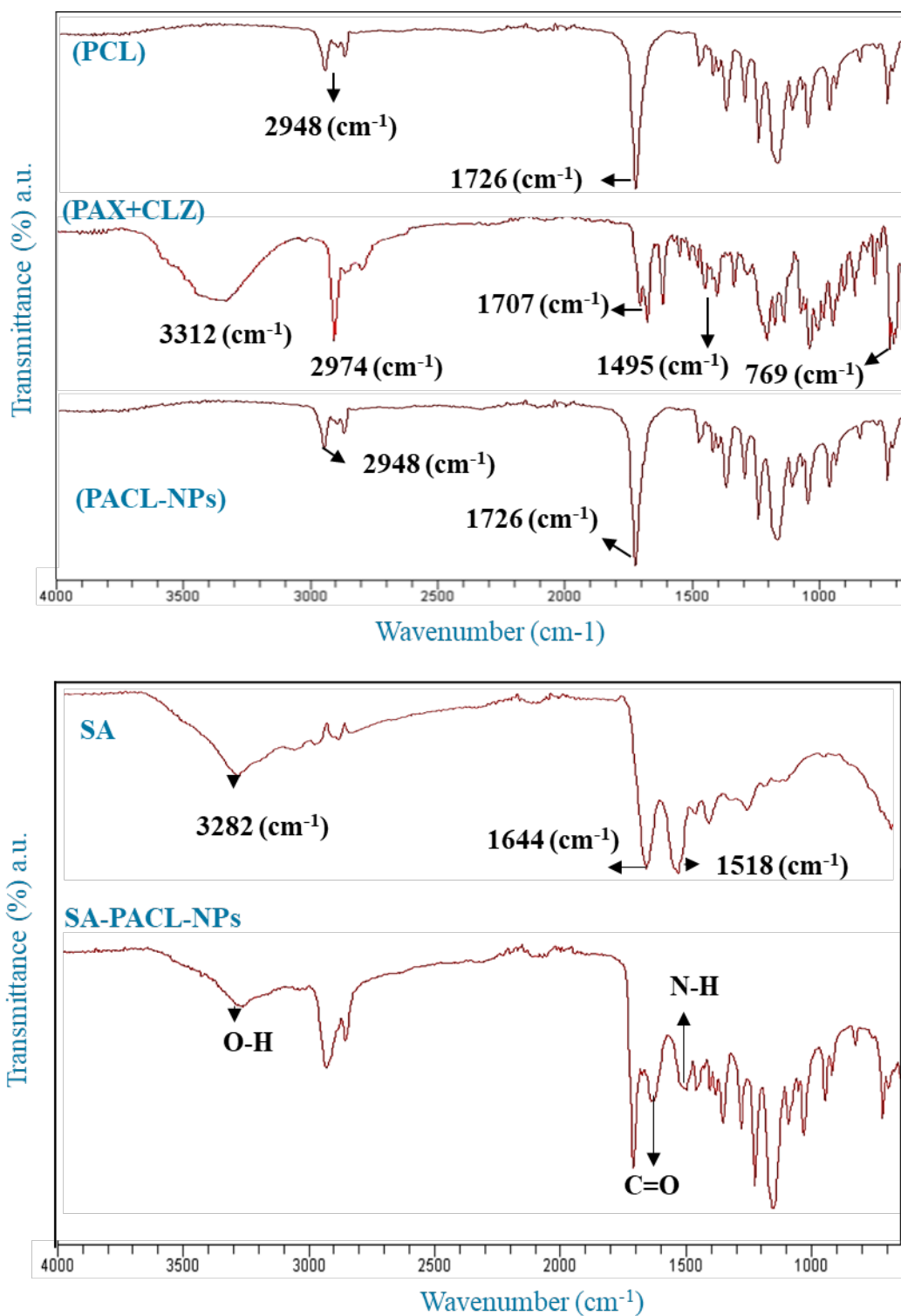


Figure 5.3. The respective Fourier-transform infrared (FTIR) spectroscopic pattern for a different formulation.

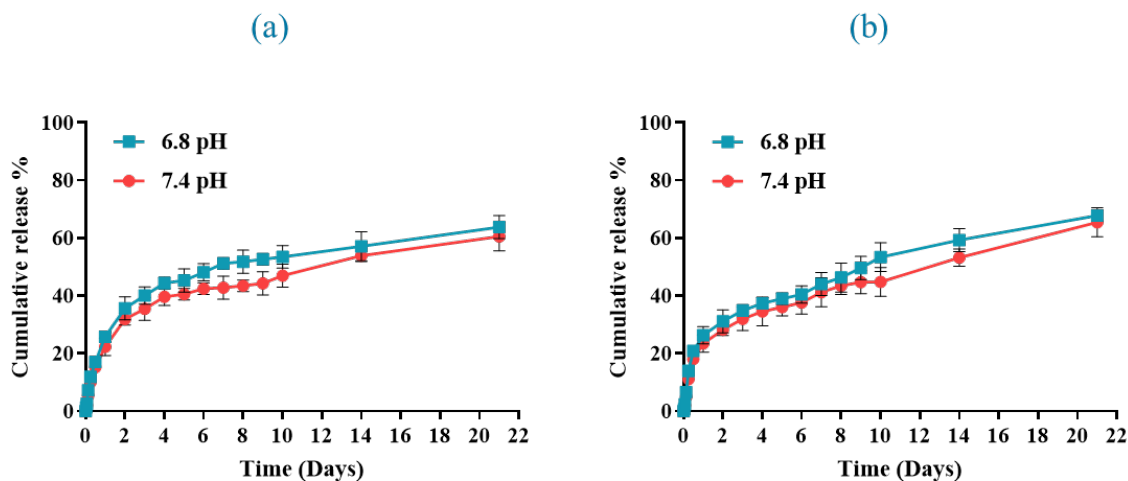


Figure 5.4 Drug release pattern from the Salic acid formulation (a) PAX and (b) CLZ (See for appendix)

To authenticate the anti-proliferative effect of synthesized NPs and to examine the alterations in nuclear morphology of HEK-293, MCF-7, and MDA-MB- 231 cells, we performed live-dead staining by using AO/EtBr staining dyes. AO stain both types of cells, live as well as dead cells and the stained cell exhibit green fluorescence when observed under a fluorescent microscope. Whereas, EtBr stains specifically cells with disoriented membrane integrity and cells demonstrate orange or red fluorescence. Corrected total cell fluorescence (CTCF) was calculated for the cells stained with EtBr (red fluorescent) representing dead cells and the graph was plotted to draw a clear conclusion from the captured fluorescent images. More importantly, only comparative fluorescent microscopic images of non-functionalized drug combination encapsulated-NPs (PCL-PACL-NPs) and sialic acid functionalized drug combination encapsulated-NPs is represented in Figure 5.6. Fluorescent images of other formulations are mentioned in APPENDIX Section -III of the thesis.

As shown in figure 5.6, HEK-293 cells exhibited no symptoms of cell death with synthesized NPs, as all the cells exhibited green fluorescence with PACL-NPs and SA-PACL-NPs. Whereas Image-J software analysis reveals a small increase in the fluorescent intensity with PCL-PACL-NPs, possibly because of passive uptake of NPs. SA-PACL-NPs exhibited significant high cellular interaction in comparison to PCL-PACL-NPs in MCF-7. Image-J software analysis also depicts the rise in the fluorescent intensity with SA-PACL-NPs on MCF-7 cells. Likewise, fluorescent microscopic images of MDA-MB-231 also depicted the similar pattern of increased intensity with SA-PACL-NPs.

Interesting, SA-PACL-NPs exhibited profound effect against MDA-MB- 231 in contrast to MCF-7 cells and the possible reason for this could be the sensitivity of MDA-MB-231 cells.

In a nutshell, SA functionalized NPs were found to be more specific toward breast cancer cells, whereas less interactive to healthy and normal cells.

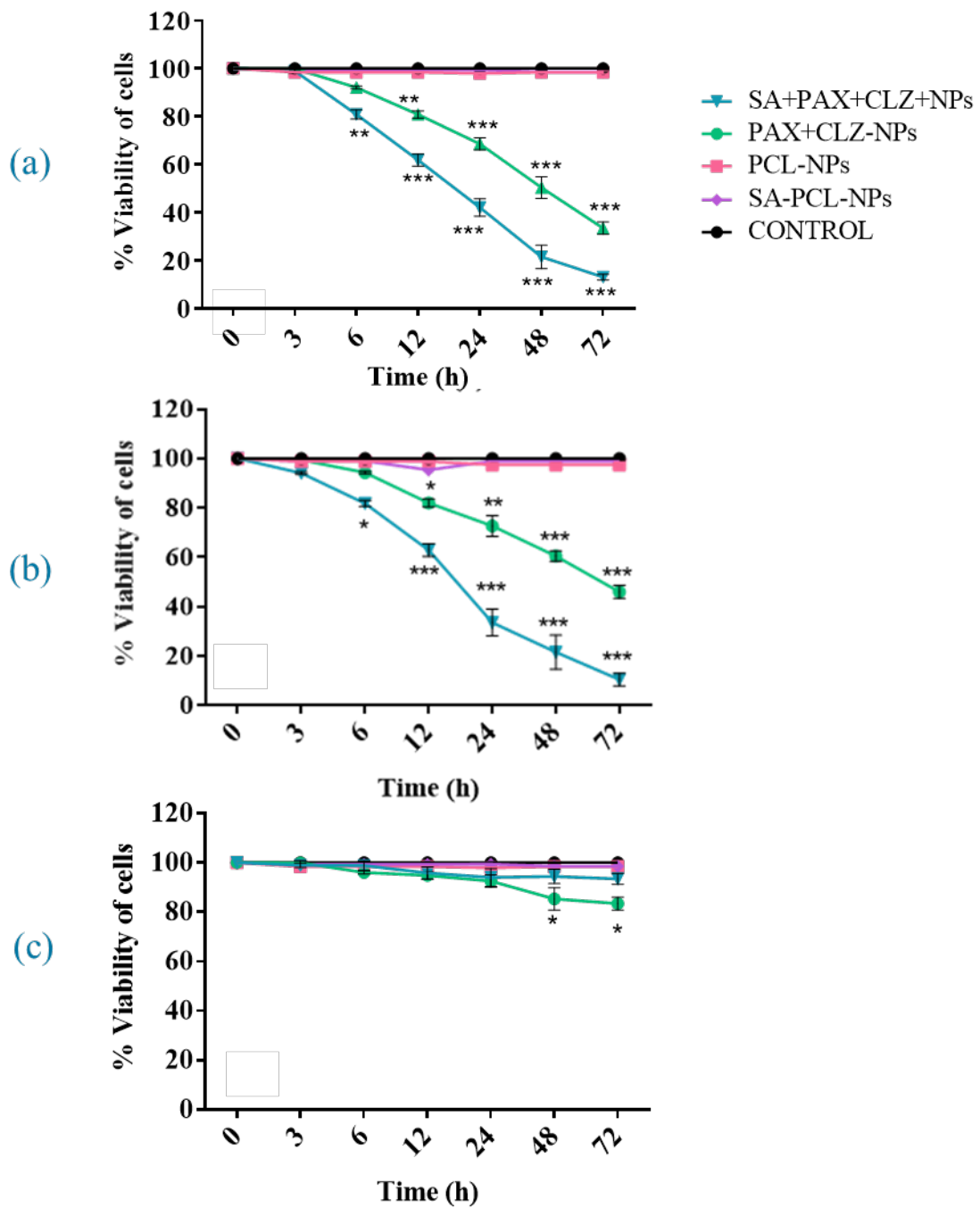


Figure 5.5. Cytotoxic effect of formulated NPs on (a) MCF-7, (b) MDA-MB-231 and (c) HEK-293 cells. Where * indicates $p < 0.05$, ** indicates $p < 0.01$ and *** indicates $p < 0.001$ when comparison made with PCL-NPs

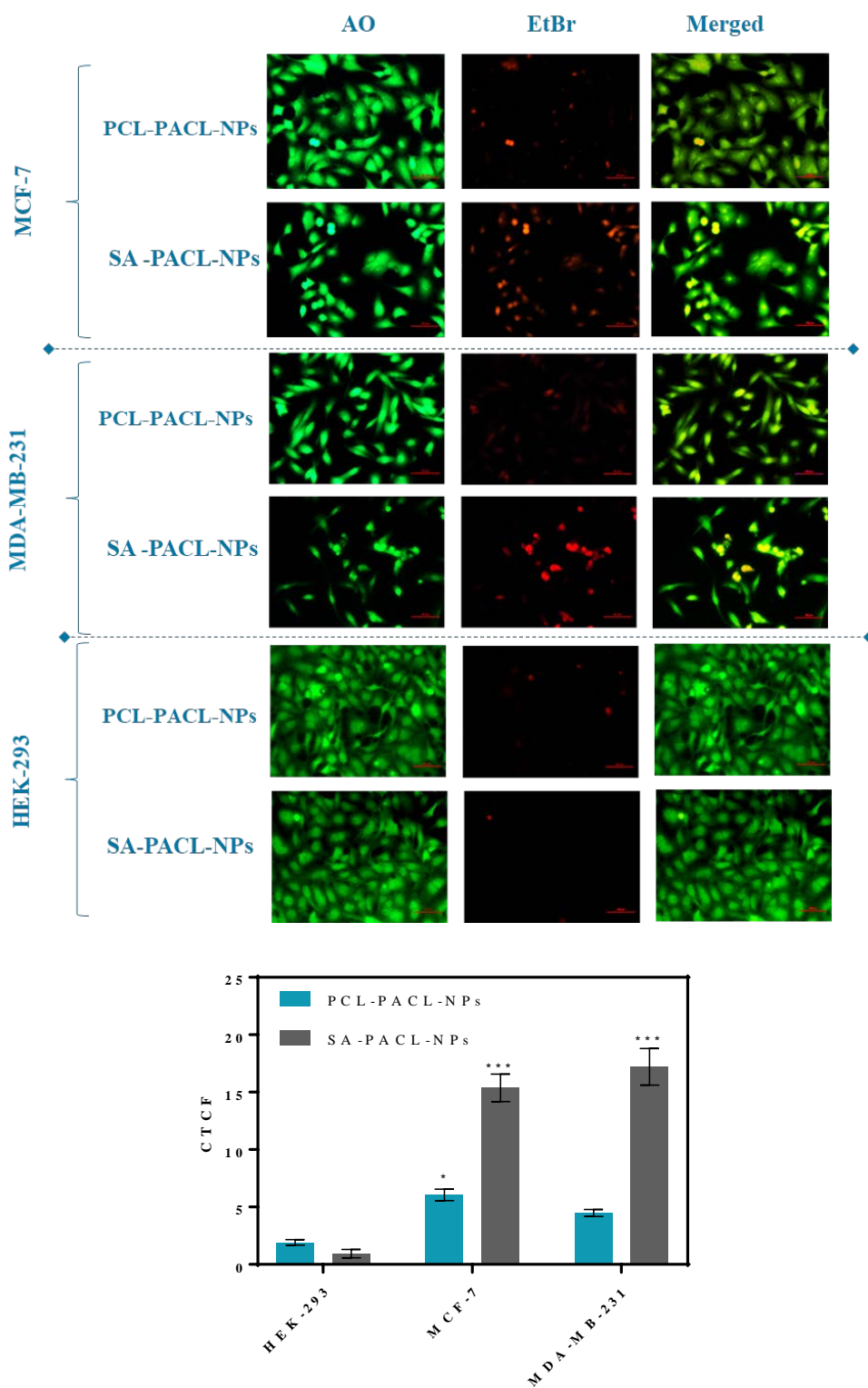


Figure 5.6 The scale bar of images corresponds to 50 μ m (200X). The graph represents the corrected total cell fluorescence (CTCF) for red fluorescence indicating dead EtBr stained cells. * indicates $p < 0.05$ and *** indicate $p < 0.001$ when comparison made with HEK-293.

5.4 SUMMARY POINTS

- Synthesized nanoparticles exhibited smooth spherical surface morphology as observed from SEM-images.
- Sialic acid functionalization on the surface of polymeric nanoparticles was confirmed through FTIR-spectral analysis.
- *In-vitro* drug release studies displayed that nano formulation have controlled drug release prolife for both the drug (PAX and CLZ).
- Optimized nano-formulation was found to be cancer-specific side by side having its minimal effect on normal cells.



APPENDIX



Section -I (Form Chapter-2)

Detailed description of CompuSyn Report and respective CI values for designed combination

Experiment Name: PAX+CLZ combination effect
Date: 08-09-2017
File Name: C:\Users\Attituder\Desktop\compusyn analysis\PX+CLZ.cse
Description: Effect of PAX and CLZ against breast cancer.
Drug: Paclitaxel (PAX) [nM]
Drug: Clotrimazole (CLZ) [μ M]
Drug Combo: Paclitaxel + Clotrimazole (PX+CLZ) (PAX+CLZ)

Data for Drug: PAX [nM]

Dose Effect

6.25 0.08
12.5 0.18
25.0 0.3
50.0 0.49

4 data points entered.

X-int: 1.71047

Y-int: -1.9436 +/- 0.06275

m: 1.13628 +/- 0.04856

Dm: 51.3417

r: 0.99818

Data for Drug: CLZ [μ M]

Dose Effect

6.25 0.16
12.5 0.22
25.0 0.32
50.0 0.49

4 data points entered.

X-int: 1.76877

Y-int: -1.3694 +/- 0.09529

m: 0.77423 +/- 0.07375

Dm: 58.7177

r: 0.99105

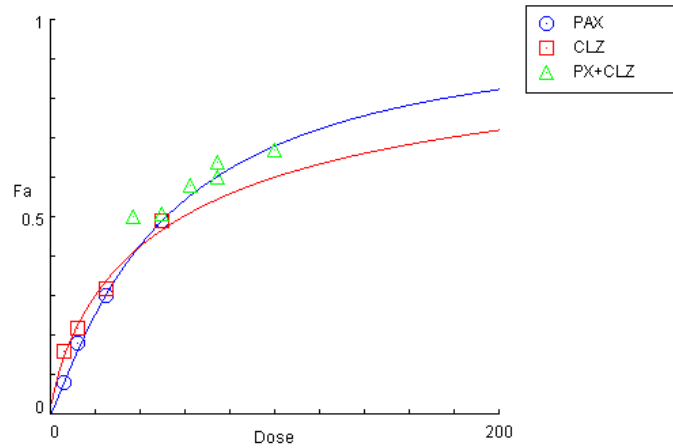
Data for Non-Constant Combo: PX+CLZ (PAX+CLZ)

Dose PAX	Dose CLZ	Effect
12.5	25.0	0.5
12.5	50.0	0.58

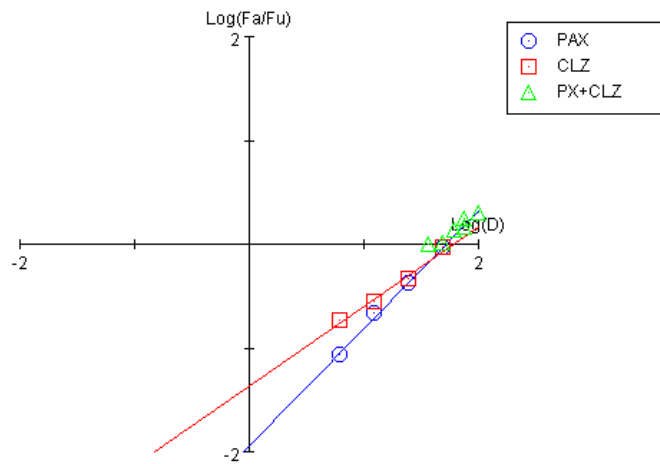
Dose PAX	Dose CLZ	Effect
25.0	25.0	0.51
25.0	50.0	0.64
50.0	25.0	0.6
50.0	50.0	0.67

6 data points entered.

Dose-Effect Curve



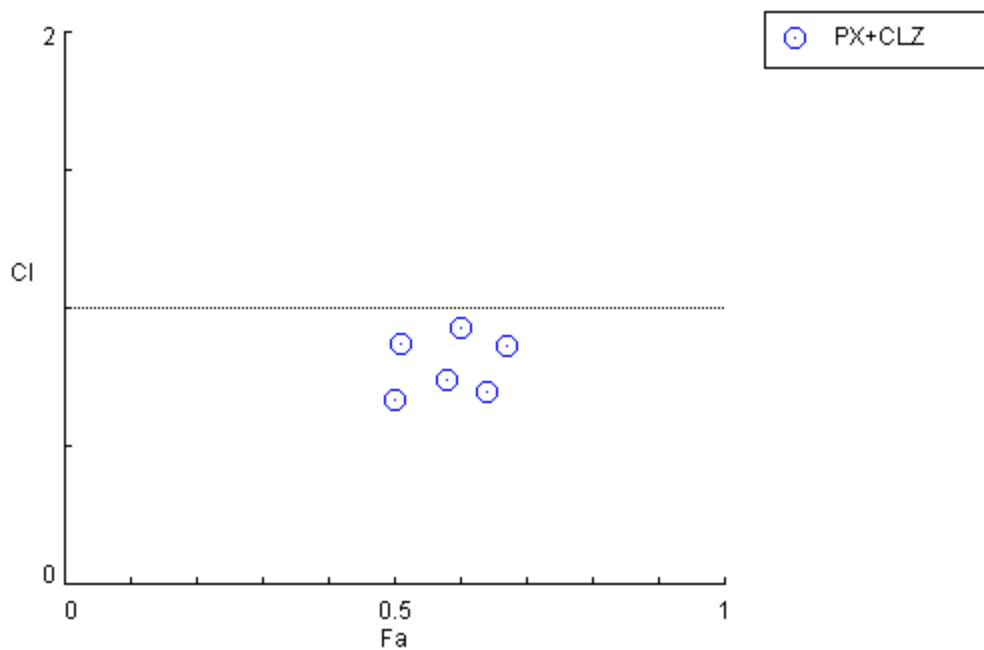
Median-Effect Plot



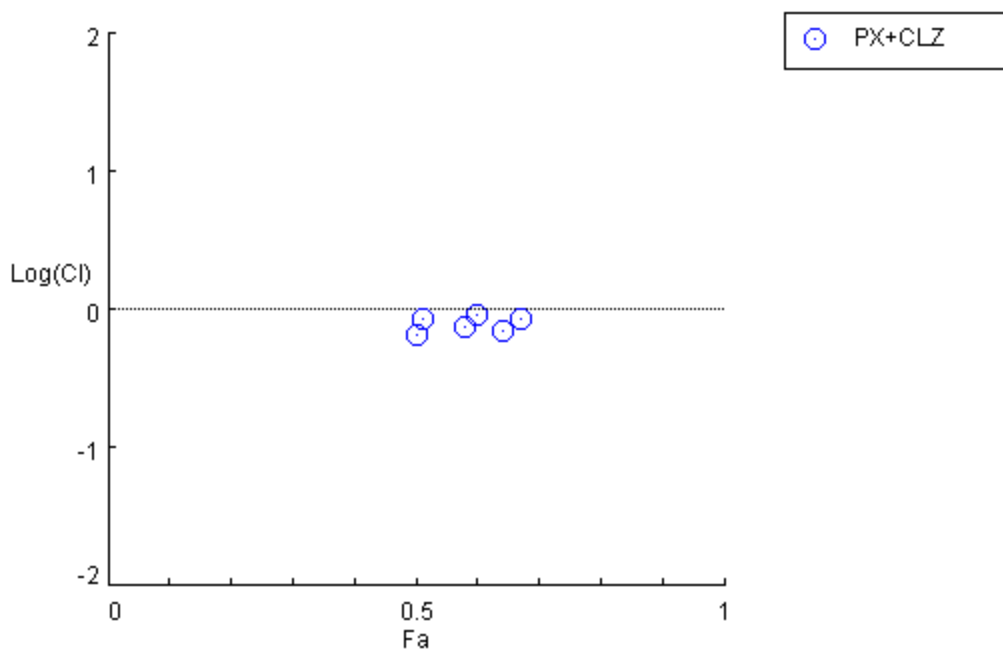
CI Data for Non-Constant Combo: PX+CLZ (PAX+CLZ)

Dose PAX	Dose CLZ	Effect	CI
12.5	25.0	0.5	0.66923
12.5	50.0	0.58	0.74450
25.0	25.0	0.51	0.87441
25.0	50.0	0.64	0.69847
50.0	25.0	0.6	0.93379
50.0	50.0	0.67	0.86334

Combination Index Plot



Logarithmic Combination Index Plot

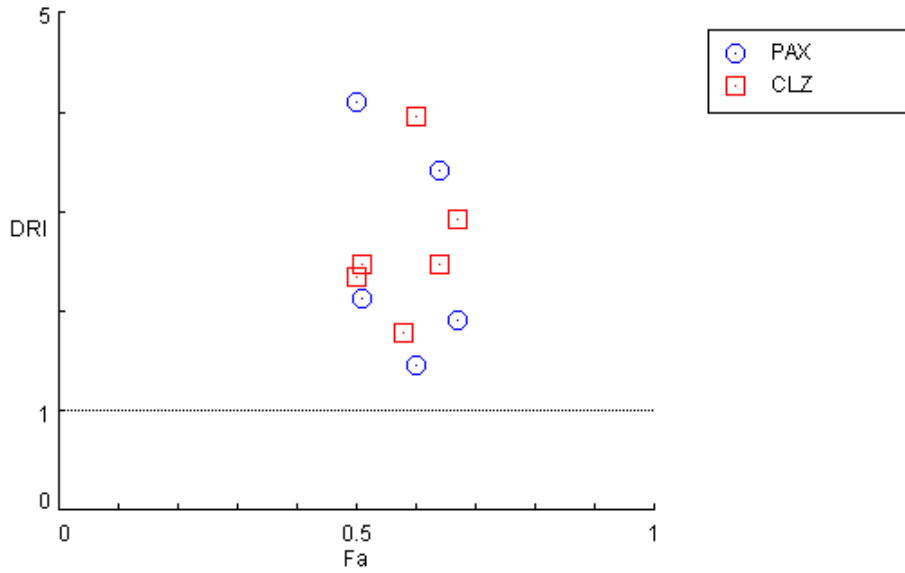


DRI Data for Non-Constant Combo: PX+CLZ (PAX+CLZ)

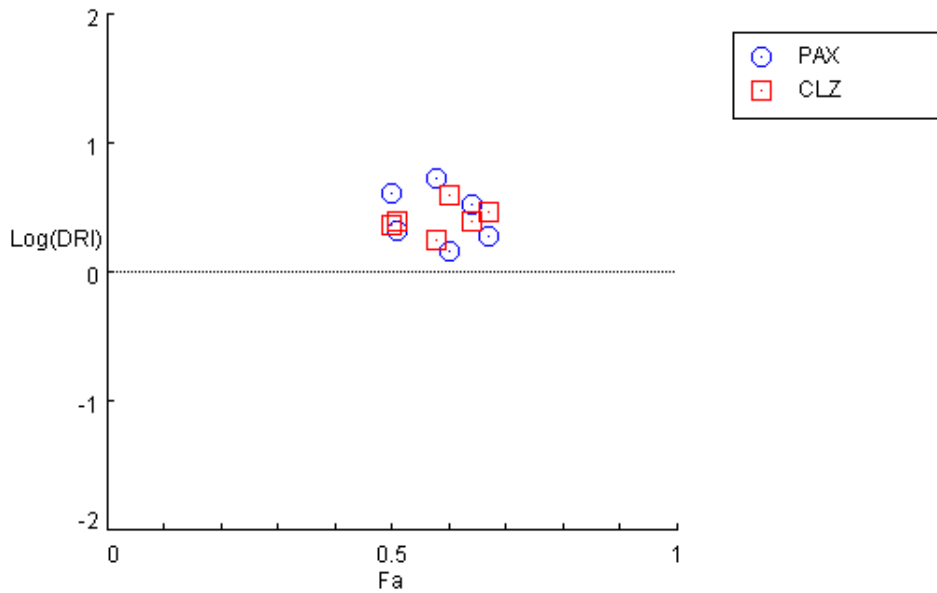
Fa	Dose PAX	Dose CLZ	DRI PAX	DRI CLZ
0.5	51.3417	58.7177	4.10733	2.34871
0.58	68.2082	89.0891	5.45666	1.78178
0.51	53.1815	61.8315	2.12726	2.47326
0.64	85.1881	123.456	3.40752	2.46912

Fa	Dose PAX	Dose CLZ	DRI PAX	DRI CLZ
0.6	73.3571	99.1310	1.46714	3.96524
0.67	95.7512	146.560	1.91502	2.93120

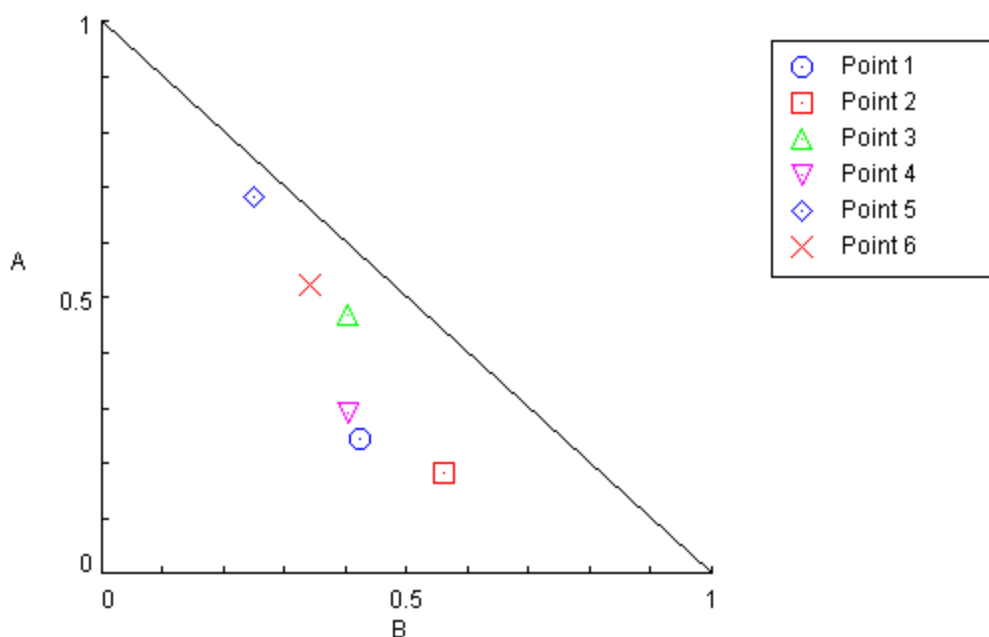
DRI Plot for Non-Constant Combo: PX+CLZ (PAX+CLZ)



Log(DRI) Plot for Non-Constant Combo: PX+CLZ (PAX+CLZ)



Normalized Isobologram for Combo: PX+CLZ (PAX+CLZ)



Summary Table

Experiment Name:	PAX+CLZ combination effect
Date:	08-09-2017
File Name:	C:\Users\Attituder\Desktop\compusyn analysis\PX+CLZ.cse
Description	Effect of PAX and CLZ against breast cancer.
Drug:	Paclitaxel (PAX) [nM]
Drug:	Clotrimazole (CLZ) [μ M]
Drug Combo:	Paclitaxel + Clotrimazole (PX+CLZ) (PAX+CLZ)

Drug/Combo	Dm	m	r
PAX	51.3417	1.13628	0.99818
CLZ	58.7177	0.77423	0.99105

CI values at:

Combo ED50 ED75 ED90 ED95

Data for Fa = 0.5

Drug/Combo	CI value	Dose PAX	Dose CLZ
PAX		51.3417	
CLZ			58.7177

Data for Fa = 0.75

Drug/Combo	CI value	Dose PAX	Dose CLZ
PAX		135.011	

Drug/Combo CI value Dose PAX Dose CLZ

CLZ 242.673

Data for $F_a = 0.9$

Drug/Combo CI value Dose PAX Dose CLZ

PAX 355.032

CLZ 1002.93

Data for $F_a = 0.95$

Drug/Combo CI value Dose PAX Dose CLZ

PAX 685.265

CLZ 2632.76

Data for $F_a = 0.97$

Drug/Combo CI value Dose PAX Dose CLZ

PAX 1094.12

CLZ 5231.66

SECTION -II (From Chapter-3)

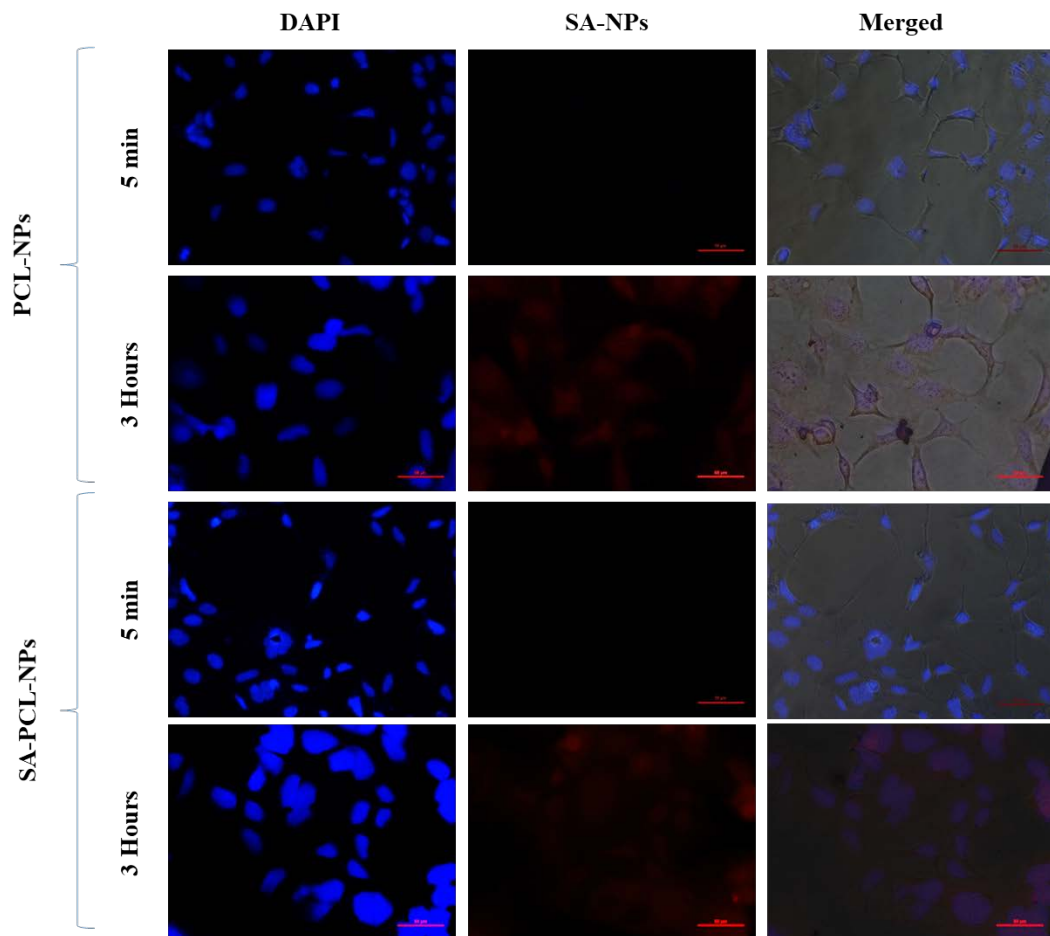


Figure 1. Fluorescent microscopic image representing the cellular uptake of Rhd-loaded-NPs in HEK-293 cell line (normal epithelial cells). The scale bar in each images corresponds to 50 μ M (200X).

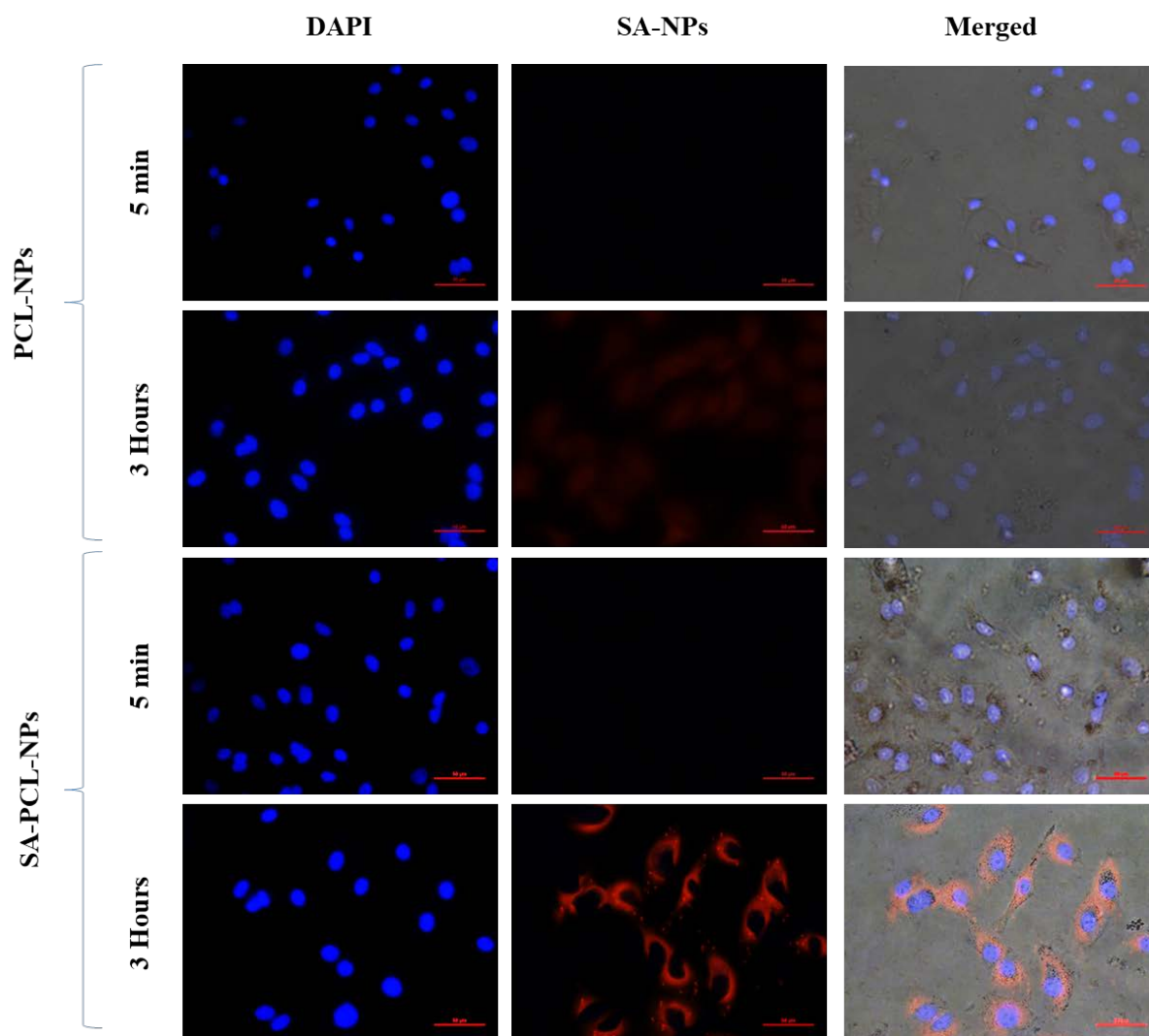


Figure 2. Fluorescent microscopic image representing the cellular uptake of Rhd-loaded-NPs in MCF-7 cell line (normal epithelial cells). The scale bar in each image corresponds to 50 μ M (200X).

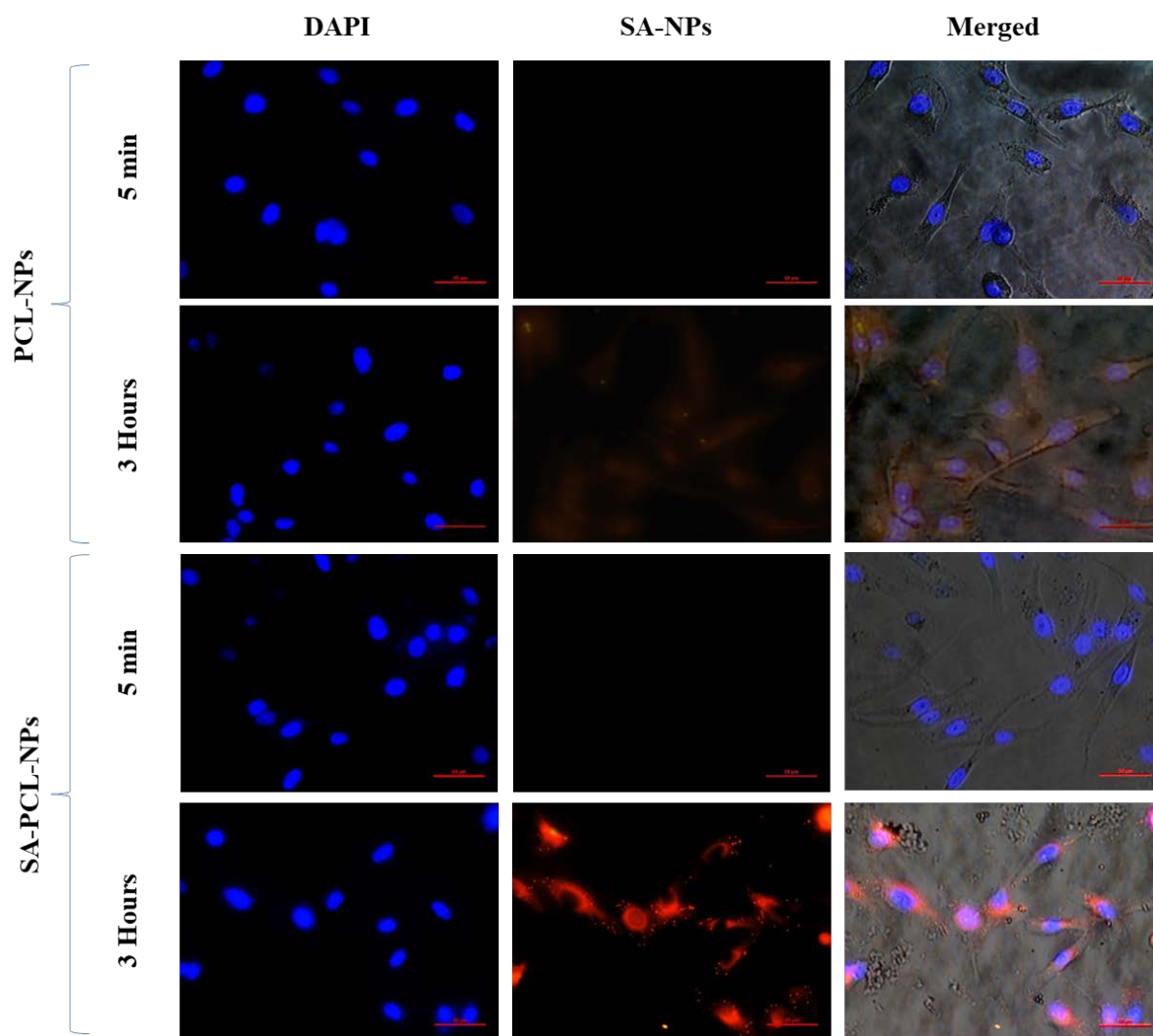


Figure 3. Fluorescent microscopic image representing the cellular uptake of Rhd-loaded-NPs in MCF-7 cell line (normal epithelial cells). The scale bar in each image corresponds to 50 μ M (200X).

SECTION -III (From Chapter-5)

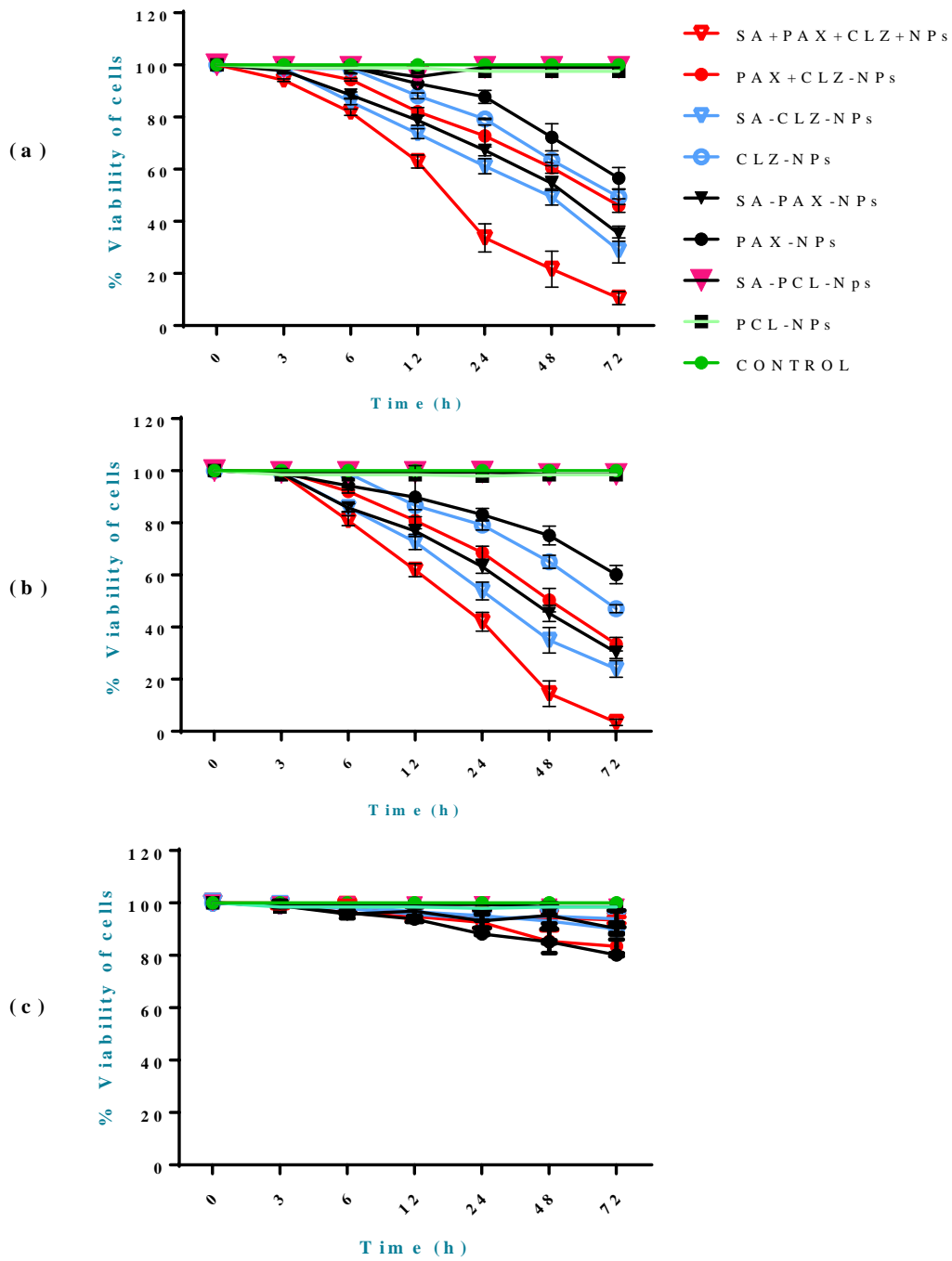


Figure 1. Time dependent cytotoxic effect of formulated NPs on (a) MCF-7, (b) MDA-MB-231 and (c) HEK-293 cells.

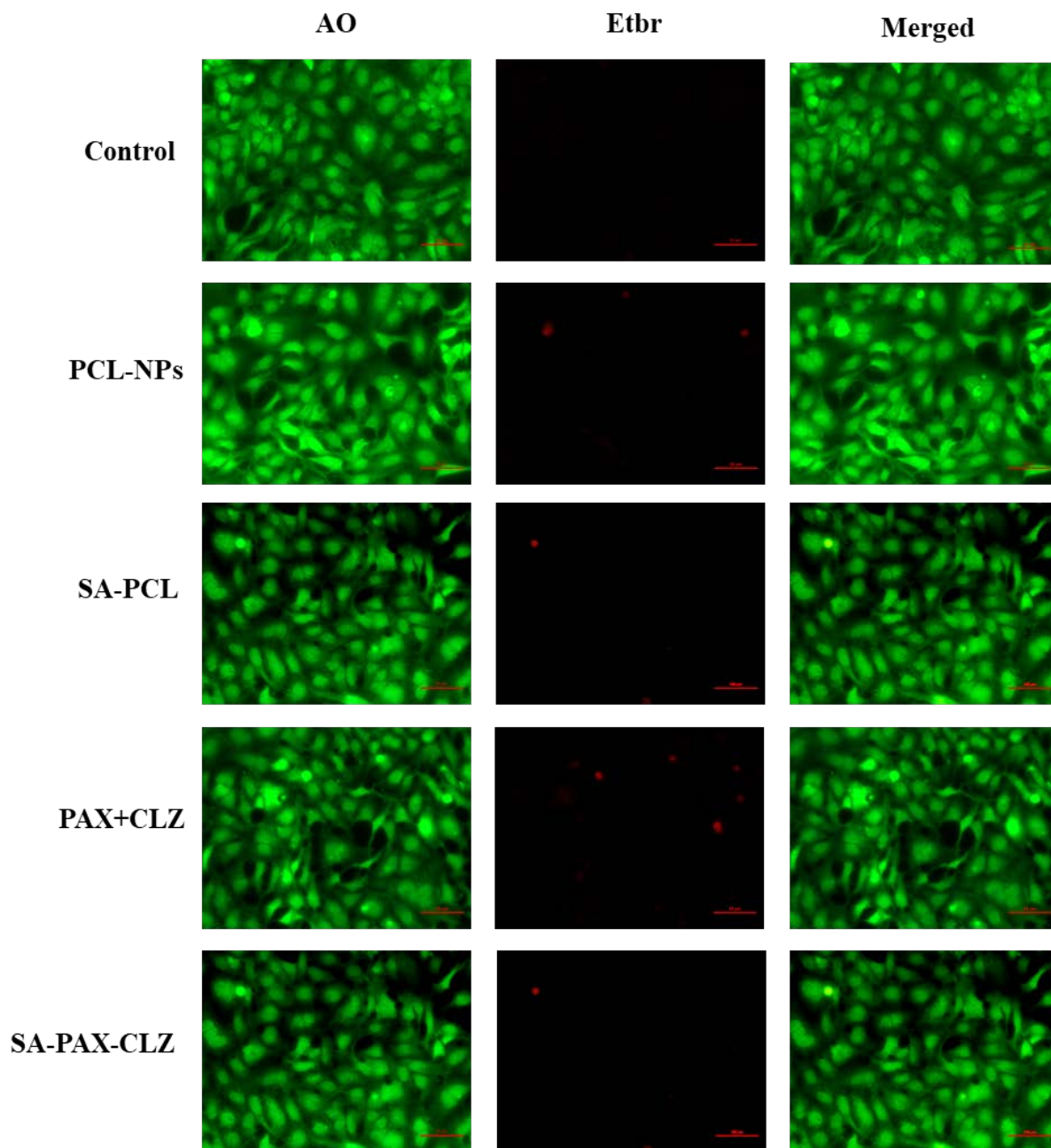


Figure 2. AO/ EtBr fluorescent images representing nuclear morphological changes as an effect of formulated-NPs on HEK-293 cell line after 24h. The sale bar in images corresponds to 50 (μ M) – 200 X.

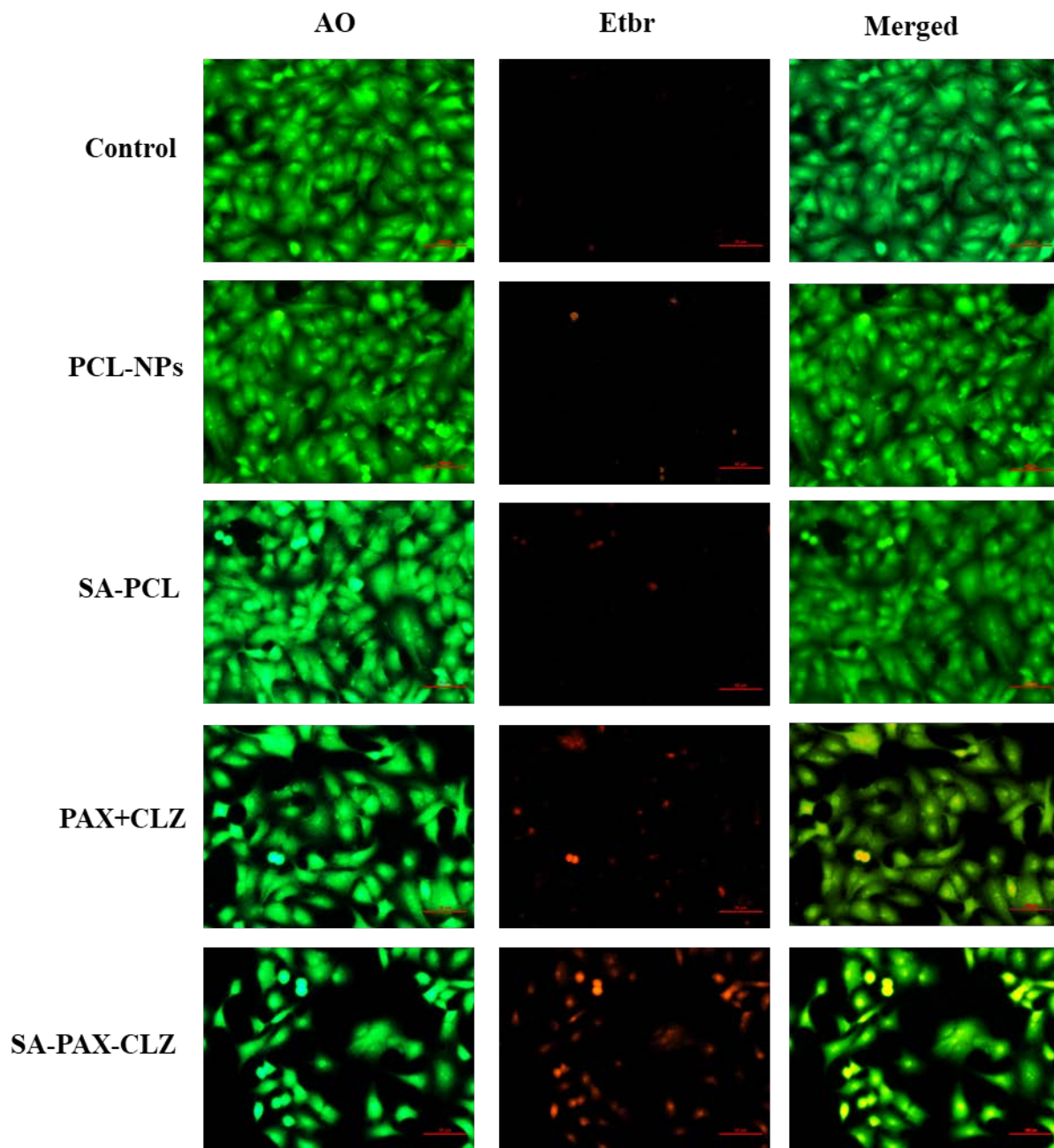


Figure 3. AO/ EtBr fluorescent images representing nuclear morphological changes as an effect of formulated-NPs on MCF-7 cell line after 24h. The sale bar in images corresponds to 50 (μ M) – 200 X.

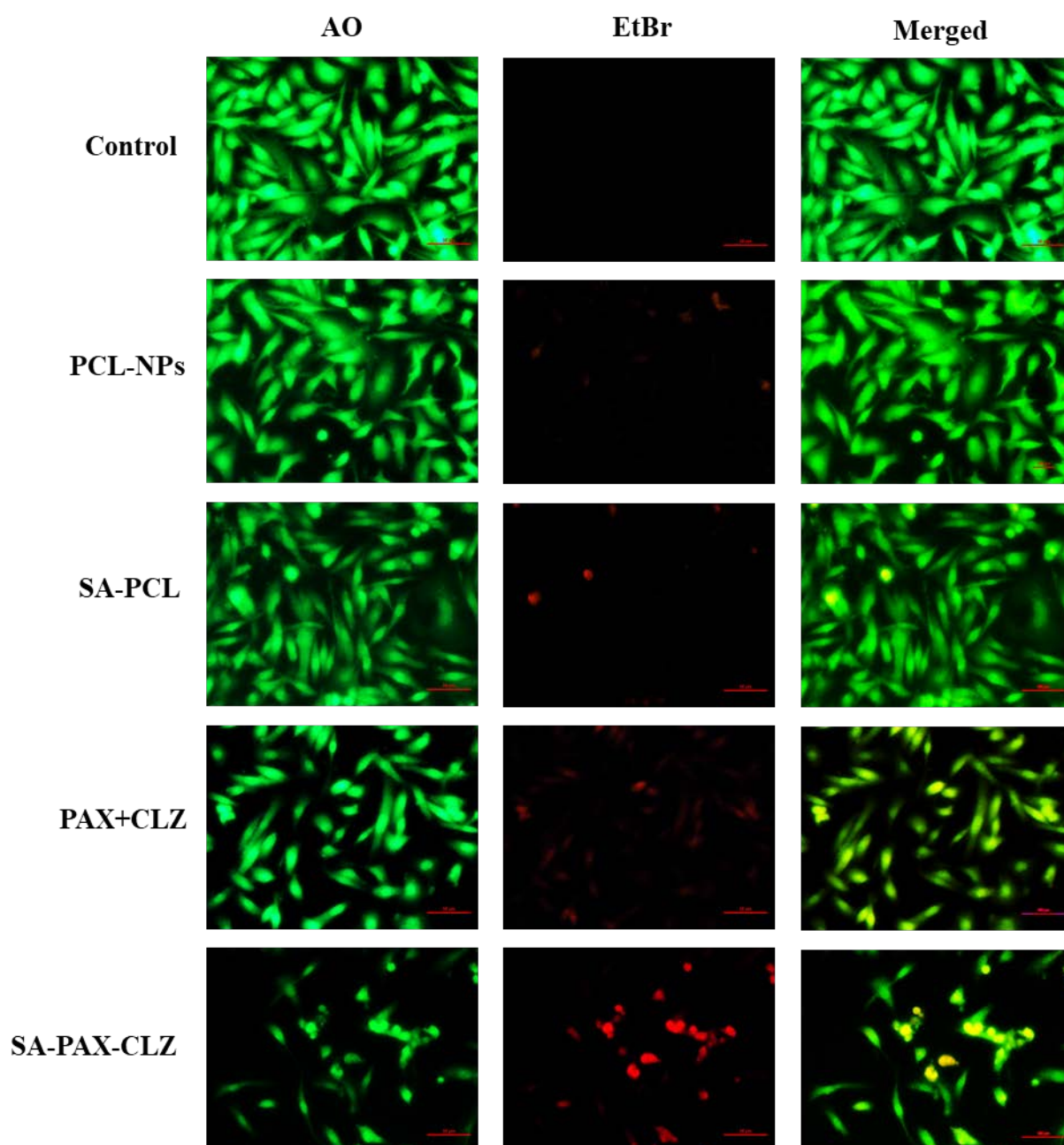
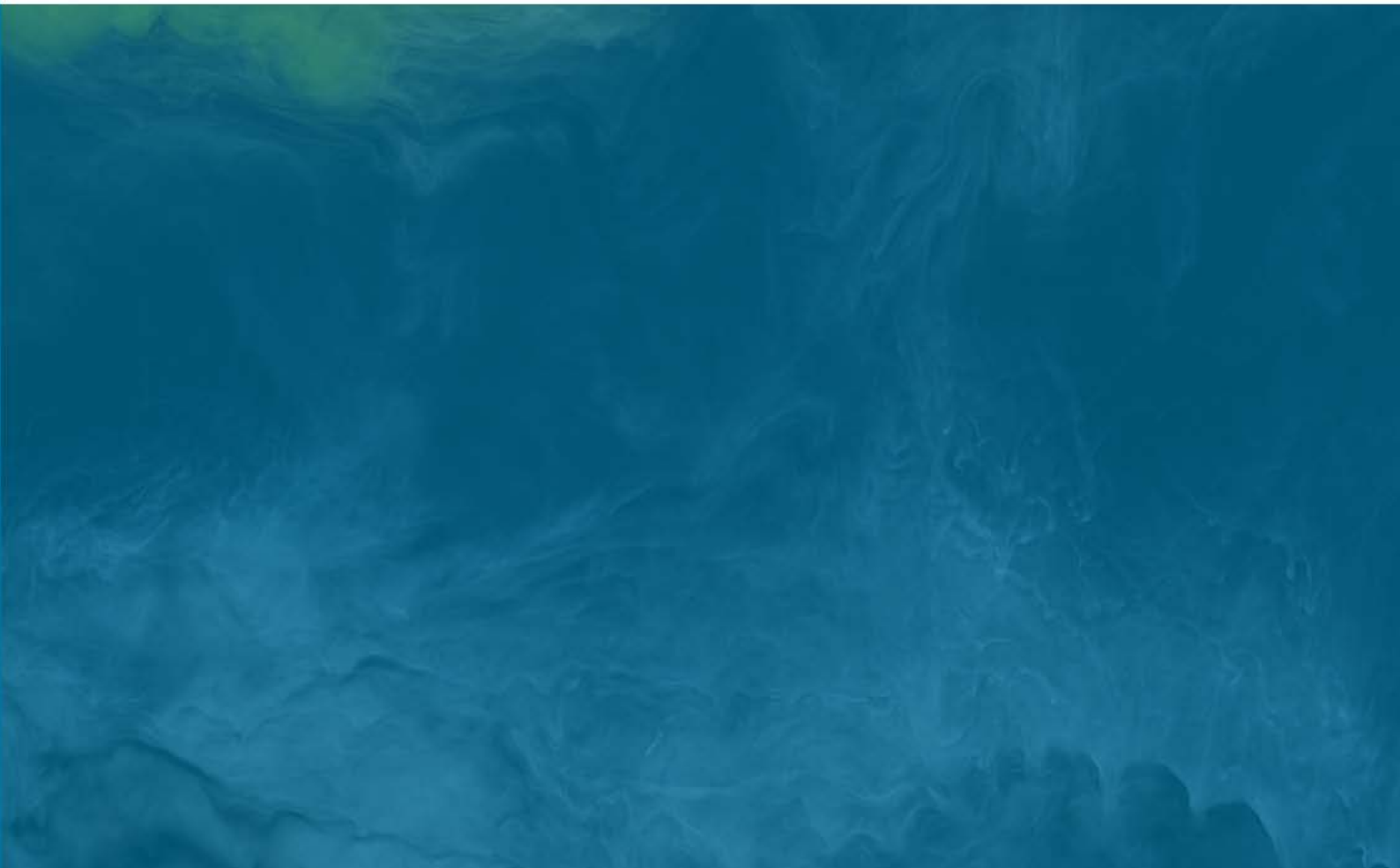


Figure 4. AO/ EtBr fluorescent images representing nuclear morphological changes as an effect of formulated-NPs on MDA-MB-231 cell line after 24h. The sale bar in images corresponds to 50 (μ M) – 200 X.



References



- 1 Kelsey, J.L., and Berkowitz, G.S.: 'Breast cancer epidemiology', *Cancer research*, 1988, 48, (20), pp. 5615-5623
- 2 Ferlay, J., Soerjomataram, I., Dikshit, R., Eser, S., Mathers, C., Rebelo, M., Parkin, D.M., Forman, D., and Bray, F.: 'Cancer incidence and mortality worldwide: sources, methods and major patterns in GLOBOCAN 2012', *International journal of cancer*, 2015, 136, (5), pp. E359-E386
- 3 Torre, L.A., Bray, F., Siegel, R.L., Ferlay, J., Lortet-Tieulent, J., and Jemal, A.: 'Global cancer statistics, 2012', *CA: a cancer journal for clinicians*, 2015, 65, (2), pp. 87-108
- 4 Bray, F., Jemal, A., Grey, N., Ferlay, J., and Forman, D.: 'Global cancer transitions according to the Human Development Index (2008–2030): a population-based study', *The lancet oncology*, 2012, 13, (8), pp. 790-801
- 5 Siegel, R., Ma, J., Zou, Z., and Jemal, A.: 'Cancer statistics, 2014', *CA: a cancer journal for clinicians*, 2014, 64, (1), pp. 9-29
- 6 Siegel, R.L., Miller, K.D., and Jemal, A.: 'Cancer statistics, 2016', *CA: a cancer journal for clinicians*, 2016, 66, (1), pp. 7-30
- 7 Liotta, L.A., Steeg, P.S., and Stetler-Stevenson, W.G.: 'Cancer metastasis and angiogenesis: an imbalance of positive and negative regulation', *Cell*, 1991, 64, (2), pp. 327-336
- 8 Cancer, A.J.C.o.: 'Breast': 'AJCC cancer staging manual' (Springer, 2002), pp. 223-240
- 9 Goldhirsch, A., Winer, E.P., Coates, A., Gelber, R., Piccart-Gebhart, M., Thürlimann, B., Senn, H.-J., members, P., Albain, K.S., and André, F.: 'Personalizing the treatment of women with early breast cancer: highlights of the St Gallen International Expert Consensus on the Primary Therapy of Early Breast Cancer 2013', *Annals of oncology*, 2013, 24, (9), pp. 2206-2223
- 10 O'shaughnessy, J., Blum, J., Moiseyenko, V., Jones, S., Miles, D., Bell, D., Rosso, R., Mauriac, L., Osterwalder, B., and Burger, H.-U.: 'Randomized, open-label, phase II trial of oral capecitabine (Xeloda®) vs. a reference arm of intravenous CMF (cyclophosphamide, methotrexate and 5-fluorouracil) as first-line therapy for advanced/metastatic breast cancer', *Annals of Oncology*, 2001, 12, (9), pp. 1247-1254
- 11 Cragg, G.M., and Newman, D.J.: 'Plants as a source of anti-cancer agents', *Journal of ethnopharmacology*, 2005, 100, (1-2), pp. 72-79

- 12 Singla, A.K., Garg, A., and Aggarwal, D.: 'Paclitaxel and its formulations', *International journal of pharmaceutics*, 2002, 235, (1-2), pp. 179-192
- 13 Holmes, F.A., Walters, R.S., Theriault, R.L., Buzdar, A.U., Frye, D.K., Hortobagyi, G.N., Forman, A.D., Newton, L.K., and Raber, M.N.: 'Phase II trial of taxol, an active drug in the treatment of metastatic breast cancer', *JNCI: Journal of the National Cancer Institute*, 1991, 83, (24), pp. 1797-1805
- 14 Gelderblom, H., Verweij, J., Nooter, K., and Sparreboom, A.: 'Cremophor EL: the drawbacks and advantages of vehicle selection for drug formulation', *European journal of cancer*, 2001, 37, (13), pp. 1590-1598
- 15 Dorr, R.T.: 'Pharmacology and toxicology of Cremophor EL diluent', *Annals of Pharmacotherapy*, 1994, 28, (5_suppl), pp. S11-S14
- 16 Bobo, D., Robinson, K.J., Islam, J., Thurecht, K.J., and Corrie, S.R.: 'Nanoparticle-based medicines: a review of FDA-approved materials and clinical trials to date', *Pharmaceutical research*, 2016, 33, (10), pp. 2373-2387
- 17 Byrne, J.D., Betancourt, T., and Brannon-Peppas, L.: 'Active targeting schemes for nanoparticle systems in cancer therapeutics', *Advanced drug delivery reviews*, 2008, 60, (15), pp. 1615-1626
- 18 Miele, E., Spinelli, G.P., Miele, E., Tomao, F., and Tomao, S.: 'Albumin-bound formulation of paclitaxel (Abraxane® ABI-007) in the treatment of breast cancer', *International journal of nanomedicine*, 2009, 4, pp. 99
- 19 Green, M., Manikhas, G., Orlov, S., Afanasyev, B., Makhson, A., Bhar, P., and Hawkins, M.: 'Abraxane®, a novel Cremophor®-free, albumin-bound particle form of paclitaxel for the treatment of advanced non-small-cell lung cancer', *Annals of Oncology*, 2006, 17, (8), pp. 1263-1268
- 20 Chidambaram, M., Manavalan, R., and Kathiresan, K.: 'Nanotherapeutics to overcome conventional cancer chemotherapy limitations', *Journal of pharmacy & pharmaceutical sciences*, 2011, 14, (1), pp. 67-77
- 21 Peer, D., Karp, J.M., Hong, S., Farokhzad, O.C., Margalit, R., and Langer, R.: 'Nanocarriers as an emerging platform for cancer therapy', *Nature nanotechnology*, 2007, 2, (12), pp. 751
- 22 Zhang, T., She, Z., Huang, Z., Li, J., Luo, X., and Deng, Y.: 'Application of sialic acid/polysialic acid in the drug delivery systems', *Asian Journal of Pharmaceutical Sciences*, 2014, 9, (2), pp. 75-81

- 23 Bader, R.A., and Wardwell, P.R.: 'Polysialic acid: overcoming the hurdles of drug delivery', *Therapeutic delivery*, 2014, 5, (3), pp. 235-237
- 24 Hayek, E.R., Speakman, E., and Rehmus, E.: 'Acute doxorubicin cardiotoxicity', *New England Journal of Medicine*, 2005, 352, (23), pp. 2456-2457
- 25 Markman, M.: 'Managing taxane toxicities', *Supportive care in cancer*, 2003, 11, (3), pp. 144-147
- 26 Furtado, C.M., Marcondes, M.C., Sola-Penna, M., De Souza, M.L., and Zancan, P.: 'Clotrimazole preferentially inhibits human breast cancer cell proliferation, viability and glycolysis', *PloS one*, 2012, 7, (2), pp. e30462
- 27 Coelho, R.G., de Castro Calaça, I., de Moura Celestrini, D., Correia, A.H., Costa, M.A.S.M., and Sola-Penna, M.: 'Clotrimazole disrupts glycolysis in human breast cancer without affecting non-tumoral tissues', *Molecular genetics and metabolism*, 2011, 103, (4), pp. 394-398
- 28 Haley, B., and Frenkel, E.: 'Nanoparticles for drug delivery in cancer treatment', in Editor (Ed.)^(Eds.): 'Book Nanoparticles for drug delivery in cancer treatment' (Elsevier, 2008, edn.), pp. 57-64
- 29 Sutradhar, K.B., and Amin, M.L.: 'Nanotechnology in cancer drug delivery and selective targeting', *ISRN Nanotechnology*, 2014, 2014
- 30 Alexis, F., Rhee, J.-W., Richie, J.P., Radovic-Moreno, A.F., Langer, R., and Farokhzad, O.C.: 'New frontiers in nanotechnology for cancer treatment', in Editor (Ed.)^(Eds.): 'Book New frontiers in nanotechnology for cancer treatment' (Elsevier, 2008, edn.), pp. 74-85
- 31 Devita Jr, V.T., Young, R.C., and Canellos, G.P.: 'Combination versus single agent chemotherapy: a review of the basis for selection of drug treatment of cancer', *Cancer*, 1975, 35, (1), pp. 98-110
- 32 Pridgen, E.M., Langer, R., and Farokhzad, O.C.: 'Biodegradable, polymeric nanoparticle delivery systems for cancer therapy', 2007
- 33 Key, T.J., Verkasalo, P.K., and Banks, E.: 'Epidemiology of breast cancer', *The lancet oncology*, 2001, 2, (3), pp. 133-140
- 34 McPherson, K., Steel, C., and Dixon, J.: 'ABC of breast diseases: breast cancer—epidemiology, risk factors, and genetics', *BMJ: British Medical Journal*, 2000, 321, (7261), pp. 624
- 35 Meric, F., Bernstam, E.V., Mirza, N.Q., Hunt, K.K., Ames, F.C., Ross, M.I., Kuerer, H.M., Pollock, R.E., Musen, M.A., and Singletary, S.E.: 'Breast cancer on the world wide web:

- cross sectional survey of quality of information and popularity of websites’, *Bmj*, 2002, 324, (7337), pp. 577-581
- 36 Khokhar, A.: ‘Breast cancer in India: where do we stand and where do we go?’, *Asian Pacific Journal of Cancer Prevention*, 2012, 13, (10), pp. 4861-4866
- 37 Agarwal, G., and Ramakant, P.: ‘Breast cancer care in India: the current scenario and the challenges for the future’, *Breast care*, 2008, 3, (1), pp. 21-27
- 38 Malvia, S., Bagadi, S.A., Dubey, U.S., and Saxena, S.: ‘Epidemiology of breast cancer in Indian women’, *Asia-Pacific Journal of Clinical Oncology*, 2017, 13, (4), pp. 289-295
- 39 Li, C., Uribe, D., and Daling, J.: ‘Clinical characteristics of different histologic types of breast cancer’, *British journal of cancer*, 2005, 93, (9), pp. 1046
- 40 Weigelt, B., and Reis-Filho, J.S.: ‘Histological and molecular types of breast cancer: is there a unifying taxonomy?’, *Nature reviews Clinical oncology*, 2009, 6, (12), pp. 718
- 41 Rouzier, R., Perou, C.M., Symmans, W.F., Ibrahim, N., Cristofanilli, M., Anderson, K., Hess, K.R., Stec, J., Ayers, M., and Wagner, P.: ‘Breast cancer molecular subtypes respond differently to preoperative chemotherapy’, *Clinical cancer research*, 2005, 11, (16), pp. 5678-5685
- 42 Yerushalmi, R., Hayes, M., and Gelmon, K.: ‘Breast carcinoma—rare types: review of the literature’, *Annals of oncology*, 2009, 20, (11), pp. 1763-1770
- 43 Fentiman, I.S., Fourquet, A., and Hortobagyi, G.N.: ‘Male breast cancer’, *The Lancet*, 2006, 367, (9510), pp. 595-604
- 44 Stevanovic, A., Lee, P., and Wilcken, N.: ‘Metastatic breast cancer’, *Australian family physician*, 2006, 35, (5), pp. 309
- 45 Network, N.C.C.: ‘Breast cancer Clinical Practice Guidelines in Oncology’, *Journal of the National Comprehensive Cancer Network: JNCCN*, 2003, 1, (2), pp. 148
- 46 Group, E.B.C.T.C.: ‘Favourable and unfavourable effects on long-term survival of radiotherapy for early breast cancer: an overview of the randomised trials’, *The Lancet*, 2000, 355, (9217), pp. 1757-1770
- 47 Seidman, A.D.: ‘Systemic treatment of breast cancer’, *Oncology (Williston Park)*, 2006, 20, pp. 983-990
- 48 GROUP, E.B.C.T.C.: ‘Systemic treatment of early breast cancer by hormonal, cytotoxic, or immune therapy: 133 randomised trials involving 31 000 recurrences and 24 000 deaths among 75 000 women’, *The Lancet*, 1992, 339, (8784), pp. 1-15

- 49 Ross, R.K., Paganini-Hill, A., Wan, P.C., and Pike, M.C.: 'Effect of hormone replacement therapy on breast cancer risk: estrogen versus estrogen plus progestin', *Journal of the National Cancer Institute*, 2000, 92, (4), pp. 328-332
- 50 Higgins, M.J., and Baselga, J.: 'Targeted therapies for breast cancer', *The Journal of clinical investigation*, 2011, 121, (10), pp. 3797-3803
- 51 Hassan, M., Ansari, J., Spooner, D., and Hussain, S.: 'Chemotherapy for breast cancer', *Oncology reports*, 2010, 24, (5), pp. 1121-1131
- 52 Hussain, S.A., Palmer, D.H., Stevens, A., Spooner, D., Poole, C.J., and Rea, D.W.: 'Role of chemotherapy in breast cancer', *Expert review of anticancer therapy*, 2005, 5, (6), pp. 1095-1110
- 53 McGrogan, B.T., Gilmartin, B., Carney, D.N., and McCann, A.: 'Taxanes, microtubules and chemoresistant breast cancer', *Biochimica et Biophysica Acta (BBA)-Reviews on Cancer*, 2008, 1785, (2), pp. 96-132
- 54 Clemons, M., Leahy, M., Valle, J., Jayson, G., Ranson, M., and Howell, A.: 'Review of recent trials of chemotherapy for advanced breast cancer: the taxanes', *European journal of cancer*, 1997, 33, (13), pp. 2183-2193
- 55 Rakha, E.A., Reis-Filho, J.S., and Ellis, I.O.: 'Basal-like breast cancer: a critical review', *Journal of clinical oncology*, 2008, 26, (15), pp. 2568-2581
- 56 Blagosklonny, M.V., and Fojo, T.: 'Molecular effects of paclitaxel: myths and reality (a critical review)', *International journal of cancer*, 1999, 83, (2), pp. 151-156
- 57 Marupudi, N.I., Han, J.E., Li, K.W., Renard, V.M., Tyler, B.M., and Brem, H.: 'Paclitaxel: a review of adverse toxicities and novel delivery strategies', *Expert opinion on drug safety*, 2007, 6, (5), pp. 609-621
- 58 Kloover, J., Den Bakker, M., Gelderblom, H., and Van Meerbeeck, J.: 'Fatal outcome of a hypersensitivity reaction to paclitaxel: a critical review of premedication regimens', *British journal of cancer*, 2004, 90, (2), pp. 304
- 59 Bonadonna, G., Brusamolino, E., Valagussa, P., Rossi, A., Brugnatelli, L., Brambilla, C., De Lena, M., Tancini, G., Bajetta, E., and Musumeci, R.: 'Combination chemotherapy as an adjuvant treatment in operable breast cancer', *New England Journal of Medicine*, 1976, 294, (8), pp. 405-410
- 60 Hryniuk, W., and Bush, H.: 'The importance of dose intensity in chemotherapy of metastatic breast cancer', *Journal of Clinical Oncology*, 1984, 2, (11), pp. 1281-1288
- 61 Citron, M.L., Berry, D.A., Cirincione, C., Hudis, C., Winer, E.P., Gradishar, W.J., Davidson, N.E., Martino, S., Livingston, R., and Ingle, J.N.: 'Randomized trial of dose-

- dense versus conventionally scheduled and sequential versus concurrent combination chemotherapy as postoperative adjuvant treatment of node-positive primary breast cancer: first report of Intergroup Trial C9741/Cancer and Leukemia Group B Trial 9741', *Journal of clinical oncology*, 2003, 21, (8), pp. 1431-1439
- 62 Kannan, P., Telu, S., Shukla, S., Ambudkar, S.V., Pike, V.W., Halldin, C., Gottesman, M.M., Innis, R.B., and Hall, M.D.: 'The "specific" P-glycoprotein inhibitor tariquidar is also a substrate and an inhibitor for breast cancer resistance protein (BCRP/ABCG2)', *ACS chemical neuroscience*, 2010, 2, (2), pp. 82-89
- 63 O'Shaughnessy, J., Schwartzberg, L., Danso, M.A., Miller, K.D., Rugo, H.S., Neubauer, M., Robert, N., Hellerstedt, B., Saleh, M., and Richards, P.: 'Phase III study of iniparib plus gemcitabine and carboplatin versus gemcitabine and carboplatin in patients with metastatic triple-negative breast cancer', *Journal of clinical oncology*, 2014, 32, (34), pp. 3840-3847
- 64 Ruttala, H.B., and Ko, Y.T.: 'Liposomal co-delivery of curcumin and albumin/paclitaxel nanoparticle for enhanced synergistic antitumor efficacy', *Colloids and Surfaces B: Biointerfaces*, 2015, 128, pp. 419-426
- 65 Recht, A., Come, S.E., Henderson, I.C., Gelman, R.S., Silver, B., Hayes, D.F., Shulman, L.N., and Harris, J.R.: 'The sequencing of chemotherapy and radiation therapy after conservative surgery for early-stage breast cancer', *New England Journal of Medicine*, 1996, 334, (21), pp. 1356-1361
- 66 Group, E.B.C.T.C.: 'Effects of chemotherapy and hormonal therapy for early breast cancer on recurrence and 15-year survival: an overview of the randomised trials', *The Lancet*, 2005, 365, (9472), pp. 1687-1717
- 67 Wright, S.E.: 'Immunotherapy of breast cancer', *Expert opinion on biological therapy*, 2012, 12, (4), pp. 479-490
- 68 Ramirez, G., Klotz, J., Strawitz, J., Wilson, W., Cornell, G., Madden, R., and Minton, J.: 'Combination chemotherapy in breast cancer', *Oncology*, 1975, 32, (3-4), pp. 101-108
- 69 Meira, D.D., Marinho-Carvalho, M.M., Teixeira, C.A., Veiga, V.F., Da Poian, A.T., Holandino, C., de Freitas, M.S., and Sola-Penna, M.: 'Clotrimazole decreases human breast cancer cells viability through alterations in cytoskeleton-associated glycolytic enzymes', *Molecular genetics and metabolism*, 2005, 84, (4), pp. 354-362
- 70 Zancan, P., Rosas, A.O., Marcondes, M.C., Marinho-Carvalho, M.M., and Sola-Penna, M.: 'Clotrimazole inhibits and modulates heterologous association of the key glycolytic

- enzyme 6-phosphofructo-1-kinase', *Biochemical pharmacology*, 2007, 73, (10), pp. 1520-1527
- 71 Aktas, H., Flückiger, R., Acosta, J.A., Savage, J.M., Palakurthi, S.S., and Halperin, J.A.: 'Depletion of intracellular Ca²⁺ stores, phosphorylation of eIF2 α , and sustained inhibition of translation initiation mediate the anticancer effects of clotrimazole', *Proceedings of the National Academy of Sciences*, 1998, 95, (14), pp. 8280-8285
- 72 Liu, H., Li, Y., and Raisch, K.P.: 'Clotrimazole induces a late G1 cell cycle arrest and sensitizes glioblastoma cells to radiation in vitro', *Anti-cancer drugs*, 2010, 21, (9), pp. 841
- 73 Khalid, M.H., Shibata, S., and Hiura, T.: 'Effects of clotrimazole on the growth, morphological characteristics, and cisplatin sensitivity of human glioblastoma cells in vitro', *Journal of neurosurgery*, 1999, 90, (5), pp. 918-927
- 74 Gomez, L.S., Zancan, P., Marcondes, M.C., Ramos-Santos, L., Meyer-Fernandes, J.R., Sola-Penna, M., and Da Silva, D.: 'Resveratrol decreases breast cancer cell viability and glucose metabolism by inhibiting 6-phosphofructo-1-kinase', *Biochimie*, 2013, 95, (6), pp. 1336-1343
- 75 Tanaka, T., Decuzzi, P., Cristofanilli, M., Sakamoto, J.H., Tasciotti, E., Robertson, F.M., and Ferrari, M.: 'Nanotechnology for breast cancer therapy', *Biomedical microdevices*, 2009, 11, (1), pp. 49-63
- 76 Suh, K., and Tanaka, T.: 'Nanomedicine in cancer', *Translational Medic*, 2011, 1, pp. 103e
- 77 Yezhelyev, M.V., Gao, X., Xing, Y., Al-Hajj, A., Nie, S., and O'Regan, R.M.: 'Emerging use of nanoparticles in diagnosis and treatment of breast cancer', *The lancet oncology*, 2006, 7, (8), pp. 657-667
- 78 Jabr-Milane, L.S., van Vlerken, L.E., Yadav, S., and Amiji, M.M.: 'Multi-functional nanocarriers to overcome tumor drug resistance', *Cancer treatment reviews*, 2008, 34, (7), pp. 592-602
- 79 Greish, K.: 'Enhanced permeability and retention of macromolecular drugs in solid tumors: a royal gate for targeted anticancer nanomedicines', *Journal of drug targeting*, 2007, 15, (7-8), pp. 457-464
- 80 Greish, K.: 'Enhanced permeability and retention (EPR) effect for anticancer nanomedicine drug targeting': 'Cancer Nanotechnology' (Springer, 2010), pp. 25-37
- 81 Bertrand, N., Wu, J., Xu, X., Kamaly, N., and Farokhzad, O.C.: 'Cancer nanotechnology: the impact of passive and active targeting in the era of modern cancer biology', *Advanced drug delivery reviews*, 2014, 66, pp. 2-25

- 82 Danhier, F., Feron, O., and Préat, V.: ‘To exploit the tumor microenvironment: passive and active tumor targeting of nanocarriers for anti-cancer drug delivery’, *Journal of controlled release*, 2010, 148, (2), pp. 135-146
- 83 Kirpotin, D.B., Drummond, D.C., Shao, Y., Shalaby, M.R., Hong, K., Nielsen, U.B., Marks, J.D., Benz, C.C., and Park, J.W.: ‘Antibody targeting of long-circulating lipidic nanoparticles does not increase tumor localization but does increase internalization in animal models’, *Cancer research*, 2006, 66, (13), pp. 6732-6740
- 84 Zhang, T., Zhou, S., Hu, L., Peng, B., Liu, Y., Luo, X., Song, Y., Liu, X., and Deng, Y.: ‘Polysialic acid-modifying liposomes for efficient delivery of epirubicin, in-vitro characterization and in-vivo evaluation’, *International journal of pharmaceutics*, 2016, 515, (1-2), pp. 449-459
- 85 Greco, F., Arif, I., Botting, R., Fante, C., Quintieri, L., Clementi, C., Schiavon, O., and Pasut, G.: ‘Polysialic acid as a drug carrier: evaluation of a new polysialic acid–epirubicin conjugate and its comparison against established drug carriers’, *Polymer Chemistry*, 2013, 4, (5), pp. 1600-1609
- 86 Tosi, G., Vergoni, A., Ruozi, B., Bondioli, L., Badiali, L., Rivasi, F., Costantino, L., Forni, F., and Vandelli, M.: ‘Sialic acid and glycopeptides conjugated PLGA nanoparticles for central nervous system targeting: in vivo pharmacological evidence and biodistribution’, *Journal of controlled release*, 2010, 145, (1), pp. 49-57
- 87 Bondioli, L., Costantino, L., Ballestrazzi, A., Lucchesi, D., Boraschi, D., Pellati, F., Benvenuti, S., Tosi, G., and Vandelli, M.A.: ‘PLGA nanoparticles surface decorated with the sialic acid, N-acetylneuraminic acid’, *Biomaterials*, 2010, 31, (12), pp. 3395-3403
- 88 Lemarchand, C., Gref, R., and Couvreur, P.: ‘Polysaccharide-decorated nanoparticles’, *European Journal of Pharmaceutics and Biopharmaceutics*, 2004, 58, (2), pp. 327-341
- 89 Zheng, J.-S., Zheng, S.-Y., Zhang, Y.-B., Yu, B., Zheng, W., Yang, F., and Chen, T.: ‘Sialic acid surface decoration enhances cellular uptake and apoptosis-inducing activity of selenium nanoparticles’, *Colloids and Surfaces B: Biointerfaces*, 2011, 83, (1), pp. 183-187
- 90 Yang, F., Tang, Q., Zhong, X., Bai, Y., Chen, T., Zhang, Y., Li, Y., and Zheng, W.: ‘Surface decoration by *Spirulina* polysaccharide enhances the cellular uptake and anticancer efficacy of selenium nanoparticles’, *International journal of nanomedicine*, 2012, 7, pp. 835
- 91 Meng, H., Mai, W.X., Zhang, H., Xue, M., Xia, T., Lin, S., Wang, X., Zhao, Y., Ji, Z., and Zink, J.I.: ‘Codelivery of an optimal drug/siRNA combination using mesoporous silica

- nanoparticles to overcome drug resistance in breast cancer in vitro and in vivo', ACS nano, 2013, 7, (2), pp. 994-1005
- 92 Bharali, D.J., Khalil, M., Gurbuz, M., Simone, T.M., and Mousa, S.A.: 'Nanoparticles and cancer therapy: a concise review with emphasis on dendrimers', International journal of nanomedicine, 2009, 4, pp. 1
- 93 Davis, M.E., Chen, Z., and Shin, D.M.: 'Nanoparticle therapeutics: an emerging treatment modality for cancer': 'Nanoscience And Technology: A Collection of Reviews from Nature Journals' (World Scientific, 2010), pp. 239-250
- 94 Panyam, J., and Labhasetwar, V.: 'Biodegradable nanoparticles for drug and gene delivery to cells and tissue', Advanced drug delivery reviews, 2003, 55, (3), pp. 329-347
- 95 Chan, J.M., Valencia, P.M., Zhang, L., Langer, R., and Farokhzad, O.C.: 'Polymeric nanoparticles for drug delivery': 'Cancer Nanotechnology' (Springer, 2010), pp. 163-175
- 96 Soppimath, K.S., Aminabhavi, T.M., Kulkarni, A.R., and Rudzinski, W.E.: 'Biodegradable polymeric nanoparticles as drug delivery devices', Journal of controlled release, 2001, 70, (1-2), pp. 1-20
- 97 Cho, K., Wang, X., Nie, S., and Shin, D.M.: 'Therapeutic nanoparticles for drug delivery in cancer', Clinical cancer research, 2008, 14, (5), pp. 1310-1316
- 98 Patel, T., Zhou, J., Piepmeier, J.M., and Saltzman, W.M.: 'Polymeric nanoparticles for drug delivery to the central nervous system', Advanced drug delivery reviews, 2012, 64, (7), pp. 701-705
- 99 Gelperina, S., Kisich, K., Iseman, M.D., and Heifets, L.: 'The potential advantages of nanoparticle drug delivery systems in chemotherapy of tuberculosis', American journal of respiratory and critical care medicine, 2005, 172, (12), pp. 1487-1490
- 100 Pillai, O., and Panchagnula, R.: 'Polymers in drug delivery', Current opinion in chemical biology, 2001, 5, (4), pp. 447-451
- 101 Mora-Huertas, C., Fessi, H., and Elaissari, A.: 'Polymer-based nanocapsules for drug delivery', International journal of pharmaceutics, 2010, 385, (1-2), pp. 113-142
- 102 Kharkwal, H., and Janaswamy, S.: 'Natural Polymers for Drug Delivery' (CABI, 2016. 2016)
- 103 Tiwari, P., Panthari, P., Katore, D.P., and Kharkwal, H.: 'Natural polymers in drug delivery', World J. Pharm. Pharm. Sci, 2014, 3, (9), pp. 1395-1409
- 104 Saito, N., Murakami, N., Takahashi, J., Horiuchi, H., Ota, H., Kato, H., Okada, T., Nozaki, K., and Takaoka, K.: 'Synthetic biodegradable polymers as drug delivery systems for bone morphogenetic proteins', Advanced drug delivery reviews, 2005, 57, (7), pp. 1037-1048

- 105 Cascone, M.G., Sim, B., and Sandra, D.: 'Blends of synthetic and natural polymers as drug delivery systems for growth hormone', *Biomaterials*, 1995, 16, (7), pp. 569-574
- 106 Dash, T.K., and Konkimalla, V.B.: 'Poly- ϵ -caprolactone based formulations for drug delivery and tissue engineering: A review', *Journal of Controlled Release*, 2012, 158, (1), pp. 15-33
- 107 Labet, M., and Thielemans, W.: 'Synthesis of polycaprolactone: a review', *Chemical Society Reviews*, 2009, 38, (12), pp. 3484-3504
- 108 Baji, A., Wong, S.-C., Srivatsan, T., Njus, G.O., and Mathur, G.: 'Processing methodologies for polycaprolactone-hydroxyapatite composites: a review', *Materials and manufacturing processes*, 2006, 21, (2), pp. 211-218
- 109 Jameela, S., Suma, N., and Jayakrishnan, A.: 'Protein release from poly (ϵ -caprolactone) microspheres prepared by melt encapsulation and solvent evaporation techniques: a comparative study', *Journal of Biomaterials Science, Polymer Edition*, 1997, 8, (6), pp. 457-466
- 110 Aliabadi, H.M., Elhasi, S., Mahmud, A., Gulamhusein, R., Mahdipoor, P., and Lavasanifar, A.: 'Encapsulation of hydrophobic drugs in polymeric micelles through co-solvent evaporation: the effect of solvent composition on micellar properties and drug loading', *International journal of pharmaceutics*, 2007, 329, (1-2), pp. 158-165
- 111 Li, R., Li, X., Xie, L., Ding, D., Hu, Y., Qian, X., Yu, L., Ding, Y., Jiang, X., and Liu, B.: 'Preparation and evaluation of PEG-PCL nanoparticles for local tetradrine delivery', *International journal of pharmaceutics*, 2009, 379, (1), pp. 158-166
- 112 Liu, Q., Li, R.-T., Qian, H.-Q., Yang, M., Zhu, Z.-S., Wu, W., Qian, X.-P., Yu, L.-X., Jiang, X.-Q., and Liu, B.-R.: 'Gelatinase-stimuli strategy enhances the tumor delivery and therapeutic efficacy of docetaxel-loaded poly (ethylene glycol)-poly (ϵ -caprolactone) nanoparticles', *International journal of nanomedicine*, 2012, 7, pp. 281
- 113 Chawla, J.S., and Amiji, M.M.: 'Biodegradable poly (ϵ -caprolactone) nanoparticles for tumor-targeted delivery of tamoxifen', *International journal of pharmaceutics*, 2002, 249, (1-2), pp. 127-138
- 114 Pulkkinen, M., Malin, M., Böhm, J., Tarvainen, T., Wirth, T., Seppälä, J., and Järvinen, K.: 'In vivo implantation of 2, 2'-bis (oxazoline)-linked poly- ϵ -caprolactone: Proof for enzyme sensitive surface erosion and biocompatibility', *European journal of pharmaceutical sciences*, 2009, 36, (2-3), pp. 310-319
- 115 Bilensoy, E., Sarisozen, C., Esendağlı, G., Doğan, A.L., Aktaş, Y., Şen, M., and Mungan, N.A.: 'Intravesical cationic nanoparticles of chitosan and polycaprolactone for the

- delivery of Mitomycin C to bladder tumors', *International journal of pharmaceutics*, 2009, 371, (1-2), pp. 170-176
- 116 Murray, C.J., and Lopez, A.D.: 'Mortality by cause for eight regions of the world: Global Burden of Disease Study', *The lancet*, 1997, 349, (9061), pp. 1269-1276
- 117 Miles, D.H., Yurjevich, S.S., Petrovna, K.O., and Goun, E.A.: 'Treatment of breast cancer', in Editor (Ed.)^(Eds.): 'Book Treatment of breast cancer' (Google Patents, 2004, edn.), pp.
- 118 Crown, J., O'Leary, M., and Ooi, W.-S.: 'Docetaxel and paclitaxel in the treatment of breast cancer: a review of clinical experience', *The oncologist*, 2004, 9, (Supplement 2), pp. 24-32
- 119 Priyadarshini, K., and Keerthi, A.U.: 'Paclitaxel against cancer: a short review', *Med chem*, 2012, 2, (7), pp. 139-141
- 120 Silvestris, N., Cinieri, S., La Torre, I., Pezzella, G., Numico, G., Orlando, L., and Lorusso, V.: 'Role of gemcitabine in metastatic breast cancer patients: a short review', *The Breast*, 2008, 17, (3), pp. 220-226
- 121 Lalla, R.V., Latortue, M.C., Hong, C.H., Ariyawardana, A., D'Amato-Palumbo, S., Fischer, D.J., Martof, A., Nicolatou-Galitis, O., Patton, L.L., and Elting, L.S.: 'A systematic review of oral fungal infections in patients receiving cancer therapy', *Supportive care in cancer*, 2010, 18, (8), pp. 985-992
- 122 Kadavakollu, S., Stailey, C., Kunapareddy, C., and White, S.: 'Clotrimazole as a cancer drug: a short review', *Medicinal chemistry*, 2014, 4, (11), pp. 722
- 123 Chou, T.-C.: 'Drug combination studies and their synergy quantification using the Chou-Talalay method', *Cancer research*, 2010, pp. 0008-5472. CAN-0009-1947
- 124 Chou, T., and Martin, N.: 'CompuSyn software for drug combinations and for general dose-effect analysis, and user's guide', Paramus: ComboSyn Inc, 2007
- 125 Chou, T., and Martin, N.: 'CompuSyn for drug combinations: PC software and user's guide: a computer program for quantitation of synergism and antagonism in drug combinations, and the determination of IC50 and ED50 and LD50 values', ComboSyn Inc, Paramus,(NJ), 2005
- 126 Motiwala, M., and Rangari, V.: 'Combined effect of paclitaxel and piperine on a MCF-7 breast cancer cell line in vitro: Evidence of a synergistic interaction', *Synergy*, 2015, 2, (1), pp. 1-6
- 127 Elumalai, P., Gunadharini, D., Senthilkumar, K., Banudevi, S., Arunkumar, R., Benson, C., Sharmila, G., and Arunakaran, J.: 'Induction of apoptosis in human breast cancer cells

- by nimbolide through extrinsic and intrinsic pathway', *Toxicology letters*, 2012, 215, (2), pp. 131-142
- 128 Vivek, R., Thangam, R., Muthuchelian, K., Gunasekaran, P., Kaveri, K., and Kannan, S.: 'Green biosynthesis of silver nanoparticles from *Annona squamosa* leaf extract and its in vitro cytotoxic effect on MCF-7 cells', *Process Biochemistry*, 2012, 47, (12), pp. 2405-2410
- 129 Oh, M., Choi, Y., Choi, S., Chung, H., Kim, K., Kim, S.I., Kim, D.K., and Kim, N.: 'Anti-proliferating effects of ginsenoside Rh2 on MCF-7 human breast cancer cells', *International journal of oncology*, 1999, 14, (5), pp. 869-944
- 130 Simon, A., Allais, D., Duroux, J., Basly, J., Durand-Fontanier, S., and Delage, C.: 'Inhibitory effect of curcuminoids on MCF-7 cell proliferation and structure-activity relationships', *Cancer letters*, 1998, 129, (1), pp. 111-116
- 131 Murphy, M.P.: 'Nitric oxide and cell death', *Biochimica et Biophysica Acta (BBA)-Bioenergetics*, 1999, 1411, (2), pp. 401-414
- 132 Koppenol, W.H., Bounds, P.L., and Dang, C.V.: 'Otto Warburg's contributions to current concepts of cancer metabolism', *Nature Reviews Cancer*, 2011, 11, (5), pp. 325-337
- 133 Abas, F., Lajis, N.H., Israf, D., Khozirah, S., and Kalsom, Y.U.: 'Antioxidant and nitric oxide inhibition activities of selected Malay traditional vegetables', *Food Chemistry*, 2006, 95, (4), pp. 566-573
- 134 Martirosyan, A.R., Rahim-Bata, R., Freeman, A.B., Clarke, C.D., Howard, R.L., and Strobl, J.S.: 'Differentiation-inducing quinolines as experimental breast cancer agents in the MCF-7 human breast cancer cell model', *Biochemical pharmacology*, 2004, 68, (9), pp. 1729-1738
- 135 Fairbairn, D.W., Olive, P.L., and O'Neill, K.L.: 'The comet assay: a comprehensive review', *Mutation Research/Reviews in Genetic Toxicology*, 1995, 339, (1), pp. 37-59
- 136 Olive, P.L., and Banáth, J.P.: 'The comet assay: a method to measure DNA damage in individual cells', *NATURE PROTOCOLS-ELECTRONIC EDITION-*, 2006, 1, (1), pp. 23
- 137 Fu, J., Zhang, N., Chou, J.H., Dong, H.-J., Lin, S.-F., Ulrich-Merzenich, G.S., and Chou, T.-C.: 'Drug combination in vivo using combination index method: Taxotere and T607 against colon carcinoma HCT-116 xenograft tumor in nude mice', *Synergy*, 2016, 3, (3), pp. 15-30

- 138 Alarifi, S.: 'Assessment of MCF-7 cells as an in vitro model system for evaluation of chemical oxidative stressors', *African Journal of Biotechnology*, 2011, 10, (19), pp. 3872-3879
- 139 Wiseman, H., and Halliwell, B.: 'Damage to DNA by reactive oxygen and nitrogen species: role in inflammatory disease and progression to cancer', *Biochemical Journal*, 1996, 313, (Pt 1), pp. 17
- 140 Cerutti, P.: 'Oxidant stress and carcinogenesis', *European journal of clinical investigation*, 1991, 21, (1), pp. 1-5
- 141 McKelvey-Martin, V., Green, M., Schmezer, P., Pool-Zobel, B., De Meo, M., and Collins, A.: 'The single cell gel electrophoresis assay (comet assay): a European review', *Mutation Research/Fundamental and Molecular Mechanisms of Mutagenesis*, 1993, 288, (1), pp. 47-63
- 142 Cotelle, S., and Ferard, J.: 'Comet assay in genetic ecotoxicology: a review', *Environmental and molecular Mutagenesis*, 1999, 34, (4), pp. 246-255
- 143 Hsu, P.P., and Sabatini, D.M.: 'Cancer cell metabolism: Warburg and beyond', *Cell*, 2008, 134, (5), pp. 703-707
- 144 Wang, A.Z., Langer, R., and Farokhzad, O.C.: 'Nanoparticle delivery of cancer drugs', *Annual review of medicine*, 2012, 63, pp. 185-198
- 145 Parveen, S., and Sahoo, S.K.: 'Polymeric nanoparticles for cancer therapy', *Journal of drug targeting*, 2008, 16, (2), pp. 108-123
- 146 Seymour, L.: 'Passive tumor targeting of soluble macromolecules and drug conjugates', *Critical reviews in therapeutic drug carrier systems*, 1992, 9, (2), pp. 135-187
- 147 Steichen, S.D., Caldorera-Moore, M., and Peppas, N.A.: 'A review of current nanoparticle and targeting moieties for the delivery of cancer therapeutics', *European Journal of Pharmaceutical Sciences*, 2013, 48, (3), pp. 416-427
- 148 Mohanraj, V., and Chen, Y.: 'Nanoparticles-a review', *Tropical journal of pharmaceutical research*, 2006, 5, (1), pp. 561-573
- 149 De Jong, W.H., and Borm, P.J.: 'Drug delivery and nanoparticles: applications and hazards', *International journal of nanomedicine*, 2008, 3, (2), pp. 133
- 150 Nagavarma, B., Yadav, H.K., Ayaz, A., Vasudha, L., and Shivakumar, H.: 'Different techniques for preparation of polymeric nanoparticles-a review', *Asian J. Pharm. Clin. Res*, 2012, 5, (3), pp. 16-23

- 151 Coombes, A., Rizzi, S., Williamson, M., Barralet, J., Downes, S., and Wallace, W.: 'Precipitation casting of polycaprolactone for applications in tissue engineering and drug delivery', *Biomaterials*, 2004, 25, (2), pp. 315-325
- 152 Kumar, A., and Sawant, K.: 'Encapsulation of exemestane in polycaprolactone nanoparticles: optimization, characterization, and release kinetics', *Cancer nanotechnology*, 2013, 4, (4-5), pp. 57-71
- 153 Ravi, P.R., Vats, R., Dalal, V., and Gadekar, N.: 'Design, optimization and evaluation of poly- ϵ -caprolactone (PCL) based polymeric nanoparticles for oral delivery of lopinavir', *Drug development and industrial pharmacy*, 2015, 41, (1), pp. 131-140
- 154 Zidan, A.S., Sammour, O.A., Hammad, M.A., Megrab, N.A., Habib, M.J., and Khan, M.A.: 'Quality by design: Understanding the formulation variables of a cyclosporine A self-nanoemulsified drug delivery systems by Box–Behnken design and desirability function', *International journal of pharmaceutics*, 2007, 332, (1-2), pp. 55-63
- 155 Gajra, B., Dalwadi, C., and Patel, R.: 'Formulation and optimization of itraconazole polymeric lipid hybrid nanoparticles (Lipomer) using box behnken design', *DARU Journal of Pharmaceutical Sciences*, 2015, 23, (1), pp. 3
- 156 Noronha, C.M., Granada, A.F., de Carvalho, S.M., Lino, R.C., de OB Maciel, M.V., and Barreto, P.L.M.: 'Optimization of α -tocopherol loaded nanocapsules by the nanoprecipitation method', *Industrial crops and products*, 2013, 50, pp. 896-903
- 157 Ferreira, S.C., Bruns, R., Ferreira, H., Matos, G., David, J., Brandao, G., da Silva, E.P., Portugal, L., Dos Reis, P., and Souza, A.: 'Box-Behnken design: an alternative for the optimization of analytical methods', *Analytica chimica acta*, 2007, 597, (2), pp. 179-186
- 158 Forastiere, A.A.: 'Use of paclitaxel (Taxol) in squamous cell carcinoma of the head and neck', in Editor (Ed.)^(Eds.): 'Book Use of paclitaxel (Taxol) in squamous cell carcinoma of the head and neck' (1993, edn.), pp. 56-60
- 159 Verweij, J., Clavel, M., and Chevalier, B.: 'Paclitaxel (TaxolTM) and docetaxel (TaxotereTM): Not simply two of a kind', *Annals of Oncology*, 1994, 5, (6), pp. 495-505



PUBLICATIONS
AND
PRESENTATIONS



PUBLICATIONS:

1. **Arun Sharma**, Ankita Rajata, Udayabanu Malairaman, Hemant Sood. “Hydroalcoholic extraction of shoot cultures from *Nothapodyte Nimmoniana* and its anti-proliferative analysis”. *International Journal of Pharmacy and Pharmaceutical Sciences*;2018 (6) 32-37 [Scopus Indexed].
2. **Arun Sharma**, Vineet Mehta, Arun Parashar, Udayabanu Malairaman. “Combinational effect of Paclitaxel and Clotrimazole on human breast cancer: Proof for synergistic interaction”. *Synergy*;2017 (5) 13-20 [Scopus Indexed].
3. **Arun Sharma**, Vineet Mehta, Arun Parashar, Riddhi Patwal, Udayabanu Malairaman. “Solid Lipid Nanoparticle: Fabricated through nanoprecipitation and their physicochemical characterization”. *International Journal of Pharmacy and Pharmaceutical Sciences*. 2016; 8(10)1- 5 [Scopus Indexed].
4. **Arun Sharma**, Aniket Sood, Vineet Mehta, Udayabanu Malairaman. “Formulation and Physicochemical evaluation of nanostructured lipid carrier for codelivery of clotrimazole and ciprofloxacin”. *Asian Journal of Pharmaceutical and Clinical Research*. 2016; 9(3) 1- 5. [Scopus Index].
5. **Arun Sharma**, Vineet Mehta, Gopal Singh Bisht, Udayabanu Malairaman. “Polymeric nanoparticles-mediated delivery system for anti-bacterial Peptides”. *International Journal of Pharmacy and Pharmaceutical Sciences*. 2016; 8(3)45. (Abstract Published) [Scopus Indexed].

ASSOCIATED PUBLICATION

1. Kumari A, **Sharma A**, Malairaman U, Singh RR. (2018) Proficient surface modification of CdSe quantum dots for highly luminescent and biocompatible probes for bioimaging: A comparative experimental investigation. *Journal of Luminescence*. 1; 199:174-82 Scopus Indexed (IF-2.6).
2. Patel SS, Ray RS, **Sharma A**, Mehta V, Katyal A, Udayabanu M (2018). Antidepressant and anxiolytic like effects of *Urtica dioica* leaves in streptozotocin induced diabetic mice. *Metabolic brain disease*. 27:1-2 Scopus Indexed (IF-2.2).
3. Mehta V, Parashar A, **Sharma A**, Singh TR, Malairaman U. (2017) “Quercetin ameliorates chronic unpredicted stress-mediated memory dysfunction in male Swiss albino mice by attenuating insulin resistance and elevating hippocampal GLUT4 levels independent of

insulin receptor expression”. *Hormones and Behavior.*;89:13-22. [Frank A. Beach Award Paper] Scopus Indexed (IF-3.3)

4. Sharma S, **Sharma A**, Mehta V, Chauhan RS, Malairaman U, Sood H. (2016) efficient hydroalcoholic extraction for highest diosgenin content from trillium govanianum (nag chhatri) and it's in vitro anticancerous activity. *AJPCR*, 4(9): 1-7 . Scopus Indexed (IF-0.49)
5. Mehta V, **Sharma A**, Tanwar S, Udayabanu M. (2016). In-vitro and in-silico evaluation of the antidiabetic effect of hydroalcoholic leaf extract of *Centella asiatica*. *International Journal of Pharmacy and Pharmaceutical Sciences*, 8, 257-362. Scopus Indexed (IF-0.51)
6. Bhardwaj V, Monga J, Sharma S, **Sharma A**, Sharma A and Sharma P. (2014). Novel surfactant immobilized micellar system of oxidation inhibitors in clotrimazole bio-adhesive gel formulation: Development, characterization, in vitro and in vivo antifungal evaluation on *Candida* clinical isolates. *RSC Adv.*, 4, 47207-21. Scopus Indexed (IF-3.1)
7. Sharma L and **Sharma A**. (2014). In vitro antioxidant, anti-inflammatory and antibacterial activity of *Withania somnifera*. *Journal of Chemical and Pharmaceutical Sciences*, 6(7):178-82. Scopus Indexed.

CONFERENCE AND WORKSHOPS

1. **Arun Sharma** and Udayabhanu Malairaman. Concept of drug repositioning and its application in breast cancer. [International Conference on “Challenges in clinical trials and pharmacovigilance of new drugs, genetically modified products and herbal drugs” on 28th & 29th March 2018]. **Received 2nd Prize in oral Presentation**
2. **Arun Sharma**, Riddhi Patwari, Gopal Bisht, Udayabhanu Malairaman. (2015) Nanoparticles-mediated delivery of the antimicrobial peptide against bacterial infection. [International Conference 4th Nanotoday Conference, JW Marriot Marquis Dubai, **United Arab Emirates**: 6-10 December 2015].
3. **Arun Sharma**, Vineet Mehta, Arun Parashar, Udayabanu Malairaman (2016). Polymeric nanoparticles-mediated delivery system for anti-bacterial peptides. *International Conference on Innovations in Pharmaceutical Sciences*. [Sri Aurobindo Institute of Pharmacy, Indore, Madhya Pradesh, India: 27-28 February 2016].
4. **Arun Sharma**, Vineet Mehta, Udayabanu Malairaman (2014). In-vitro and IN-vivo evaluation of solid dispersion of Rosuvastatin. *International Conference on Pharmaceutical*

Sciences- Present Trends and Future Prospects in Pharmaceutical Sciences [Shri Guru Ram Rai Institute of Technology & Science, Dehradun, Uttarakhand, India: 14 - 15 February 2014].

5. **Arun Sharma** (2016). National Symposium on Computational Systems Biology (NSCSB). [Jaypee University of Information Technology, Wagnaghat, Himachal Pradesh, India: 18-20 March 2016]
6. **Arun Sharma** (2016). Workshop on Statistical Techniques in Biological and Medical Sciences (STBMS). [Jaypee University of Information Technology, Wagnaghat, Himachal Pradesh, India: 13-18 June 2016].
7. **Arun Sharma**, Varun Bhardwaj, Udayabanu Malairaman (2014) National Conference on “Recent Advancement in Novel Drug Delivery System and Technology” [ASBASJSM college of pharmacy Bella (Ropar) Punjab. India ;15-16 November 2014] **Received 1st Prize in poster presentation**
8. **Arun Sharma**. One day workshop on “Hands on Training Analytical Instrument Expertise- In collaboration with Industrial Experts” [Laureate Institute of Pharmacy, Kangra, H.P. India; 6 April 2014].